

Chiral separation of arginine based on tailor-made FhuA β -barrel protein

Von der Fakultät für Mathematik, Informatik und Naturwissenschaften der
RWTH Aachen University zur Erlangung des akademischen Grades eines
Doktors der Naturwissenschaften

vorgelegt von

**Master of Science (M.Sc.)
Biotechnologie**

Deepak Anand

aus India

**Berichter: Universitätsprofessor Dr. Ulrich Schwaneberg
Universitätsprofessor Dr. Alexander Böker**

Tag der mündlichen Prüfung: 20 April 2020

Diese Dissertation ist auf den Internetseiten der Universitätsbibliothek verfügbar.

WHERE THERE IS A WILL THERE IS A WAY

Table of Contents

Abbreviations	v
Abstract	viii
1 Introduction.....	1
1.1 Enantioselectivity and chiral separation	1
1.2 Ferric hydroxamate uptake protein component A (FhuA).....	3
1.3 Membrane proteins in technical applications	5
1.4 Protein engineering	7
1.5 Omnichange.....	9
1.6 Arginine diminase (ADI)	10
1.7 Pig kidney D-amino acid oxidase (pkDAO)	12
1.8 Liposomes and polymersomes.....	13
1.9 Detergents for membrane protein and use of 2-methyl-2,4-pentanediol (MPD) as refolding agent.....	15
1.10 Objectives	17
2 Computational analysis based engineering of FhuA WT for generation of selectivity filter regions	18
2.1 Computational identification/selection of loops to be shortened for generation of filter regions.....	18
2.1.1 Identification of loops.....	18
2.1.2 Rational prediction for stabilization of the cork domain.....	18
2.1.3 Steered molecular dynamic (SMD) simulations of FhuA WT and FhuA Δ L variant.....	19
2.2 Result and discussion.....	20
2.2.1 Generation of filter regions	20
2.2.2 Stabilization of cork domain at identified positions with site directed mutagenesis (SDM).....	21
2.3 Experimental section	24
2.3.1 Cloning of gene encoding FhuA WT and generation of FhuA Δ L variant.....	24
2.3.1.1 Cloning of pPRIBA1_FhuA WT in expression strain	26
2.3.1.2 Channel generation in FhuA WT	26
2.3.2 Production of FhuA WT and FhuA Δ L	27
2.3.2.1 Preparation of chemical competent cells and transformation.....	27
2.3.2.2 Expression of FhuA WT and FhuA Δ L	28
2.3.2.3 Extraction of FhuA WT and FhuA Δ L	28
2.3.2.4 Refolding of FhuA WT and FhuA Δ L	29
2.3.3 Calcein release assay	29
2.3.3.1 Polymersome preparation with entrapped calcein.	29
2.3.3.2 Insertion of FhuA variants.....	30

2.4	Result and discussion	31
2.4.1	Channel generation in FhuA WT and stabilization of cork domain	31
2.4.2	Expression and extraction of FhuA WT and FhuA Δ L	32
2.4.3	Extraction of FhuA WT and FhuA Δ L	33
2.4.4	Calcein release assay	35
3	Structure guided OmniChange libraries generation	37
3.1	Computational analysis for selection of amino acid residues for OmniChange libraries generation	37
3.2	Result and discussion	37
3.3	Experimental section	39
3.3.1	Iodine cleavage	43
3.3.2	Hybridization of DNA fragments	43
3.3.3	Transformation of assembled OmniChange library	43
3.4	Result and discussion	44
3.4.1	Generation of OmniChange libraries	44
4	Development and validation of high-throughput screening system for identification of enantioselective FhuA variants	47
4.1	Experimental section	47
4.2	Development of whole cell screening system	50
4.2.1	Cloning and expression of FhuA with amino acid utilizing enzymes (ADI)	50
4.2.2	Cultivation and expression in 96-well plates	50
4.2.3	Screening of OmniChange libraries	50
4.3	Development of characterization system	51
4.3.1	Cloning and expression for characterization system	51
4.3.2	Chiral HPLC	51
4.3.3	Characterization of identified variants	52
4.3.4	Quantification of FhuA Δ L and FhuAF4	52
4.3.5	Steered molecular dynamics simulations	53
4.4	Recombination with site directed mutagenesis	53
4.5	Result and discussion	55
4.5.1	Expression in autoinduction media	55
4.5.2	Whole cell citrulline detection assay	56
4.5.3	Screening of OmniChange libraries	59
4.5.4	Characterization of identified variants	60
4.5.5	Steered molecular dynamics (SMD) simulations	64
4.6	Recombination of beneficial mutations	66

4.7 Quantification of FhuA variants on cell surface	68
4.7.1 Strep tag insertion by PCR and PLICing.....	68
4.7.2 Expression of strep tagged FhuA variants	69
4.7.3 Quantification of FhuA on cell surface	70
5 Summary and conclusion	72
References.....	75
Appendix	88
Publications and patent	103
Declaration	104
Acknowledgement	105
Curriculum Vitae.....	107

Abbreviations

AA	Amino acid(s)
Abs₆₀₀	Absorption at the wavelength of 600 nm
AcN	Acetonitrile
ADI	Arginine deiminase
AI	After induction
AMBER	Assisted model building with energy refinement
ARGET	Activator regenerated by electron transfer
ASL	Argininosuccinate lyase
ASS	Argininosuccinate synthetase
bp	Base pair(s)
BCA	Bicinchoninic acid
BI	Before induction
BLOSUM 62	Blocks substitution matrix 62
BSA	Bovine serum albumin
CBB	Coomassie brilliant blue, Coomassie
CD	Circular dichroism
cfu	Colony forming unit(s)
CMC	Critical micelle concentration
CSP	Chiral stationary phase
Δ	Deletion of amino acid(s)
ΔΔG	Stabilizing energy
Da, kDa	Dalton, kilo Dalton
DAM	Diacetyl monoxime
DAO	D-amino acid oxidase
DNA	Deoxyribonucleic acid
dNTP	Desoxy nucleic triphosphate(s)
DAO	D-amino acid oxidase
<i>E. coli</i>	<i>Escherichia coli</i>
EDTA	Ethylenediaminetetraacetic acid
epPCR	Error-prone PCR
<i>e.g.</i>	<i>exempli gratia (for example)</i>
<i>et al.</i>	<i>et alii</i>
Ex₄₉₅, Em₅₁₄	Wavelength for excitation and emission, respectively
FAD	flavin adenine dinucleotide
FhuA	Ferric hydroxamate uptake protein component A
For	Forward primer for PCR
g	Gravitational force
h	Hour(s)
HCC	Hepatocellular carcinomas
IPTG	Isopropyl-β-D-thiogalactopyranoside

LB	Luria Broth
LBA	Luria Broth with ampicillin
LBK	Luria Broth with kanamycin
LCST	Lower critical solution temperature
m	Mass
M	Protein and DNA marker, respectively
MD simulation	Molecular dynamic simulation
min	Minute(s)
MPD	2-Methyl-2,4-pentanediol
MTP	Microtiter plate(s)
MWCO	Molecular weight cut-off
NaCl	Sodium chloride
NTP	Nucleoside triphosphate
OD₆₀₀	Optical density of cell suspensions at 600 nm
OE-PCR	overlap extension polymerase chain reaction
OMP	Outer membrane protein(s)
oPOE	Octyl-polyoxyethylene
P	Pellet
PAGE	Polyacrylamide gel electrophoresis
PCR	Polymerase chain reaction
PDB	Protein Data Bank
PE-PEG	Polyethylene-polyethyleneglycol
PfuS	DNA polymerase found in <i>Pyrococcus furiosus</i>
pkDAO	Pig kidney D-amino acid oxidase
PLICing	Phosphorothioate-based ligase-independent gene cloning
Pp	<i>Pseudomonas plecoglossicida</i>
PTO	Phosphorothioate nucleotides
Rev	Reverse primer for PCR
rpm	Rounds per minute
sec	Second(s)
S	Supernatant
SDM	Site-directed mutagenesis
SDS	Sodium dodecyl sulfate
SSM	Site-saturation mutagenesis
StdDev	Standard deviation
Taq Pol	DNA polymerase found in <i>Thermus aquaticus</i>
TSC	Thiosemicarbazide
TYA	TY media with ampicillin
U	Unit(s)
UV	Ultraviolet light
VIS	Visible light
v_t	Terminal velocity

v/v	Volume per volume
w/v	Weight per volume
w/w	Weight per weight
WT	Wildtype
YASARA	Yet Another Scientific Artificial Reality Application

Abstract

Chirality of chemical compound is ubiquitous in nature performing central function in metabolism of many nutrients and pharmaceuticals. Even-though enantiomers of a compound have similar chemical and physical properties it can have completely different biological activity. Thus chiral molecules are of large economic value in chemical, pharmaceutical, and food industries. Many applications in these industries require the isolation and use of single chiral isomers (enantiomers) of chiral compounds. As a result, there is an ever increasing necessity of optically pure compounds but it is a challenging task to obtain it. Since the first optical resolution of tartaric acid, performed by Louis Pasteur in early 1848, various techniques have been developed for chiral resolutions of enantiomeric compounds. Methods such as chromatographic or enzymatic techniques are commonly used. However, they are limited by difficulties for large-scale productions. Crystallization can be used in large-scales but often several rounds of crystallization and recrystallization are required to obtain enantiopure compounds due to entrapments of the unwanted enantiomer during crystal growth, which often leads to significant reduction in yields (up to 50 %).

Each and every one of these techniques has their own advantages and disadvantages but the membrane based approach is of particular interest because of its use in continuous operation and its ease of scale-up. But the problem with the membrane based technology developed till now is that of non-uniform pore size and limited number of pores. Inspired by nature, membrane-based approaches for chiral separation using a barrel protein can be a suitable alternative. Chiral protein-polymer membranes would be an attractive, cost-effective, and scalable method. However, the main challenges lie in the design of “filter regions” and the generation of “screening systems” to identify chiral channel proteins. In the present thesis, ferric hydroxamate uptake component A (FhuA) was engineered to generate chiral channel for separation of arginine enantiomers which can be used as a scaffold for the generation of protein-polymer membrane. FhuA is a large monomeric transmembrane protein of *Escherichia coli* which folds into a barrel consisting of 22 antiparallel β -strands and a barrel-plugging “cork domain”. FhuA was chosen as a functional nanopore because of its high tolerant towards organic solvents, thermal resistant, and has a high robustness towards reengineering.

Structurally, FhuA contains a water channel wherein two flexible loops in the cork domain (loop1; residue 35-40 and loop2; residues 135-145) were shortened to generate two selectivity filter regions (filter1 and filter2). Additionally, cork domain was stabilized inside the barrel by substituting three amino acids (Q62D, R81W, and N117L) resulting in generation of FhuA Δ L variant having higher interaction between barrel and cork domain. In order to generate a chiral selective variant, a directed evolution protocol was developed to generate a chiral FhuA Δ L variant.

A novel whole cell calorimetric screening system based on amino acid utilizing enzyme (arginine deiminase) was developed in order to identify the enantioselective variant from mutant libraries of FhuA Δ L. Screening of mutant libraries led to the identification of FhuAF4 variant (amino acid substitutions: G134S, G146T) showing approximately two times higher transport of L-arginine compared to parent FhuA Δ L with E-value=1.92; ee %=23.91 at 52.39 % conversion.

Steered molecular dynamics (SMD) simulations were carried out for molecular understanding of observed altered enantiopreference of FhuAF4 variant towards L-arginine compared to the FhuA Δ L variant. In FhuA Δ L variant, less interactions of both D- and L-arginine with the filter region 2 were observed and both enantiomers pass freely. Interestingly, in FhuAF4 variant, transport of D-arginine is hindered and steered transport is slowed down, indicated by a longer residence time close to the selectivity filter region 2.

The obtained results provide first proof of principle of engineering of a membrane protein towards chiral separation of amino acids and provide insight into the mechanism of chiral separation within the FhuA channel. It is likely that with the identified filter region and OmniChange libraries further improvements are achievable for other amino acids and a broader range of enantiomers. The chiral FhuA channel proteins would be an excellent scaffold for generation of chiral membrane based on protein polymer conjugates with a high potential for novel and scalable downstream processes in pharmaceutical and food industries.

1 Introduction

1.1 Enantioselectivity and chiral separation

Isomers are molecules that have the same molecular formula, but have a different arrangement of the atoms in space. There are two different classes of isomers: structural isomers and stereoisomers. Structural isomers have the same molecular formula but different structural formula whereas Stereoisomers have the same structural formula but differ in their spatial arrangement. Stereoisomers are further classified into two categories: Geometric isomers and optical isomers/enantiomers (Figure 1).¹ Optical isomers or Enantiomers are the chiral molecules that have a central atom to which different side chains are attached and are non-superposable mirror image of each. Enantiomers have similar physical and chemical properties except for their ability to rotate plane polarized light. L-enantiomer of a compound rotates plane polarized light to left (levorotatory) and D-enantiomer rotates it to right (dextrorotatory).¹ Eventhough enantiomers have similar physical and chemical properties, they can have very different biological activity. In some cases, only one of the enantiomers of a compound contributes to its positive effect, while the other shows no or a much weaker effect as well as side-effects or even toxicity.^{2,3} These differences in biological activities can be attributed to the high degree of stereoselectivity of enzymatic reactions and other biological processes.^{4,5} Therefore, there is tremendous interest in producing pure enantiomers for the food and agrochemical industries, and in particular for the pharmaceutical industry.⁶⁻⁸

Since the first optical resolution of tartaric acid, performed by Louis Pasteur in early 1848,⁹ various techniques have been developed for chiral resolutions of enantiomeric compounds.¹⁰ One method is chiral crystallization,^{11,12} in which a racemate is complexed with another chiral compound that selects the desired enantiomer, resulting in a chemical distinction between the two enantiomers that allows one to crystallize out.^{13,14} In other cases, a solution is seeded with chiral crystals, causing the desired enantiomer to crystallize out preferentially.^{15,16} However, this approach works only for the approximately 10 % of known compounds that crystallize into distinct enantiopure crystallites. A second method employs chiral chromatography,^{17,18} such as high performance liquid chromatography (HPLC), which is used in batch mode, or a continuous chromatographic process. But these methods present scalability challenges. Third method is chiral catalysis,^{19,20} which uses chiral catalysts to produce enantiomerically pure compounds. However, matching catalysts and target molecules can be difficult.

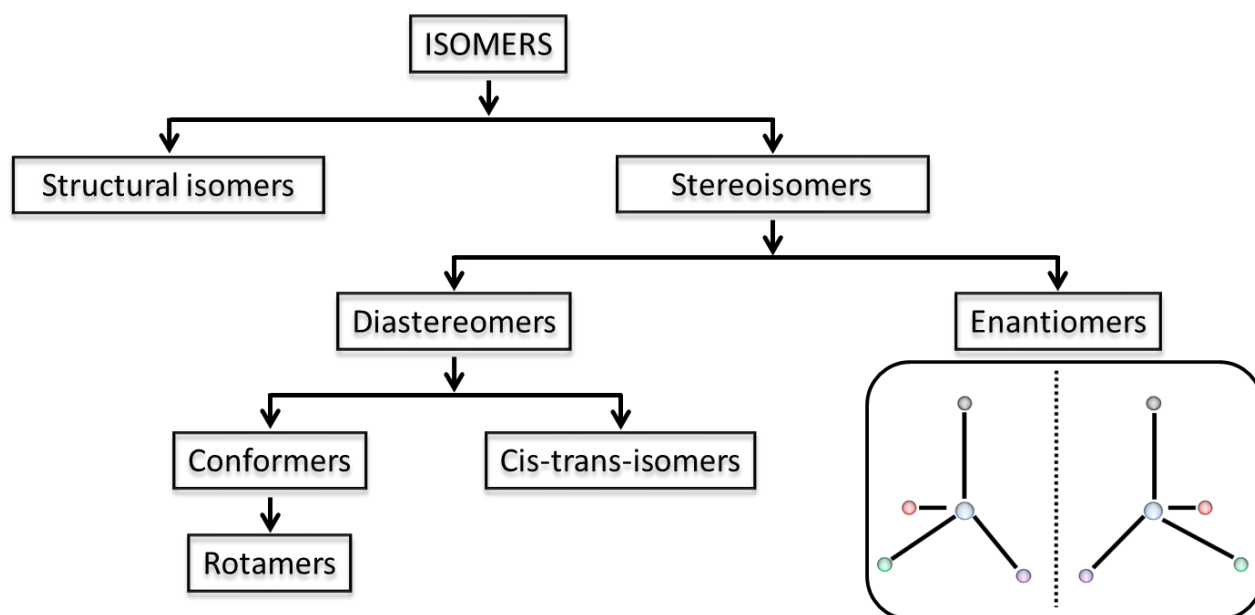


Figure 1. Classification of isomer. Enantiomers/optical isomers are a class of stereoisomers that form non-superimposable mirror images of each other.

1.2 Ferric hydroxamate uptake protein component A (FhuA)

Biological membranes are crucial component of cells enabling separation between inside and outside of an organism by providing natural compartment. In gram-negative bacteria, such as *Escherichia coli* (*E.coli*), these biological membranes consist of inner (cytoplasmic) membrane (IM), a thin peptidoglycan layer, and an outer membrane (OM) containing lipopolysaccharide. The outer membrane is the first barrier which acts as a selective and permeable layer to control compound flux^{21,22} while protecting the interior from the toxic substances.²³ This selective transport of compounds is mediated by outer membrane proteins (OMPs) which is encoded by as much as 3 % of gram-negative bacterial genome.²⁴ Approximately 15% of the membrane proteins are β -barrel proteins consisting of β -strands that are generally oriented antiparallel to each other.²⁴

Ferric hydroxamate uptake protein component A (FhuA) is one of the largest known monomeric β -barrel proteins consisting of 714 amino acids (78.9 kDa) with a height of 6.9 nm and an elliptical cross section of 3.9-4.6 nm (Figure 2). It consists of two domains: C-terminal β -barrel domain (amino acid residues 161-714) and N-terminal cork domain (amino acid residues 1-160). Like most of the membrane proteins, the β -barrel of FhuA consists of highly hydrophobic middle part which helps in stable incorporation into the lipid membrane. Its barrel is arranged in 22-antiparallel β -strands connected together by short loops towards periplasm and longer surface exposed loops. The barrel wall is connected to cork domain by extensive hydrogen bonding. The cork domain consists of four-stranded β -sheets which are arranged in the barrel at an inclined angle of 45° sterically occluding the channel. FhuA together with an energy transducing protein TonB mediates the active transport of ferrichrome-iron through the outer membrane of *E. coli*. It binds to specific siderophore-iron complexes that can barely cross the membrane through passive diffusion, and exploit the electrochemical potential of the cytoplasmic membrane. In addition to ferrichrome-siderophores, FhuA acts as a primary receptor for antibiotics albomycin and microcin, several bacteriophages and the bacterial toxin colicin M.²²

FhuA has been extensively reengineered in order to use it in medical applications (triggered drug release) and in catalysis (hybrid catalysts). FhuA acts as an attractive scaffold for these applications since it have a remarkable resistance towards, high temperatures (*e.g.* $T_m \sim 60^\circ\text{C}$), chaotropic salts (*e.g.* 8 M urea), alkaline pH, organic solvents (*e.g.* $\leq 40\%$ tetrahydrofuran, $\leq 10\%$ ethanol) and proteolysis (*e.g.* subtilisin, trypsin).²⁵⁻³⁰ Additionally, FhuA has shown high tolerance towards genetic modification. Active channel of FhuA was converted to a passive diffusion channel by the deletion of cork domain ($\Delta 5-160$).³¹ Other cork domain deletion variants were generated (FhuA $\Delta 1-129$, FhuA $\Delta 1-160$) which even allowed the translocation of single stranded DNA molecules.³² FhuA without this cork domain can function as a passive diffusion channel and has been used as a nanopore integrated in liposome/polymersome membranes for the translocation of compounds.³²⁻³⁴ Other derived variants of FhuA $\Delta 1-160$

were generated in order to widen the channel diameter^{30,35} and to overcome the hydrophobic mismatch for a more efficient insertion into synthetic membranes.³⁶ FhuA embedded in liposomes, residue Lys545 (equal to Lys556 of published FhuA variants with a His-tag) was identified as key residue for controlled compound flux. Based on this principle, an engineered variant FhuA Δ CVF^{tev} (FhuA Δ 1-159 K545C/N548V/E501F_{tev}) was generated; it exhibits accessibility of free cysteine group inside the channel which can be covalently attached to metal catalyst to generate hybrid catalysts.³⁷

Due to the aforementioned features such as the comparably large pore-size, its rigid structure and wide possibilities of modification, the well-characterized FhuA is more attractive than other membrane proteins for investigation as a scaffold for generation of stable chiral protein channel with possibility of its used for protein-polymer membrane generation.

In the present thesis, FhuA Wild Type (FhuA WT) functioned as starting variant for investigation towards the generation of chiral membranes for separation of enantiomeric amino acids (arginine) as model compound.

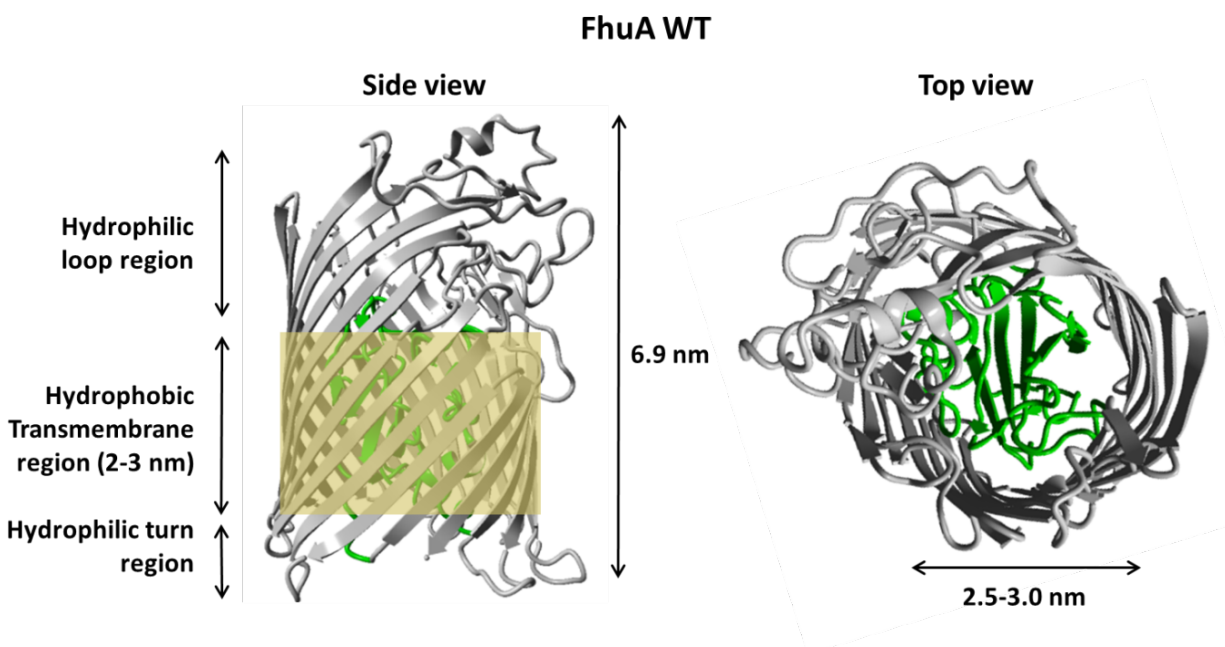


Figure 2. Crystal structure of Ferric hydroxamate uptake component A (FhuA, side and top view) an outer membrane protein of *E. coli*. The structure is based on PDB ID 1BY3 showing 22 β -sheets forming a β -barrel (C-terminus, gray), blocked by the N-terminal cork domain (green). It has a height of ~ 6.9 nm and channel size of 2.5 nm-3.0 nm.

1.3 Membrane proteins in technical applications

Nature has evolved cells to generate highly specific and selective membranes which allow only specific compounds to pass through it. Therefore, it is very hard to develop an artificial membrane which has higher performance parameters than a natural membrane. Hence it is only logical to use biomaterials like membrane proteins for generation of selective membranes, but the amphiphilic nature of membrane proteins makes it harder to purify as it cannot maintain its 3D structure and precipitate under hydrophilic conditions. Because of this, utilization of membrane proteins in technical applications is a hard task. However, many alpha-helical and beta barrel proteins have been recently used in various applications.

Alpha-helical protein like α -Hemolysin in polymer membrane has been used for translocation of single stranded DNA and RNA³⁸ which later led to its utilization in determining the sequence of DNA and RNA during its translocation.³⁹ Similarly, engineered MspA protein was also studied for DNA sequencing and translocation of small compounds.^{40,41} Membrane associated enzymatic proteins like Acetylcholinesterase has also been utilized for generation of biosensors for compounds such as pesticides, chemical agents and natural toxins.⁴²

One of the biggest success stories of commercial utilization of membrane protein is that of use of aquaporin for water purification. Aquaporin is an intrinsic membrane protein which facilitates transport of water in all kinds of life. Unique structure of aquaporin channel allows only water molecules to pass through preventing transport of any protons or ions due to electrostatic repulsions.⁴³ Study done by Kumar *et al.* has shown that the biomimetic aquaporin membranes shows 200 times higher water permeability compared to any other commercial membranes⁴⁴ leading to first commercial launch of aquaporin biomimetic membrane by Aquaporin A/S.

Although considerable progress has been achieved in chiral resolution of amino acids in past decade, the design of a simple and effective system for the enantiomeric resolution of amino acids still remains as a challenging task. Crystallization and recrystallization methods have mostly been used in the industry to separate enantiomers from racemic mixtures; quite often recrystallization has to be repeated with corresponding loss of yield and turnover.¹⁰ Chiral protein-polymer membranes would be an attractive, cost-effective, and scalable alternative to crystallization methods. With the best of our present knowledge a controlled production of protein-polymer-conjugate-membranes via amino-functionalized polymerization of tailored and selective channel proteins for separation of enantiomer mixtures is a new interdisciplinary approach. Membranes with highly uniform pore size could not be chemically produced until now. Current approaches, which are targeting this aim, are using cylindrical diblock copolymers as a template. Using this, small pores with a size up to 20 nm can be generated, but these pores are too large for certain applications (e.g. selectivity of enantiomers) and due to the process of their generation, they are chemical inert. So a subsequently functionalization is excluded. Other methods like electron beam lithography are generating pores with a higher pore size

distribution are not economical, and so they are only of academic interests. Long term goal of this work goes far beyond the state of the art of the techniques used till now and will enable generation of highly uniform selective functional pores with a high functional loading density on the membrane ($> 10,000,000$ channel proteins per cm^2). Work done in this thesis focuses on crucial step of generating selective pores which are the basis of generation of these membrane in future.

1.4 Protein engineering

Proteins are the macromolecules that play crucial part in survival of living organisms because of its versatile function in life. It not only performs important biochemical reactions (biocatalysis) but also are involved in structural stability and regulation process. Because of their different functions, proteins are important for broad industrial applications in food industries, laundry applications and in pharmaceuticals. Proteins are especially used as biocatalysts for the industrial production of fine chemicals and pharmaceuticals. Native proteins are mostly not suitable for an efficient application and need to be modulated or optimized to fulfil all desired properties. Often properties of proteins like regioselectivity, chemoselectivity and stereoselectivity need to be optimized, as well as process-related aspects, such as temperatures, pH-values, activity in presence of high substrate concentrations or other stability related aspects to achieve maximal productivity.⁴⁵⁻⁴⁹ Since proteins are built up of amino acids, extensive and at the same time very specific protein-engineering can be performed in order to improve functions or even to obtain new functions. Modification of natural enzymes and proteins by protein engineering is an increasing important scientific field. Protein engineering is the process of designing new enzymes or proteins with novel and desirable functions. It is based on the use of recombinant DNA technology to change amino acid sequences. It provides unprecedented expansion of scope and applications of improved enzymes with desired physical and catalytic properties. Two most common complementary strategies for protein engineering are rational design and directed evolution.^{50,51}

Directed evolution is a random process of imparting mutations by changing amino acids randomly and it does not require prior information about structure and its structure related functions.^{52,53} The first direct and dramatic proof of directed evolution was given in the famous experiments by Spiegelman and coworkers on the concept of “evolution in a test tube” in 1967 with an *in vitro* Darwinian experiment using self-replicating RNA.⁵⁴ Although the term had been occasionally applied for decades to describe adaptive evolution experiments, the first directed evolution experiment linked to an evolved enzyme was reported in the mid-1990s. In 1993, Chen and Arnold showed a successful example of tuning the activity of subtilisin E (a serine protease useful in several industrial applications) for unusual environments by sequential random mutagenesis.⁵⁵ Until 2006 a rapid blossom of the field could be observed (~320 reports in 2006 Core collection; search term “Directed Evolution”) follow by slowdown in growth to around 450 reports since 2012 (2012: ~450; 2013: ~480; 2014: ~450). Up to now, directed evolution has been used to expand and boost various enzyme properties, such as enantioselectivity, specificity, activity, stability and solubility. In broad terms, one round of directed enzyme evolution usually consists of three steps: i) Diversity generation; ii) Screening for improved variants; and iii) Isolating the gene encoding for the improved protein variant. In step I, diversity is generated on the gene level by random mutagenesis using enzyme-based, chemical, whole cell or hybrid methods.⁵⁶ In the second step, an improved variant is identified

on the protein level using high throughput screening methods. In the third step, the gene encoding for the improved variant is isolated and responsible mutations are identified. Iterative cycles are usually required until the desired property has been changed or improved significantly. Main challenges for directed evolution are the generation of mutant libraries with high diversity and development of a high-throughput screening method for identification of mutants with improved properties.⁵⁷ A common method to generate random mutagenesis is error-prone polymerase chain reaction (ep-PCR) based on inaccurate amplification of gene.^{58,59} This method has been widely used in directed enzyme evolution experiments due to their versatility and simplicity but it is significantly limited in the ability to create diversity on the gene level.⁶⁰ Disadvantageous, mutation hot spots, consecutive mutations and bias towards transition mutagenesis are observed while performing epPCR. Sequence Saturation Mutagenesis (SeSaM) improved the diversity generation of random mutagenesis by eliminating hot spots and reducing the transition bias as well as consecutive mutations.⁶¹

In contrast to directed evolution, rational design requires detailed knowledge of protein structure, function and mechanism of action.⁶² Based on this knowledge, precise changes in amino acid sequence can be made which are predicted to change the enzymatic properties towards desired properties. It is a powerful tool to generate focused mutant libraries to improve enzyme properties such as activity and selectivity with amino acid substitutions mainly close to the active site.⁶³⁻⁶⁵ This process limits the size of the library tremendously. Also the knowledge about protein structure simplifies the redesign of the active site structures for modification purposes. It also greatly enhances our basic understanding of enzyme binding and catalytic mechanisms, thus increasing the success of future enzyme engineering efforts and laying the foundation for functional prediction of new protein sequences in databases.

Although either directed evolution or rational redesign can be very effective, a combination of both strategies probably represent the most successful route to improving the properties and function of an enzyme. This Semi-rational protein design involves the identification of possible beneficial residues through computational analysis of a homology model or a crystal structure and the subsequent randomization of the selected positions.⁶⁶

1.5 Omnichange

Omnichange is a ligase-free and sequence independent multiple saturation mutagenesis method. It is cost-effective, robust and a fast method that allows simultaneous and efficiently saturation of up to five independent codons.⁶⁷ Furthermore, it is possible to show cooperative effects on desired enzyme characteristic by exploring novel combination of substitutions that may interact with each other.⁶⁸ The advantage of Omnichange is being an enzyme free method for DNA- modification such as restriction digestion and ligation of insert and plasmid DNA. It is fully sequence and fragment size-independent and generates libraries of high genetic diversity in a single PCR step.⁶⁷ The Omnichange multi-site-saturation method comprises four steps (Figure 3): Step 1: Vector and insert amplification by standard PCR with phosphorothiolated oligonucleotides (PTO) containing the degenerate (NNK) codons; Step 2: Iodine cleavage of PTO oligonucleotides in order to generate complementary 5'-overhangs; Step 3: Assembly of mutated plasmids via complementary DNA hybridization; and Step 4: Transformation of plasmid constructs in host organism.^{67,69}

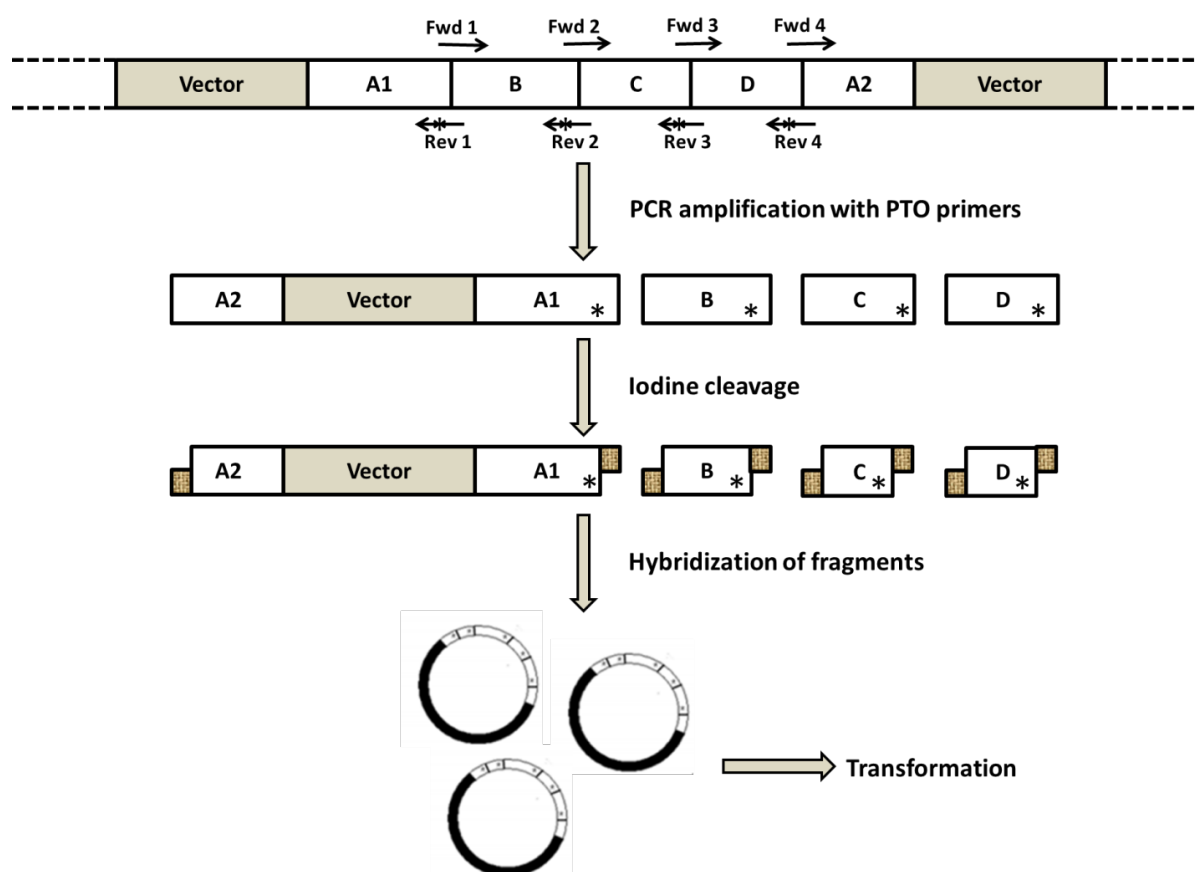


Figure 3. Schematic representation of steps involved in Omnichange multiple saturation mutagenesis method. Image has been adapted from reference ⁶⁷.

1.6 Arginine deiminase (ADI)

Arginine deiminase (ADI, EC 3.5.3.6) is an arginine degrading enzyme that catalyses the first step of the arginine dehydrolase pathway by the conversion of arginine to citrulline and ammonia. ADI is widely spread among prokaryotes with very few exceptions in eukaryotes. ADI was first reported in *Bacillus pyocyaneus* by F. Horn in 1933.⁷⁰ Since then several ADI genes have been characterized from many microorganisms such as *Pseudomonas aeruginosa*,⁷¹ *Mycoplasma arginine*,⁷² *Pseudomonas plecoglossicida*,⁷³ *Giardia intestinalis*,⁷⁴ *Hexamita inflata*,⁷⁵ *Trichomonas fetus*,⁷⁶ and *Trichomonas Vaginalis*.⁷⁷

Arginine deiminase has been studied as a potential anticancer drug for the treatment of arginine-auxotrophic tumors such as hepatocellular carcinomas (HCCs) and melanomas. Arginine is not considered as an essential amino acid for adult humans and is synthesized from citrulline using two enzymes, argininosuccinate synthetase (ASS) and argininosuccinate lyase (ASL). Cells that cannot express ASS can be sensitive to arginine-depleting enzymes such as arginine deiminase (ADI). Human melanoma and hepatocellular cell lines have been found to lack ASS expression and hence are auxotrophic for arginine. Amino acid depletion is one of the methods of treating certain cancers and studies have suggested that arginine depletion can be effective in treating these tumors.⁷⁸⁻⁸⁵ With the hydrolysis of arginine, ADI is able to exert antitumor activity because of its ability to deplete the nonessential amino acid arginine from human blood and other extracellular fluids and thus has a potential to be used as a therapy against arginine-auxotrophic tumors.

The first example of directed evolution of ADI from *Pseudomonas plecoglossicida* (PpADI, Figure 4a) by our group provides a simple and effective screening system to improve activity of PpADI at physiological pH. Within this system a microtiter plate (MTP) format calorimetric screening system based on citrulline detection with diacetyl monoxime (DAM) and thiosemicarbazide (TSC) was used (Figure 4b) leading to detection of improved ADI variants showing higher activity at physiological pH values.⁷³ Inspired by previous work within our group, we used PpADI and modified citrulline detection system within a whole cell format to identify FhuA variants showing preferential transport of enantiomers of arginine (D- or L-arginine).

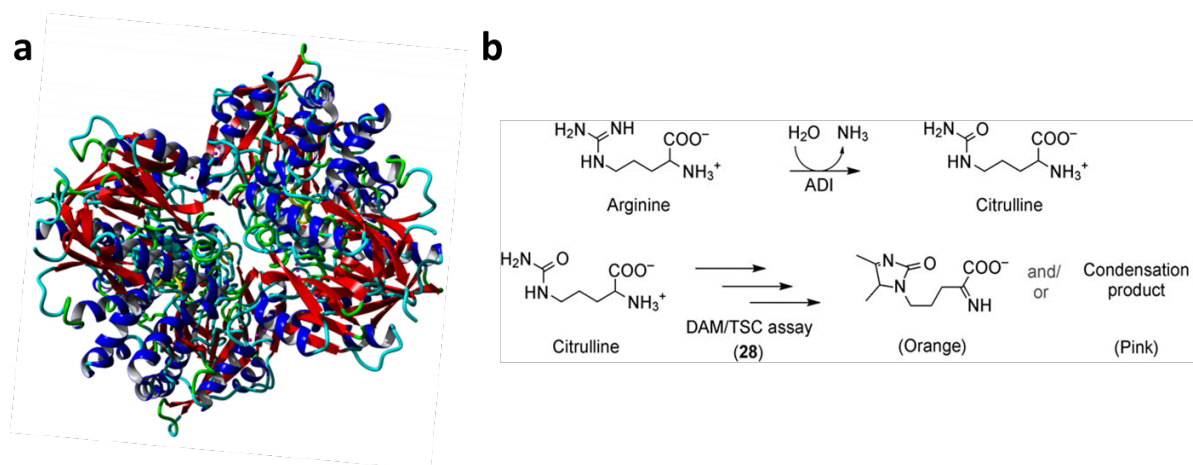


Figure 4. (a) Crystal structure of PpADI showing overview of its tetramer structure (PDB ID: 2A9G). **(b)** Scheme of the conversion of arginine by ADI and detection of citrulline using the DAM-TSC assay.

1.7 Pig kidney D-amino acid oxidase (pkDAO)

D-amino acid oxidase (EC 1.4.3.3., DAO, Figure 5) is a flavoprotein that catalyzes the oxidative deamination of D-amino acids to corresponding imino acids which is further hydrolyzed non-enzymatically to α -keto acid and ammonia.^{86,87} It is a flavin dependent oxidoreductase that acts on the CH-NH₂ group of D-amino acids with oxygen as an acceptor.⁸⁸ DAO exists as a dimer with each monomer containing a FAD binding domain (FBD) and a substrate binding domain (SBD).⁸⁹ After first identification of DAO by Krebs in 1935⁹⁰ in porcine kidney, many other DAO had been studied and characterized in a variety of species ranging from microorganisms to mammals. DAO plays an important role in microbial metabolism,⁹¹ regulation of the nervous system,^{92,93} utilization of endogenous D-amino acids,⁹⁴ and aging in mammals.⁹⁵⁻⁹⁷

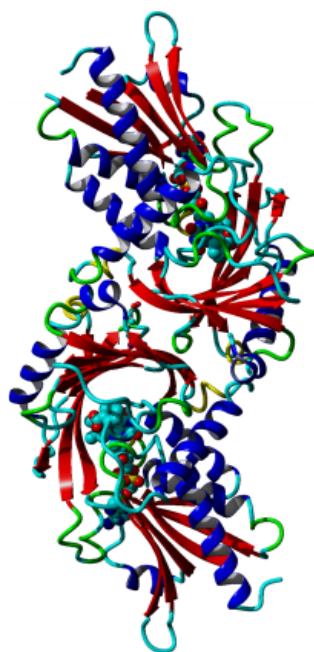


Figure 5. Crystal structure showing dimeric structure of pkDAO (PDB ID: 1VE9)

Within this thesis pig kidney D-amino acid (pkDAO) was used for characterization of FhuA variants for its enantiopreference. An engineered variant of pkDAO (222D 224G)⁹⁸ was chosen because of its activity towards D-arginine.

1.8 Liposomes and polymersomes

The cell is the basic structure of the biosystem consisting of a membrane which provides stable compartmentalization of various organelles performing different function for survival of life. Cell membrane has a basic structure consisting of phospholipids and embedded membrane proteins for the selective permeation of nutrient and ions.⁹⁹ Synthetic biology offers plenty of exciting and potential possibilities to mimic cell membrane and have a deeper insights and understanding to fundamentals of transport mechanism through nanochannels.^{44,100-103} In the interest of mimicking nature's compartmentalization strategies, forming vesicle structures, have gained tremendous attention because of the reaction space available in the interior of aqueous compartment and at the interface between membrane and the exterior. At the same time, vesicle membranes can enclose proteins and enzymes for a certain biochemical reaction and allow the communication with the exterior.¹⁰⁴⁻¹⁰⁶

One such artificial nanocompartment system is the liposomes. Liposomes are spherical vesicles composed of phospholipids bilayers.¹⁰⁷⁻¹⁰⁹ Similar to natural membranes, liposomes consists of a hydrophobic membrane compartmentalizing a hydrophilic environment. As a result liposomes can carry both hydrophobic molecules in its membrane and hydrophilic solutes inside the compartment. Liposomes can be used in delivery of hydrophilic drugs and nutrients which would normally not pass through hydrophobic membrane.¹¹⁰⁻¹¹⁴ But liposomes usually have shorter shelf life depending upon chemical compositions of lipids used for generation of liposomes. Additionally, liposomes are readily removed from blood circulation when used in a drug delivery system.¹¹⁵ Because of these drawbacks more stable alternative was required for these studies.

Polymersomes, like liposomes, are the family of artificial vesicles made of amphiphilic block copolymers.^{116,117} The polymer membrane provides a barrier between the compartmentalized compounds from external environment similar to lipid membrane in liposomes. However, the polymeric membrane of polymersomes provides more rigidity, stability and reduced permeability through the membrane.¹¹⁸

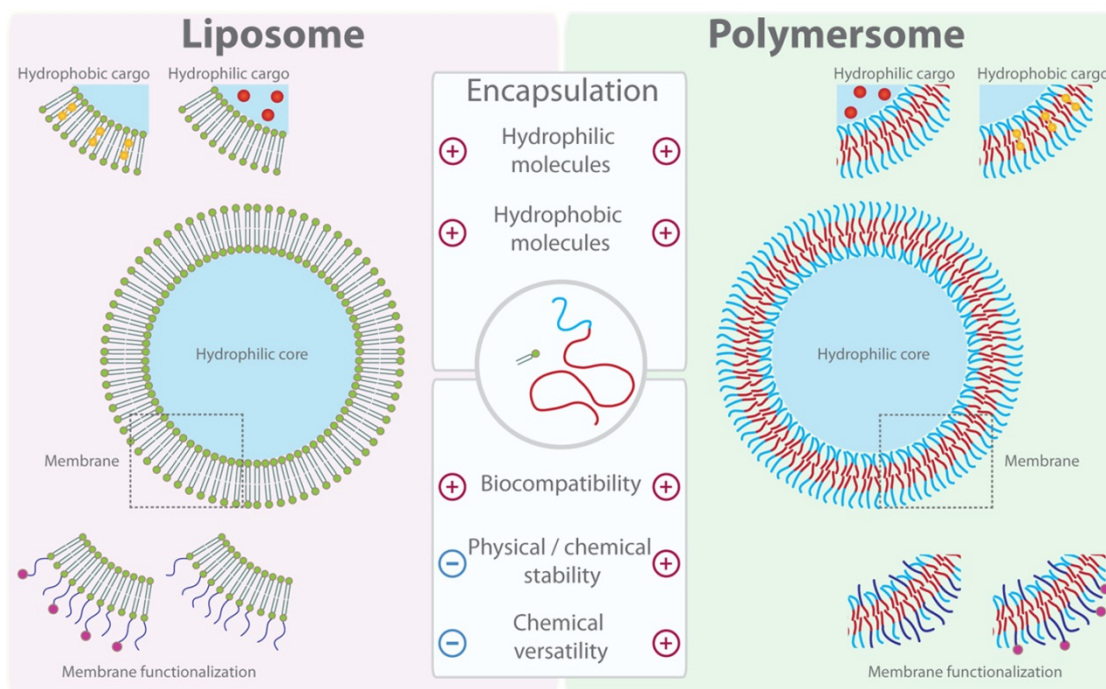


Figure 6. Schematic representation of liposomes and polymersomes. Adapted from reference¹¹⁹

Polymersomes have been successfully used to study membrane protein for their translocation properties in the form of synthosomes.^{27,32,120} Synthosomes are the polymersomes having a protein nanochannel inserted in its polymer membrane.²⁷ Protein nanochannel provides a passage for controlled translocation of certain compounds. Additionally, translocation of compounds can be altered by engineering the size of nanochannel.^{30,35} Onaca *et. al.* reported an exclusive translocation of calcein through an engineered transmembrane FhuA Δ 1-160 which had been embedded in a tri-block copolymer membrane PMOXA-PDMS-PMOXA; where PMOXA = poly(2-methyl-2-oxazoline) and PDMS = poly(dimethyl siloxane); and could be opened up through a reduction triggered system.³²

1.9 Detergents for membrane protein and use of 2-methyl-2,4-pentanediol (MPD) as refolding agent

Most common method for extraction of membrane protein is the use of detergents. The amphiphilic structure of detergent molecule consists of a hydrophilic head group connected to a hydrophobic alkyl chain which gives it the ability to solubilize hydrophobic molecules such as membrane proteins. The head group provides the molecule water solubility whereas the hydrophobic chain interacts with the hydrophobic residues of membrane proteins shielding them from water and lead to protein solubilization.¹²¹⁻¹²³

Free detergent molecules have limited solubility. Detergents exist as monomers in solution up to their critical micelle concentration (CMC). Exceeding CMC, detergent molecules self-assemble by orientating the hydrophobic chains together. The soluble structures called micelles remain in equilibrium with the remaining free detergent molecules. The number of detergent molecules forming a micelle is variable and depends on the size and charge of the head group and the length of the hydrophobic chain. The shorter the chain the lower is the number of molecules per micelle and vice versa.¹²⁴ Their amphiphilic properties allow detergents to solubilize embedded membrane proteins by disassemble membranes.^{121,122}

Sodium dodecylsulfate (SDS) are known to efficiently solubilize membrane proteins and belong to the group of ionic detergents with charged head group. But SDS usually has denaturing effect for solubilization of protein.¹²² In contrast to that, nonionic detergents are much milder. Commonly used are polyoxyethylene detergents as octyl-polyoxyethylene (oPOE) and also detergents with glycosidic head groups as n-dodecyl- β -D-maltoside (DDM).¹²⁵ The head groups of zwitter-ionic detergents have a positive and a negative charge resulting in a neutral net charge.

Detergents like oPOE, DDM and block-copolymers like PE-PEG have previously been used for successful refolding of FhuA.^{27,33,126,127} However, these molecules with longer chain length are not suitable within this work due to steric hindrances caused by shielding effects. These effects lead to coverage of exposed Lys residues, which are supposed to be nucleation sites for polymerization reaction. Therefore, in the present work a small water-miscible alcohol 2-methyl-2,4-pentanediol (MPD) was used for solubilization of FhuA. The amphipathic MPD is used as co-solvent as originally investigated by Michaux *et al.* to refold membrane proteins such as PagP and bacteriorhodopsin, which were denatured by SDS.^{128,129} Molecular dynamic (MD) simulations were performed in collaboration with Dr. M. Bocla (RWTH Aachen University, Institute of Biotechnology) to analyze the stabilizing effect of MPD on FhuA. MD simulations showed that MPD covers the hydrophobic region of the transmembrane protein FhuA in an average of around 200 molecules, broadly distributed in the range of about 150-300 molecules. Based on this a minimum of 10 mM MPD was obtained and five times excess was chosen for the

dialysis buffer to ensure a proper folding of FhuA. The stabilizing effect of MPD was proven by performing SDS extraction of FhuA in unfolded state followed by dialysis in refolding buffer containing MPD. The secondary structure was proven with CD spectroscopy and spectra of FhuA WT and the engineered variants show characteristic spectra of β -sheet proteins.¹³⁰

1.10 Objectives

The present thesis entitled '**Chiral separation of arginine based on tailor-made FhuA β -barrel protein**' focused on the engineering of the transmembrane protein FhuA for chiral separation of arginine enantiomers. This work provides the proof of principle for a long-term goal of using engineered membrane proteins for an application potential for the separation of other enantiomeric amino acids as well as further compound classes such as epoxides and amines. FhuA was chosen for this work because of its robustness (T_m 60.0-65.0°C and resistance against tetrahydrofuran up to 40.0 %), unique pore size (0.7-3.0 nm) and tolerance towards reengineering.

Main aim of this study was to generate a chiral selective nanopore from otherwise non (chiral) selective nanopore and to provide insight into the mechanism of chiral separation within the engineered nanopore. It is a well-known fact that interaction between a selector and a chiral compound enable chiral recognition. In order to develop a chiral recognition site within the FhuA channel a rational protein engineering approach was developed. Two selectivity filter regions within FhuA WT were generated by deletion of two short loops within the cork domain of FhuA providing a channel for translocation and interaction points for chiral resolution of arginine enantiomers. Additionally, OmniChange mutant libraries were generated to impart enantioselectivity within the selectivity filter regions. For investigation of amino acid binding to the engineered FhuA interior a screening system was necessary, in which the engineered FhuA channels were presented in their natural environment. Therefore, a whole cell screening system with amino acid utilizing enzymes produced inside the cell was investigated to identify selective variants.

Based on the identified variants from screening system, a deeper understanding of translocation mechanism was aimed to provide insight and knowledge about the mechanism of chiral discrimination performed by engineered channel. For this purpose, steered molecular dynamics (SMD) simulations were aimed to be carried out for molecular understanding of observed altered enantiopreference of identified variant towards arginine enantiomers.

The mentioned approach faces the main challenges of designing of filter regions and generation of screening system for identification of chiral channel proteins. The results and gained knowledge from present thesis provide the proof of principle for utilization of membrane protein towards new application of chiral separation. It is likely that with the identified filter region and mutant libraries further improvements are achievable for other amino acids and a broader range of enantiomers. The chiral FhuA channel proteins would be an excellent scaffold for generation of chiral membrane based on protein polymer conjugates with a high potential for novel and scalable downstream processes.

2 Computational analysis based engineering of FhuA WT for generation of selectivity filter regions

Interaction between a selector and a chiral compound can enable chiral recognition. A rational protein engineering approach was chosen for generation of selectivity filter regions in the interior of FhuA WT. This work was performed in collaboration with Dr. M. Bocola, RWTH Aachen University, Institute of Biotechnology.

2.1 Computational identification/selection of loops to be shortened for generation of filter regions

2.1.1 Identification of loops

The starting coordinates of FhuA was downloaded from protein data bank (PDB ID: 1BY3¹³¹). The respective loop residues to be deleted within the cork domain were selected on a structural basis, to create a cavity within the water channel visually identified from the X-ray structure of FhuA with bound crystal waters. Water channel was visually inspected using YASARA Structure Version 17.8.9¹³² and two loops (residues 35-40 and 135-145) hindering the flow of water within the cork domain were identified. The selected residues were computationally deleted and the fragments of the cork domain were manually rejoined. Thereafter all structures were relaxed by several rounds of steepest descent minimization and simulated annealing. Afterwards, the structure was initially minimized using first steepest descent without electrostatics to remove steric clashes and subsequently relaxed by steepest descent minimization and simulated annealing from 298 K (time step 2 fs, atom velocities scaled down by 0.9 every 10th step) until convergence was reached, i.e. the energy improved by less than 0.05 kJ/mol per atom during 200 steps.

2.1.2 Rational prediction for stabilization of the cork domain

The stabilizing substitutions to increase the interaction between cork and barrel domain of FhuA was predicted by employing the FoldX method in YASARA software.¹³³ The starting coordinates for the FoldX *in silico* mutagenesis experiment were taken from the X-ray structure of the FhuA protein (PDB ID: 1BY3¹³¹). A FoldX mutation run including rotamer search, exploring alternative conformations (3 independent runs) were performed during the FoldX energy minimization employing a probability-based rotamer library. Stabilization energy calculations (defined as the difference in free energy ($\Delta\Delta G$) given by $\Delta G_{\text{variant}} - \Delta G_{\text{wt}}$) were computed with FoldX version 3.0 Beta¹³³ using default settings. For the stabilizing of the cork domain of the generated loop variants, all residues at the inner interface located between barrel and cork-domain were investigated by full computational saturation mutagenesis utilizing FoldX and the best three variants with highest stabilization energy $\Delta\Delta G > 1\text{ kcal/Mol}$ and largest distance from the

generated loop cavity were selected. These substitutions were performed by site directed mutation (SDM) to generate variant FhuA Δ L.

2.1.3 Steered molecular dynamic (SMD) simulations of FhuA WT and FhuA Δ L variant

A SMD simulation protocol was developed for diffusion of D- and L- arginine through the channel of FhuA WT, FhuA Δ L, and FhuA Δ 1-159 variants. These variants were generated *in silico* within YASARA Structure version 17.8.9¹³² based on the crystal structure of FhuA WT (PDB ID: 1BY3¹³¹). The D- and L- arginine was placed above the channel entrance of these variants, respectively. For the pulling of arginine from the top of the FhuA channel, D487 located at the bottom of the FhuA channel was defined as an end point. The size of the simulation box was 100.39 x 76.00 x 61.16 Å with alpha = 90.00, beta = 90.00 and gamma = 90.00. AMBER03 force field¹³⁴ was applied at a temperature of 298 K. During SMD simulations, distances of the arginine and the end point (D487) were analyzed. A pulling force of 5000 pm/ps² on the transported arginine was applied per time step as implemented in YASARA steered MD macro. The arginine was passed through the channel and the selectivity filter regions, which was monitored by time recorded with md_runsteered.mcr script within YASARA.

2.2 Result and discussion

2.2.1 Generation of filter regions

FhuA WT in its natural state consists of an N-terminal cork domain which occludes the channel. Engineering campaign in past decade has led to generation of different variants of FhuA with different applications. An open passive diffusion channel was generated by removing pore-blocking domain by deletion of the 159 N-terminal amino acids (FhuA Δ 1-159).¹²⁶ FhuA Δ 1-159 has been investigated in stability studies as well as the translocation of single-stranded DNA through FhuA by inserting into artificial membranes.^{135,136} Further modifications such as the insertion of a free accessible Cys (D501F, K545C, N548V; amino acid numbering according to FhuA WT PDB ID: 1BY3) led to the generation of a catalytically active channel (FhuA Δ CVFtev).^{37,137} For the aim of the present thesis, engineering of FhuA WT channel was performed in order to generate a small channel and selectivity filter region in FhuA.

Water channel within FhuA was visually inspected using YASARA Structure Version17.8.9 and two loops (loop 1: residues 35-40 and loop 2: residues 135-145) hindering the flow of water within the cork domain were identified (Figure 7). The respective loop residues to be deleted within the cork domain were selected on a structural basis, to create a cavity within the water channel visually identified from the X-ray structure of FhuA WT (PDB ID: 1BY3) with bound crystal waters. FhuA WT based loop deletion variant was generated to create a small cavity and steered molecular dynamics simulation was performed with FhuA WT, FhuA Δ L and FhuA Δ 1-159 (FhuA variant with a passive diffusion channel).¹²⁶ In a simulation box, the D-/L-arginine was placed at the tunnel entrance and a constant force along the diffusion path through FhuA passing the selectivity filter regions (indicated with two circles in blue and green) near loop 1 and loop 2 was applied during steered MD simulation using AMBER99 force field at 298K. The simulation results indicated no diffusion of arginine enantiomers through FhuA WT whereas diffusion of arginine was observed through FhuA Δ L which is controlled by a longer residence time in the two selectivity filter regions near the engineered loop 1 and 2 (Figure 8).

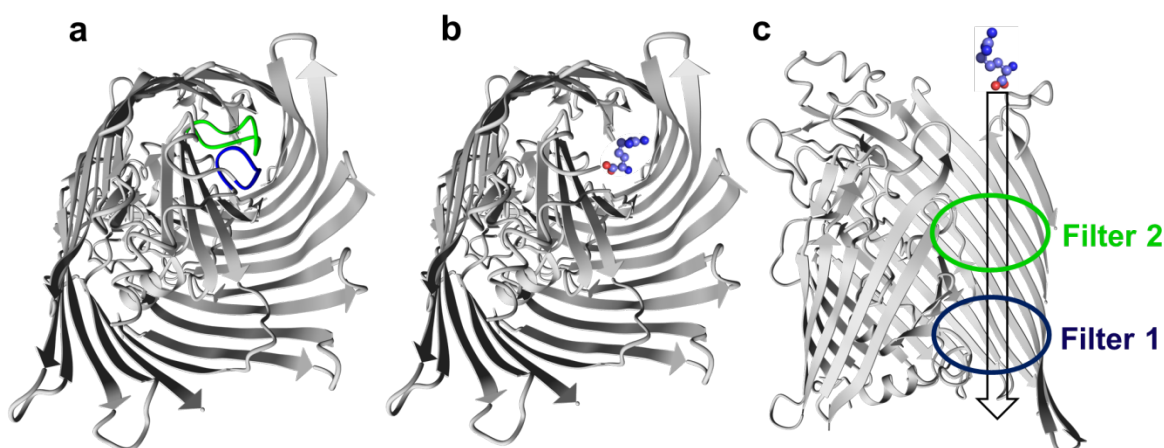


Figure 7. Identification and shortening of loops (1 and 2) to generate two filter regions (1 and 2) in FhuA WT (PDB ID: 1BY3¹³¹). **(a)** Position of two identified loops in FhuA WT (loop 1: blue; loop 2: green). **(b)** FhuA loops shortened variant (FhuAΔL) accommodating an arginine molecule (ball and stick representation). **(c)** Side view of FhuAΔL showing transport path of D-/L-arginine (indicated by an arrow) along the selectivity filter regions (green and blue circles) generated by shortening of loop 1 and loop 2. (Reprinted figure with permission of RSC)¹³⁸

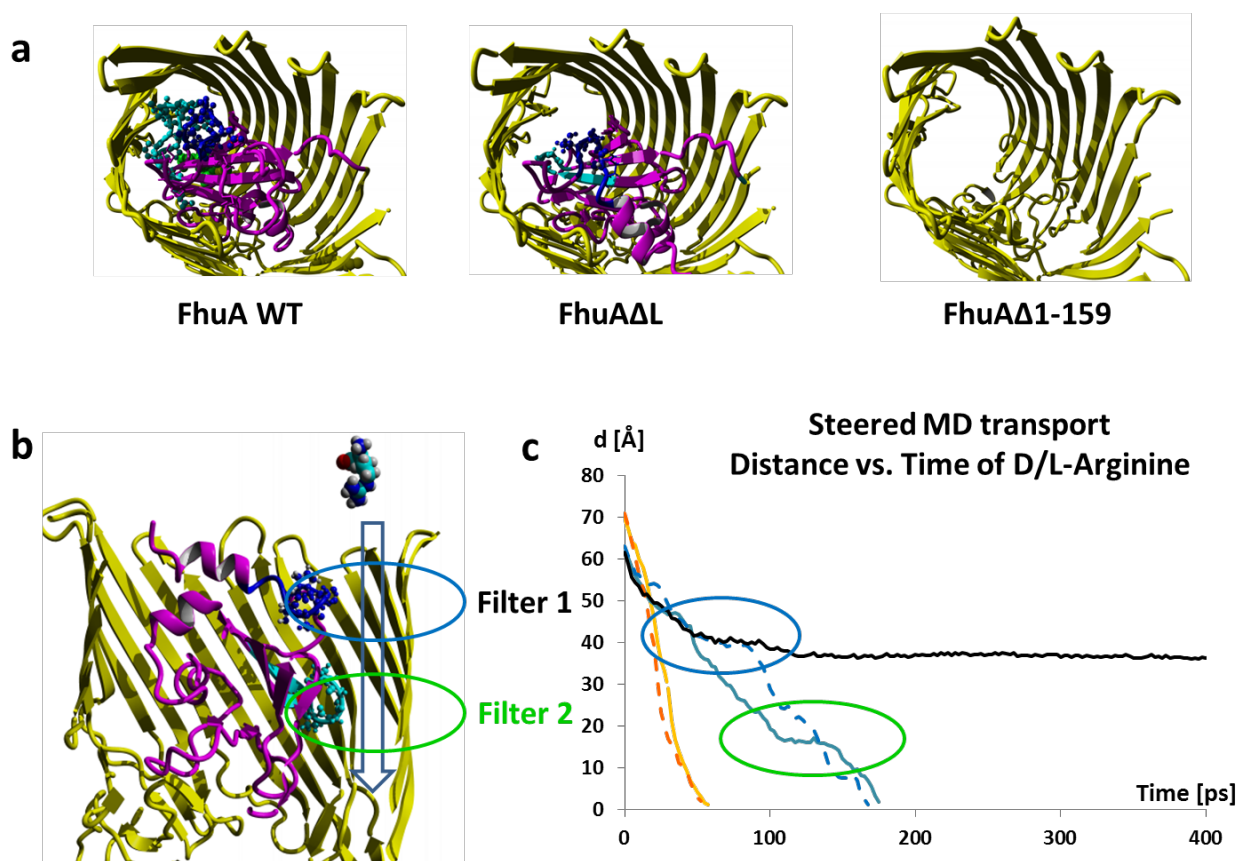


Figure 8 **(a)** Top view of FhuA WT, FhuAΔL and FhuAΔ1-159 showing the difference in channel diameter of different variants. **(b)** The path for the steered MD simulation is indicated by an arrow, encircling the two selectivity filter regions generated by deletion of loop 1 and 2. **(c)** The diffusion time for D-/ L-arginine along the simulation path at constant force is shown for FhuA WT (black); FhuAΔL (blue); L-arginine (solid line); D-arginine (dotted line).

2.2.2 Stabilization of cork domain at identified positions with site directed mutagenesis (SDM)

In *E. coli*, transport of iron in the form of siderophore occurs through the FhuA channel. Transport from outside to inside of cell is a dynamic process which involves conformational changes in FhuA.¹³¹ In order to avoid fluctuations of cork domain during transport of compound, new interaction points were introduced within the barrel and cork domain of FhuA. For the

identification of stabilizing amino acid substitutions within FhuA WT *in silico* prediction of Gibbs free energy ($\Delta\Delta G$) was calculated. YASARA Structure Version17.8.9 was used for the generation of structural models of the FhuA WT with the YASARA-FoldX plugin and FoldX method.¹³³

The importance of the interactions that contribute to the stability of protein variants was estimated quantitatively by determination of the difference in folding free energy upon substitutions compared to FhuA WT ($\Delta\Delta G = \Delta G(\text{variant}) - \Delta G(\text{WT})$). These substitutions were selected on the basis of stabilization energy ($\Delta\Delta G$) values and the distance of these stabilizing substitutions from the generated filter regions. For the stabilizing of the cork domain, all residues at the inner interface located between barrel and cork-domain were investigated by full computational saturation mutagenesis utilizing FoldX. A substitution is likely beneficial for improving stability of FhuA WT if the change in the Gibbs free energy ($\Delta\Delta G$) is decreased (Figure 9).

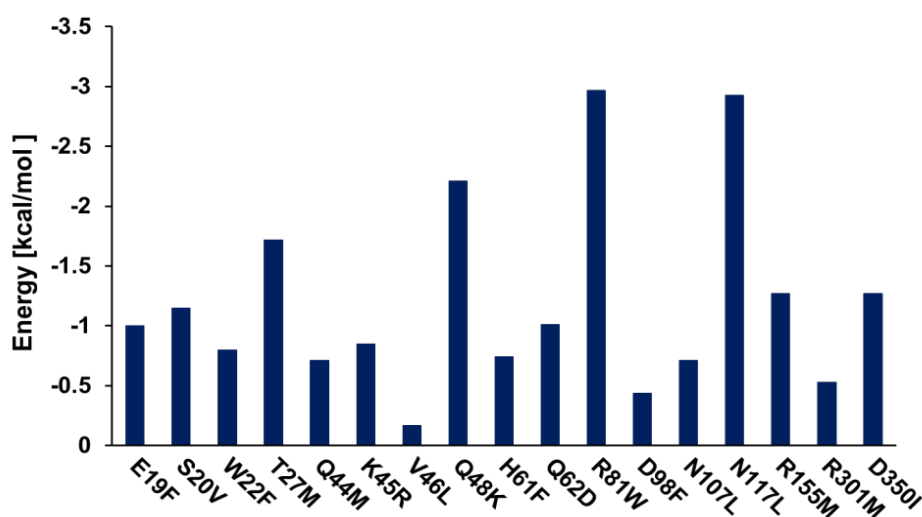


Figure 9. Calculated stabilization energy ($\Delta\Delta G$) of the substitutions using FoldX method¹³³. Three amino acid substitutions (Q62D, R81W, N117L) were identified to enhance the interactions between the cork domain and the β -barrel domain. These substitutions were chosen based on the highest stabilization energy and largest distance from generated filter regions. (Reprinted figure with permission of RSC)¹³⁸

To find the most contributing positions, we exchanged each position with all 20 amino acids. Three substitutions (Q62D, R81W, and N117L) were selected based on stabilization energy ($\Delta\Delta G < -1$ kcal/mol) and largest distance from the generated filter region to enhance the interactions between the cork domain and the β -barrel (**Figure 10**).

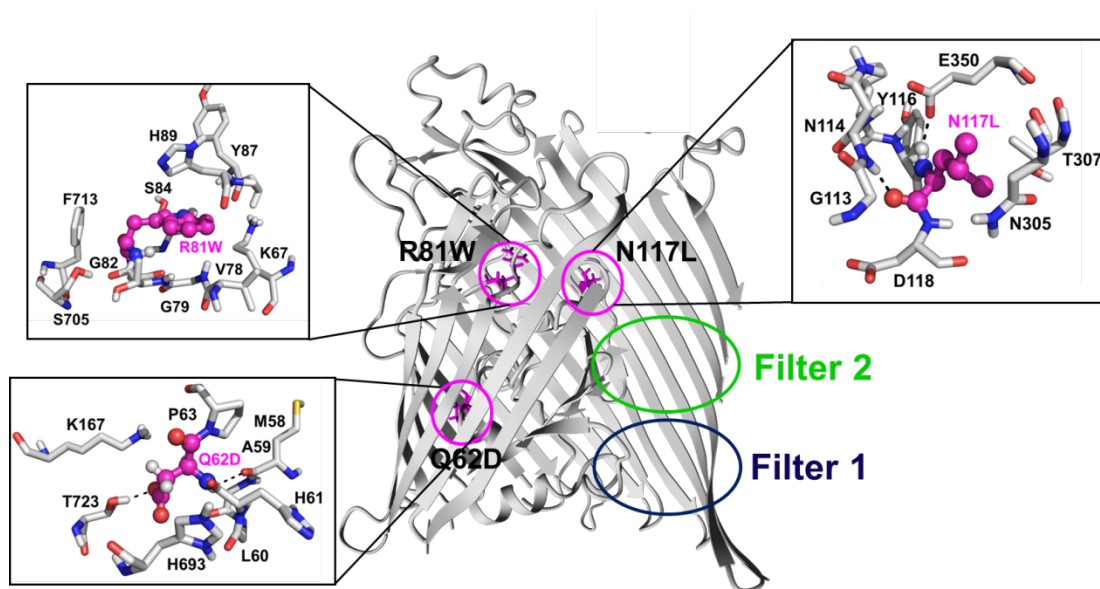


Figure 10. Side view of FhuAΔL. FhuAΔL showing selectivity filter regions 1 and 2 (blue and green circles) and the stabilizing substitutions (magenta sticks) identified by FoldX analysis. Inset showing location and interactions of selected amino acid substitutions (Q62D, R81W and N117L) within FhuA. (Reprinted figure with permission of RSC)¹³⁸

2.3 Experimental section

All used chemicals in this section were of analytical reagent grade or higher quality, purchased from Applichem (Darmstadt, Germany), New England Biolabs (Ipswich, USA) or Sigma-Aldrich Chemie (Taufkirchen, Germany), if not stated otherwise.

The buffer used for refolding of FhuA consisting of 10 mM sodium phosphate, 50 mM MPD, 1 mM ethylenediaminetetraacetic acid (EDTA), pH 7.4 and is termed as MPD buffer in the following sections.

Thermal cycler (Mastercycler gradient; Eppendorf, Hamburg, Germany) and thin-wall polymerase chain reaction (PCR) tubes (Multi-ultra tubes; 0.2 mL; Carl Roth, Germany) were used in all PCRs. The amount of DNA in cloning experiments was quantified by using a Nano-Drop photometer (NanoDrop Technologies, Germany).

2.3.1 Cloning of gene encoding FhuA WT and generation of FhuA Δ L variant

Target gene

FhuA WT (PDB ID: 1BY3) gene in pPR-IBA1 plasmid was obtained from strain collection of our lab. The gene encoding for FhuA WT was used as starting point for investigation in this work.

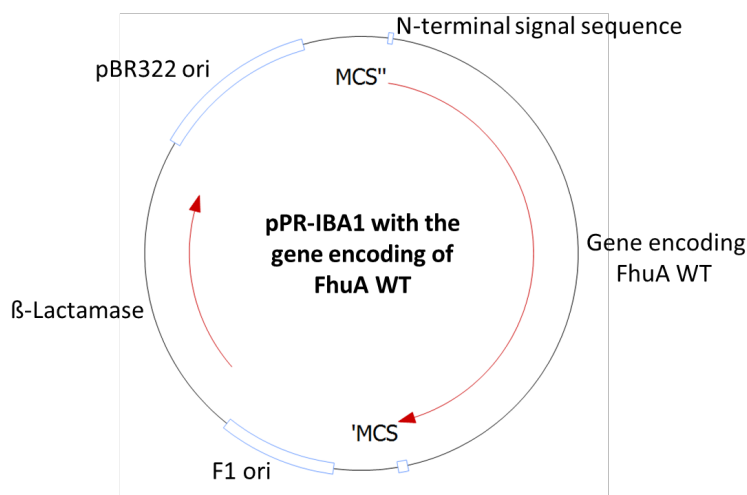


Figure 11. Vector map of FhuA WT gene in pPR-IBA1 plasmid.

Bacterial strains

All bacterial strains and plasmids used in this section are given in Table 1. The strain *E. coli* DH5 α was used for generation of high copy numbers of respective plasmids and *E. coli* BE BL21 (DE3) omp8 (*E. coli* omp8) strain was used as an expression strain.

Table 1. Summary of bacterial strains used in this part of thesis

Bacterial strain	Genotype	Function
<i>E. coli</i> DH5 α	F-mcrA Δ (mrr-hsdRMS-mcrBC) endA1 recA1 s ϕ 80dlacZ Δ M15 Δ lacX74 araD139 Δ (ara,leu)7697 galU galK rpsL nupG λ tonA	Plasmid construction and amplification
<i>E. coli</i> BE BL21 (DE3) omp8 (<i>E. coli</i> omp8) strain	F- <i>hsdSB</i> (rB- mB-) <i>gal ompT dcm</i> (DE3) Δ <i>lamB ompF::Tn5 Δ<i>ompA</i> Δ<i>ompC</i></i>	Expression strain

Primers

Following tables shows the list of primers used for shortening of loops and anchoring of cork domain in FhuA WT. All primers were ordered in a salt-free form Eurofins MWG Operon, Ebersberg, Germany.

Table 2. Sequences of the primers used for shortening of loops in cork domain and generation of filter regions in FhuA WT.

Primer name	Sequence (5' \rightarrow 3')	GC (%)	T _m (°C)
loop 1 del_Fwd	CGCGACAGTCTGCTACGCCGATTCAAAAAG	53.1	64.5
loop 1 del_Rev	CTGTGGCACTTTTGAATCGGCGTAGCAGA	50.5	63.3
loop 2 del_Fwd	CGCTGAAATTATGCGTGGCGGCGGCTGTT	60.8	67.8
loop 2 del_Rev	GCTGACCATATTCAACAGGCCGCCGCCACG	63.2	68.7

Table 3. Sequences of the primers used to perform site directed mutagenesis for stabilization of cork domain. Bold letters represents substitution codon.

Targeted mutations	Oligoname	Sequence	GC (%)	T _m (°C)
Gln (62) \rightarrow Asp	G62D_Fwd	GAGATGGCGCTGCAT GAC CCGAAGTCGGTAAAAGAAGC	55.3	68.3
	G62D_Rev	GCTTCTTTTACCGACTTCGG GTC ATGCAGCGCCATCTC	55.3	68.3
Arg (81) \rightarrow Trp	R81W_Fwd	GTCTCTGTTGGTAC GTG GGGCGCATCCAACACC	60.6	68.7
	R81W_Rev	GGTGTTGGATGCGCC CC ACGTACCAACAGAGAC	60.6	68.7
Asn (117) \rightarrow Leu	N117L_Fwd	GCAGGGCAACTTCTAT CTC TGATGCGGTCATTGACC	55.6	67.5
	N117L_Rev	GGTCAATGACCGCATCG AG ATAGAAGTTGCCCTGC	55.6	67.5

Media and buffer

Table 4. Summary of media and buffer in this part of thesis

Media/Buffer	Components
LB media	5 g/L yeast extract, 10 g/L trypton, 10 g/L NaCl
LB plates	5 g/L yeast extract, 10 g/L trypton, 10 g/L NaCl, 15 g/L Agar
TY media	5 g/L yeast extract, 10 g/L trypton, 5 g/L NaCl
SOC media	2 % trypton, 0,5 % yeast extract, 10 mM NaCl, 2.5 mM KCl, 10 mM MgCl ₂ , 10 mM MgSO ₄ , 20 mM glucose
TFBI buffer	pH = 5.8, 30 mM KAc, 50 mM MnCl ₂ , 100 mM RbCl ₂ , 10 mM CaCl ₂ , 15 % (w/v) glycerol
TFBII buffer	pH = 6.8, 10 mM MOPS, 75 mM CaCl ₂ , 10 mM RbCl ₂ , 15 % (w/v) Glycerol,
Tris-KCl buffer	pH 7.4, 10 mM Tris-HCl, 100 mM KCl,

2.3.1.1 Cloning of pPRIBA1_FhuA WT in expression strain

For plasmid isolation cells were cultivated in Luria Broth (LB) medium supplemented with the ampicillin (100 µg/ml final concentration). Cultivation was done overnight at 37°C, 250 rpm, 4 ml/glass vial with metal cap, 16-18 h (Minitron, Infors AG, Bottmingen, Switzerland). Overnight grown cells were harvested in 1.5 ml reaction tubes and pPR-IBA1 plasmid containing FhuA WT genes was isolated from *E. coli* DH5α cells using NucleoSpin Plasmid isolation kit (Machery and Nagel). Isolated plasmids from *E. coli* DH5α cells were stored at -20°C until transformation into *E. coli* omp8 strain for expression or to use as template for shortening of loops for generation of filter regions. Chemically competent cells were used for transformation into *E. coli* DH5α cells as well as *E. coli* omp8 cells, which were prepared in-house with the rubidium chloride method.

2.3.1.2 Channel generation in FhuA WT

The identified loops predicted to open up a small channel in FhuA WT (loop 1: 35-40 and loop 2: 135-145) were shortened by PCR using two set of primers (Table 2). Primer pairs (loop 1 del_Fwd and loop 1 del_Rev) were used to shorten loop 1 and primer pairs (loop 2 del_Fwd and loop 2 del_Rev) were used to shorten loop 2. Shortening of loops was done in two steps. In first step loop 1 was shortened and the PCR product of first round was used as templet for second round of loop shortening using second set of primers. Conditions used for PCR is given in the Table 5 and 6. The final PCR products were digested (20 U *DpnI*: 16 h, 37°C), purified using PCR cleanup kit (Macherey-Nagel) and transformed into *E. coli* Omp8 competent cells. The extraction of the plasmid was performed with the NucleoSpin Plasmid DNA Purification Kit (Macherey-Nagel GmbH & Co. KG, Düren, Germany). The plasmid DNA was eluted by adding

30 μ L distilled water. The concentrations of the plasmids were measured by Nano Drop 2000 spectrophotometer (Thermo Fisher Scientific Inc., Rockford, USA). Deletion of loops was subsequently verified by sequencing.

Table 5. Composition of standard reaction mixture for shortening of both loops in FhuA WT.

PCR components	Amount
PfuS DNA polymerase buffer (10X)	5 μ l
Plasmid template DNA	15-20 ng
dNTP mix	0.2 mM
Forward primer	0.4 μ M
Reverse primer	0.4 μ M
PfuS DNA polymerase	2 U
ddH ₂ O	Up to 50 μ l

Table 6. General PCR conditions used for shortening of both loops in FhuA WT. 25 cycles of PCR extension were used for amplification. Any difference in conditions is given in the text (if any).

Step	Temperature (°C)	Time
Initial denaturation	98	2 min
Denaturation	98	30 sec
Annealing	60	45 sec
Extension	72	5 min
Final extension	72	10 min

2.3.2 Production of FhuA WT and FhuA Δ L

2.3.2.1 Preparation of chemical competent cells and transformation

To prepare *E. coli* chemical competent cells, 20 mL pre-cultures (LB-medium) in 100 mL flask with single *E. coli* colony were incubated at 37°C (CERTOMAT RM, 250 rpm, 37°C, Sartorius AG, Goettingen, Germany) overnight. OD₆₀₀ of samples was measured and main-culture (200 mL in 1 L flask) was started to culture at 37°C with a start OD₆₀₀ of 0.1 by dilution of pre-culture. The main-cultures were grown to an OD₆₀₀ of 0.4 and then cooled down on ice. The cells were collected by centrifugation (Eppendorf centrifuge 5810R, A-4-81, 1258 g, 4°C, 15 min, Eppendorf, Hamburg, Germany). The supernatant was discarded and the pellet was resuspended in cooled TFB I buffer (pH 5.8, 30 mM potassium acetate, 100 mM RbCl₂, 10 mM CaCl₂, 50 mM MnCl₂, 15 % (v/v) glycerol) by gently pipetting on ice. The suspended solution was centrifuged (Eppendorf centrifuge 5810R, A-4-81, 1258 g, 4°C, 15 min, Eppendorf, Hamburg, Germany). The supernatant was discarded and the pellet was resuspended in TFB II buffer (pH 6.5, 10 mM MOPS, 75 mM CaCl₂, 10 mM RbCl₂, 15 % (v/v) glycerol). Aliquots of 100 μ L were frozen in liquid nitrogen and stored at -80°C. Transformation was performed by heat shock method. 100 μ L *E. coli* chemical competent cells were incubated with the plasmid on ice

for 5 min. After heat shock at 42°C for 45 s, the cells were put back on ice for 5 min. 1 mL SOC medium was added and the cells were incubated for 40 min (CERTOMAT RM, 250 rpm, 37°C, Sartorius AG, Goettingen, Germany). Finally, the transformed cells were transferred to LB agar plate containing respect antibiotics and cultivated overnight at 37°C (CERTOMAT RM, 250 rpm, 37°C, Sartorius AG, Goettingen, Germany).

2.3.2.2 Expression of FhuA WT and FhuA Δ L

E. coli BE BL21 (DE3) Omp8 cells were used as a host for expression of FhuA WT and variant FhuA Δ L. Precultures were grown overnight in LB media supplemented with 0.1 mM ampicillin (30°C, 250 rpm, 20 ml/ 250 ml shaking flask). Cell density was analyzed after overnight cultivation. Main-culture was grown in TY media with supplementation of 0.1 mM ampicillin. Inoculated of main culture was done with the preculture to obtain an initial OD₆₀₀ of 0.1 and incubated (37°C, 250 rpm, 200 ml/1 l shaking flask) until OD₆₀₀ of 0.6-1.0 was reached. Expression was induced by addition of isopropyl- β -D-1- thiogalactopyranoside (IPTG, final concentration of 1 mM). Culture incubation was continued for 16-18 h. Afterwards, cells density was analyzed, cells were harvested (4°C, 3,220 g, 20 min; centrifuge 5810R, rotor A-4-81, Eppendorf, Hamburg, Germany) and cell pellets stored at -20°C until FhuA extraction was carried out. Expression was monitored by sodium dodecyl sulfate-polyacrylamide gel electrophoresis (SDS-PAGE, 10 % acrylamide) and apparent molecular weights were compared to pre-stained marker (#SM0671, Fermentas). For SDS-PAGE analysis, 1 ml culture of an OD₆₀₀ of 1 taken before (BI) and after induction (AI) were pelleted and supplemented with lysis buffer (1 % SDS, 0.2 M EDTA, 20 mM Tris-HCl, pH 8). Cells were lysed using amplitude of 65 % for 45 sec (VibraCell VCX-130, SONICS, Newtown, USA). Subsequently, samples were supplemented with four times loading dye (200 mM Tris-HCl, 40 % glycerol, 8 % SDS, 400 mM dithiotreitol, 0.4 % bromophenol blue, up to 15 ml ddH₂O) and samples were heated at 95°C for 10 min (Thermostat, Eppendorf, Hamburg, Germany). Samples were electrophoretically separated on 10 % polyacrylamide gels (100 V, 18 mA per gel, 50 W, 1 h, Mini-PRO TEAN® Electrophoresis System-Bio-Rad, München, Germany). Thereafter, gels were stained with Coomassie brilliant blue (CBB) for 5-10 min. Destaining was performed with either destaining solution for 2 h (30 % ethanol, 10 % acetic acid, 60 % MilliQ water) followed by storage in storage solution for 16-18 h (10 % acetic acid, 90 % MilliQ water).

2.3.2.3 Extraction of FhuA WT and FhuA Δ L

Pellet obtained after successful expression of FhuA WT and FhuA Δ L were used for extraction using SDS extraction protocol. Pre-extraction was performed in MilliQ water using a high pressure homogenizer for cell disruption (three times 1300 bar, EmulsiFlex®-C3, Avestin, Ottawa, Canada) as previously reported.¹³⁵ SDS was used as solubilizing agent according to Philippart *et al.* in a low concentration of 0.1 % (w/v) to remove membrane bound impurities from the pre-extracted pellet.³⁷ After incubation for 1 h in 0.1 % SDS and following ultracentrifugation (Beckman Coulter XPN-80, rotor 70.2 Ti, 29,500 g, 45 min), the obtained

pellet was resuspended with 1.25 % (w/v) SDS solution to isolate the transmembrane protein FhuA. The FhuA containing supernatant was obtained by ultracentrifugation (Beckman Coulter XPN-80, rotor 70.2 Ti, 118,000 g, 20 min) and analyzed by SDS-PAGE (Figure 14) and protein concentration determined by bicinchoninic acid assay (BCA, Thermo Fisher Scientific, Rockford, USA). For long-term storage of extracted FhuA, samples were lyophilized and stored at -20°C before refolding was performed.

2.3.2.4 Refolding of FhuA WT and FhuA Δ L

FhuA variants were refolded either directly after extraction with SDS or after lyophilization by dialyzing two times for 24 h against 10 mM sodium phosphate pH 7.4, 50 mM MPD and 1 mM EDTA (MPD buffer) including a buffer exchange after the 24 h (dialysis membrane, molecular weight cut-off (MWCO) of 12-14 kDa, Spectral/POR, Spectrum Laboratories, California, USA). Samples were stored at 15°C after refolding until further used. During extraction and refolding steps, samples were taken at different steps and analyzed by SDS-PAGE, BCA assay (Pierce™ BCA Protein Assay Kit, Thermo Fisher Scientific, Darmstadt, Germany) and CD spectroscopy for monitoring extraction process. For electrophoretic analyses, FhuA extraction and refolding samples were supplemented with four times loading dye. Subsequent procedure is the same as for expression sample as outlined in the previous section. For CD analyses, FhuA samples were normalized to concentration of 0.4 mg/ml. A quartz cuvette with a path length of 0.5 mm (Hellma® SUPRASIL cuvette, Hellma GmbH & Co. KG, Mülheim, Germany) was used to obtain CD spectra at room temperature on Olis SDM 17 (Olis, Bogart, USA, software Olis GlobalWorks version 4.7.40). The following parameters were applied for all CD spectroscopy measurements: bandwidth of 2 nm, data pitch of 1 nm, integration time of 1 sec and scan speed of 20 nm/min. Three spectra were analyzed, averaged and Savitzky-Golay filter was used for smoothening (Figure 16).¹³⁹

2.3.3 Calcein release assay

2.3.3.1 Polymersome preparation with entrapped calcein.

ABA tri-block copolymer poly(2-methyloxazoline)–poly(dimethylsiloxane)–poly(2-methyloxazoline) (PMOXA–PDMS–PMOXA; Mn X 103: 1.2-4.8-1.2) was used to generate polymersomes using direct dispersion method.^{27,120} 10 mg polymer was dissolved in 1 mL of 50 mM calcein solution dissolved in Tris buffer (10 mM Tris, 100 mM KCl, pH 7.4) by gently stirring (Cimarec i Poly 15 and Multipoint Stirrers, 300 rpm, Thermo Scientifics, MA, USA) at room temperature in darkness. The obtained solution was sonicated twice (Sonics vibra cell VCX130, 40 % power, 1 min, Sonics & Materials, Inc., Connecticut, USA) with 15 min interval stirring followed by 10 times freeze-thaw cycles. Afterwards, generated polymersomes were subjected to freeze thaw cycles by freezing in liquid nitrogen for 3 min and heating at 60°C for 3 min. Unilamellar vesicles were obtained by extrusion 4-6 times (Avanti polar lipids extruder, Alabama, USA) through 0.2 μ m filter membrane (Millipore) using 2 ml syringe. Polymersomes

with encapsulated calcein (50 mM) were collected by performing size exclusion chromatography through a sepharose 6B column (Sigma-Aldrich Chemie, Steinheim, Germany).

2.3.3.2 Insertion of FhuA variants

Extracted and refolded FhuA samples were diluted in FhuA refolding buffer (10 mM sodium phosphate buffer, 50 mM 2-methyl-2,4-pentandiol (MPD), 1 mM EDTA, pH 7.4) to get final concentration of 3.91 μ M. 50 μ L of prepared polymersomes was supplemented with 150 μ L Tris buffer (10 mM Tris, 100 mM KCl, pH 7.4) in black microtiterplate and measurement were taken with Tecan infinite M200 Pro (Tecan Group AG, Zürich, Switzerland). The release of calcein was determined by applying the following settings: number of cycles: first 15 cycles and then 45 cycles, shaking: 3 sec, number of flashes: 10, integration time: 20 μ s, manual gain: 49, excitation: 495 nm, emission: 525 nm. After the first 15 cycles without addition FhuA samples, 3.91 μ M of FhuA WT and FhuA Δ L were separately added stepwise in 10 μ L batches (after every 45 cycles) to the polymersome suspension and the fluorescence increase was recorded at 520 nm.

2.4 Result and discussion

In order to generate an enantioselective FhuA channel, a small cavity need to be generated within FhuA with stabilized cork domain inside the barrel. In the following section, expression and purification of the starting variant FhuA WT and the derived variants FhuA Δ L are described. Afterwards, calcein release study was performed to analyze the stability of cork domain.

2.4.1 Channel generation in FhuA WT and stabilization of cork domain

Through computational analysis two loops were identified in the water channel of FhuA WT. These two loops (residues 35-40 in loop1 and residues 135-145 in loop2) in the cork domain of FhuA WT were shortened using the primer pair given in Table 2. pPR-IBA1_FhuA WT was used as a template plasmid with *fhuA* gene in it. Figure 12 shows the successful shortening of these two loops from FhuA WT analyzed on an agarose gel. Whole plasmid was amplified and the product obtained was further transformed into *E. coli* DH5 α strain. Shortening of both loops was confirmed by sequencing.

Additionally, in order to stabilize cork domain in the barrel of FhuA, three amino acid substitutions (Q62D, R81W, N117L, numbering of positions is based on PDB ID 1BY3) were identified to enhance the interactions between the cork domain and the β -barrel domain (Table 7). These substitutions were chosen based on the highest stabilization energy and largest distance from generated filter regions. Plasmid obtained after shortening of loops was used as template to perform stepwise site directed mutagenesis in order to incorporate all substitutions using primers given in table 3 (Figure 13).

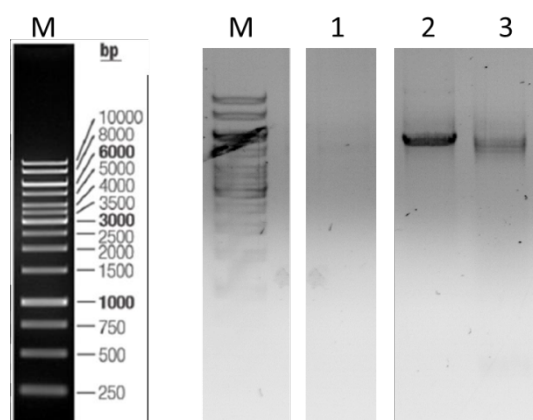


Figure 12. Agarose gel image showing amplification of whole plasmid (pPR-IBA1_FhuA WT) and after shortening of two loops. M: ladder (GeneRuler 1 kB, Fermentas), Lane 1: Negative control without addition of primers, lane2: FhuA WT and lane 3: FhuA after shortening of two loops. 5 μ l of each sample were analyzed on 0.8 % agarose gel.

Table 7. Three amino acid positions were identified by FoldX of the YASARA software to enhance the interactions between the cork domain and the β -barrel domain. The following amino acid substitutions were introduced by directed mutagenesis to reduce fluctuations of the cork domain.

Substitutions in FhuA	Stabilizing energy FoldX $\Delta\Delta G$ (kcal/mol)	New Interaction
Q62D	-1.0	Salt bridge
R81W	-2.9	Aromatic Interaction
N117L	-2.9	Hydrophobic Interaction

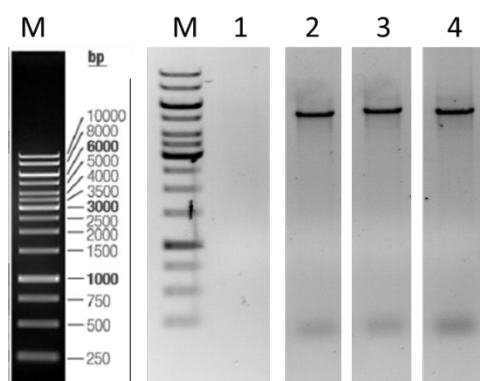


Figure 13. Agarose gel showing site-directed mutagenesis result for insertion of stabilizing mutations. M: ladder (GeneRuler 1 kB, Fermentas), Lane 1: Negative control without addition of primers, lane2: SDM for substitution of Q62D, lane 3: SDM for substitution of R81W and lane 3: SDM for substitution of N117L. 5 μ l of each sample were analyzed on 0.8 % agarose gel.

2.4.2 Expression and extraction of FhuA WT and FhuA Δ L

Overexpression of membrane protein FhuA was done in *E. coli* BE BL21 (DE3) Omp8 strain. This specific strain was chosen because the strain is deficient for several outer membrane proteins (OMP). Since expression of membrane protein only in membrane would lead to low yield, expression was performed in cytoplasm in form of inclusion bodies. The expression of these variants was checked by 8 % SDS gel. Samples loaded on acrylamide gels showed successful overexpression of both FhuA WT and FhuA Δ L variant (Figure 14). No FhuA band was observed in case of the empty vector as well as in the samples before induction, which were used as negative controls (gel image not shown). Successful expression demonstrates that loops deletion and additional amino acid substitutions of FhuA WT did not harm the cell growth and FhuA expression. The next step comprises the extraction of FhuA WT and engineered FhuA variant from *E. coli* cells, which is described in the following section.

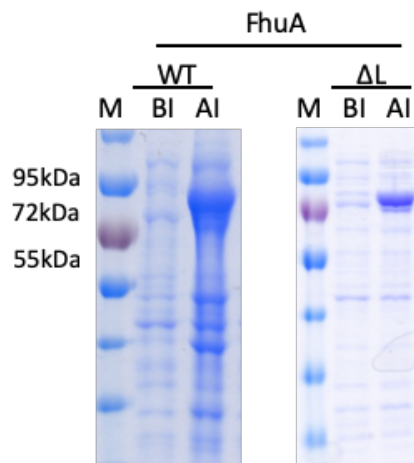


Figure 14. SDS-PAGE gel image showing successful expression of FhuA WT and engineered variant FhuA Δ L. M, marker (pre-stained PageRuler, Fermentas); BI, before induction; AI, after induction.

2.4.3 Extraction of FhuA WT and FhuA Δ L

Being a transmembrane protein, FhuA is embedded in phospholipid bilayer in its natural form. Structure of OMP is naturally optimized to interact with the cell membrane in a way that side chains of amino acids in hydrophobic region are exposed to outer surface of protein and interacts with lipid bilayer by hydrophobic interactions. For this reason detergents are used for extraction of membrane proteins. Detergents are amphiphilic molecules with hydrophobic head and hydrophilic tail similar to natural cell membranes. The head group provides the molecule water solubility whereas the hydrophobic chain interacts with the hydrophobic residues of membrane proteins shielding them from water and lead to protein solubilization.^{122,140-142}

In the present thesis, FhuA WT and the engineered FhuA variants were extracted according to the successful established purification protocol by Philippart et al.³⁷ This method has been used to purify FhuA variants in larger amount using 1.25 % SDS (CMC \sim 0.2 %/8.2 mM).¹⁴³ Extraction using SDS method resulted in at least 0.5 g FhuA from 1.5 liter of overnight grown culture with protein concentration of 4-5 mg/ml with a purity of 90-95 %. Dialysis is performed after extraction in order to regain the proper folded state of the transmembrane protein FhuA after denaturing by SDS.^{144,145} Initially, polyethylene- polyethyleneglycol (PE-PEG) was used in the as refolding agent in a ratio of protein to dialysis of 1:200 (v/v).^{185,214} However, these molecules with longer chain length are not suitable within this work due to steric hindrances caused by shielding effects. These effects lead to coverage of exposed Lys residues, which are supposed to be nucleation sites for polymerization reaction. Therefore, in the present work a small water-miscible alcohol 2-methyl-2,4-pentanediol (MPD) was used for solubilization of FhuA (10 mM sodium phosphate pH 7.4, 50 mM MPD and 1 mM EDTA (MPD buffer)). Proper folding of FhuA after extraction and refolding was monitored by performing CD spectrometry (Figure 16).

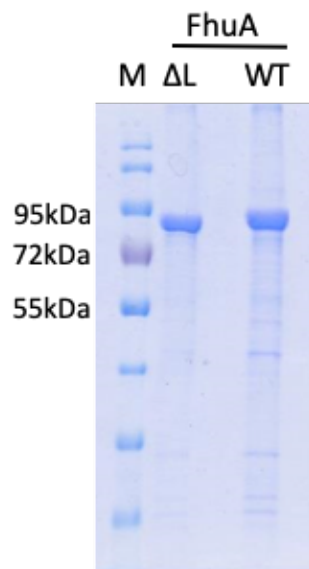


Figure 15. SDS-PAGE gel for FhuA extraction. One major band with correct apparent molecular weight shows successful extraction of both FhuA WT and FhuA Δ L. M, marker (pre-stained PageRuler, Fermentas).

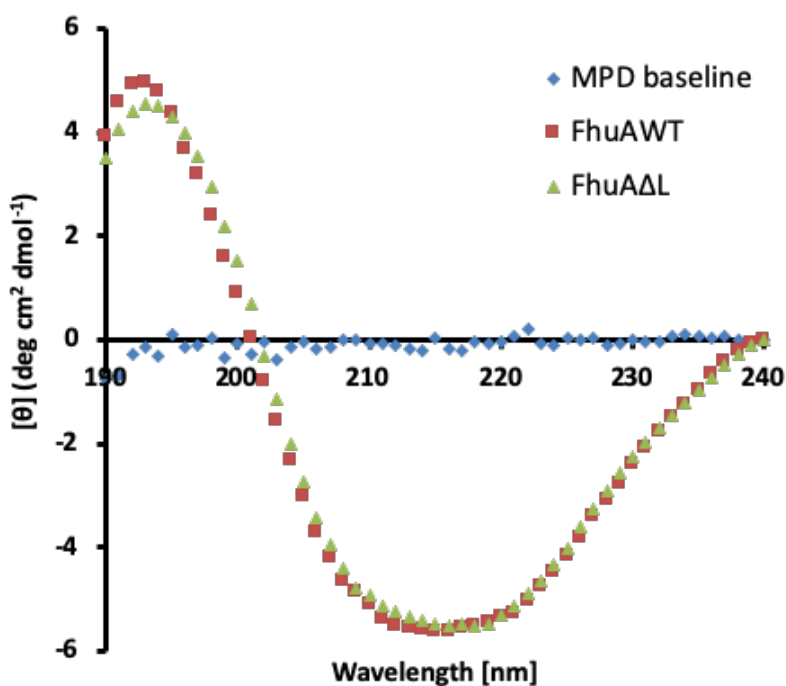


Figure 16. CD spectra of FhuA WT and FhuA Δ L variant refolded in MPD buffer. Both spectra show characteristic of β -barrel protein with minima at 215 nm and maxima at 195 nm. (Reprinted figure with permission of RSC)¹³⁸

2.4.4 Calcein release assay

Aim of calcein release study was to observe the influence of stabilizing mutations between cork domain and barrel of FhuA. Fluctuations of cork domain was monitored during transport of calcein through the channels of FhuA WT and FhuA Δ L. We expected to observe lower release of calcein from FhuA Δ L compared to FhuA WT due to stability or less movement of cork inside the barrel of FhuA while the compound is being transported through.

Polymersomes were prepared in collaboration with L. Zhanzhi, RWTH Aachen University, Institute of Biotechnology. Direct dispersion method was used to prepare polymersomes using poly(2-methyloxazoline)–poly(dimethylsiloxane)–poly(2-methyloxazoline) (PMOXA–PDMS–PMOXA; Mn X 103: 1.2-4.8-1.2) (see section 2.3.3.1). Initial characterization of prepared polymersomes using cryo-TEM was performed by L. Zhanzhi.

Calcein is a fluorescent compound that quenches itself at a concentration higher than 50 mM.^{146,147} FhuA variants has previously been characterized by entrapment of self-quenching concentration in synthosomes.^{27,120} Similarly in this study, self-quenching concentration of calcein (50 mM) was entrapped inside the polymersomes and its release after insertion of FhuA variants into polymer membrane was monitored by performing calcein release assay in a 96 well black MTP. Extracted and refolded FhuA samples were diluted in FhuA refolding buffer to get final molar concentration of 3.91 μ M. 50 μ L of prepared polymersomes was supplemented with 150 μ L Tris buffer in black microtiterplate and measurement were taken with Tecan infinite M200 Pro. Two negative controls were also performed by adding 40 μ L Tris-KCl buffer and 40 μ L dialysis buffer, respectively. The release of calcein was determined by applying the following settings: number of cycles: first 15 cycles and then 45 cycles, shaking: 3 sec, number of flashes: 10, integration time: 20 μ s, manual gain: 49, excitation: 495 nm, emission: 525 nm. After the first 15 cycles without addition FhuA samples, 3.91 μ M of FhuA WT and FhuA Δ L were separately added stepwise in 10 μ L batches (after every 45 cycles) to the polymersome suspension and the fluorescence increase was recorded at 520 nm. Higher release of calcein in case of FhuA WT compared to FhuA Δ L supports the stabilization effect of inserted substitutions (Q62D, R81W, and N117L) by reducing fluctuations of cork domain.

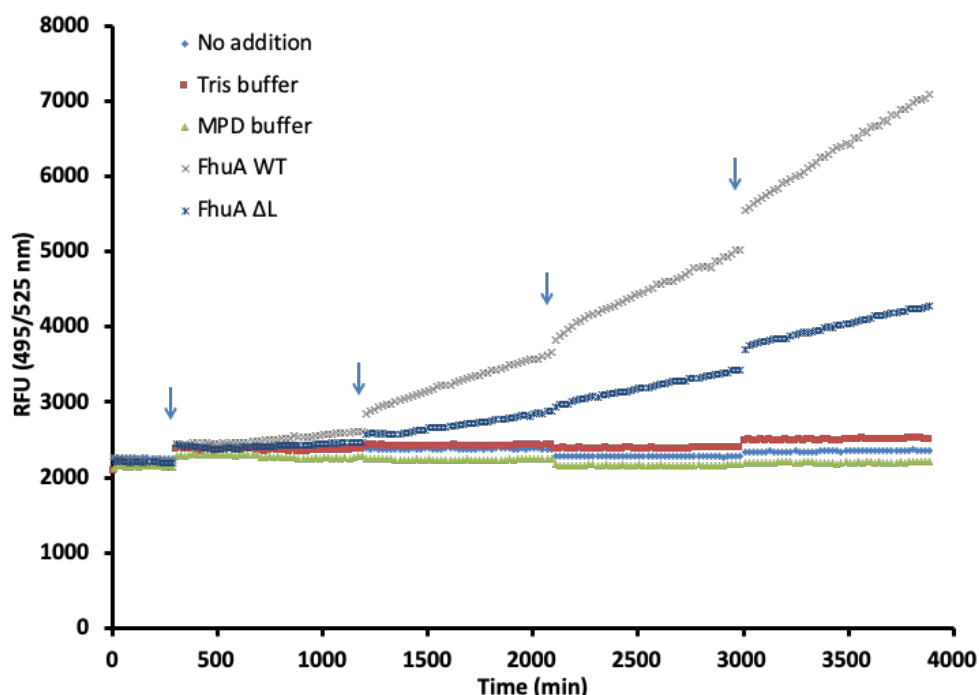


Figure 17. Calcein release assay. Increase in fluorescence intensity due to dilution of self-quenching concentration of calcein (50mM) as a result of diffusion through FhuA channels. Two FhuA variants (3.91 μ M FhuA WT (grey) and 3.91 μ M FhuA Δ L (dark blue)), FhuA refolding buffer (10 mM sodium phosphate buffer, 50 mM MPD, 1 mM EDTA, pH 7.4, green) and Tris buffer (10 mM Tris, 100 mM KCl, pH 7.4; red) were added step-wise to calcein loaded polymersomes (indicated by arrows). Another control without addition of any sample (light blue) was also run. (Reprinted figure with permission of RSC)¹³⁸

3 Structure guided OmniChange libraries generation

Interaction between a selector and a chiral compound can enable chiral recognition. The following section focuses on computational analysis of FhuA channel for generation of chiral environment in its interior. FhuA Δ L with its two filter regions was used as template. This work was performed in collaboration with Dr. M. Bocla, RWTH Aachen University, Institute of Biotechnology.

3.1 Computational analysis for selection of amino acid residues for OmniChange libraries generation

After generation of small channel in FhuA WT selectivity need to be imparted into the generated channel. In order to achieve it, the passive diffusion channel of FhuA Δ L needs to be converted into chiral selector for arginine enantiomers. Therefore, FhuA Δ L variant was rationally designed. The rational design was performed based on X-ray crystal structure of FhuA WT (PDB ID: 1BY3, reference for numbering of positions) as structural template. In the channel interior, arginine enantiomers were placed within two selectivity filter regions one by one. The amino acid residues in a distance of 5 Å around the placed arginine were chosen to perform saturation to all 20 proteogenic amino acids.

3.2 Result and discussion

Six libraries with up to five targeted positions were selected on the basis of the two selectivity filter regions of FhuA Δ L variant. The geometric design criteria were introduced by identification of contact residues (sidechain distance to aa < 5 Å) of arginine placed within the respective selectivity filter region. In total 23 amino acid positions were selected out of which 11 positions were located within the selectivity filter region 1 and the remaining 12 positions were located in selectivity filter region 2. Amino acids positions listed in Table 8 were selected to impart enantioselectivity within the filter regions.

Table 8. 23 selected positions near the loop deletion region to create the OmniChange libraries. The numbering of positions is based on crystal structure PDB IB: 1BY3. For example, Gly134 the Gly146 in 1BY3.

Region	Libraries	Position
Filter region 1	Library 1	Ala34, Thr295, Arg297, Gln362
	Library 2	Thr41, Tyr435, Gln437, Gln439
	Library 3	Thr448, Gly450, Arg479
	Library 4	Asn103, Tyr105, Gly134, Gly146
Filter region 2	Library 5	Gln431, Gly433, Arg452, Asp454, Phe500
	Library 6	Gly134, Ser499, Glu501

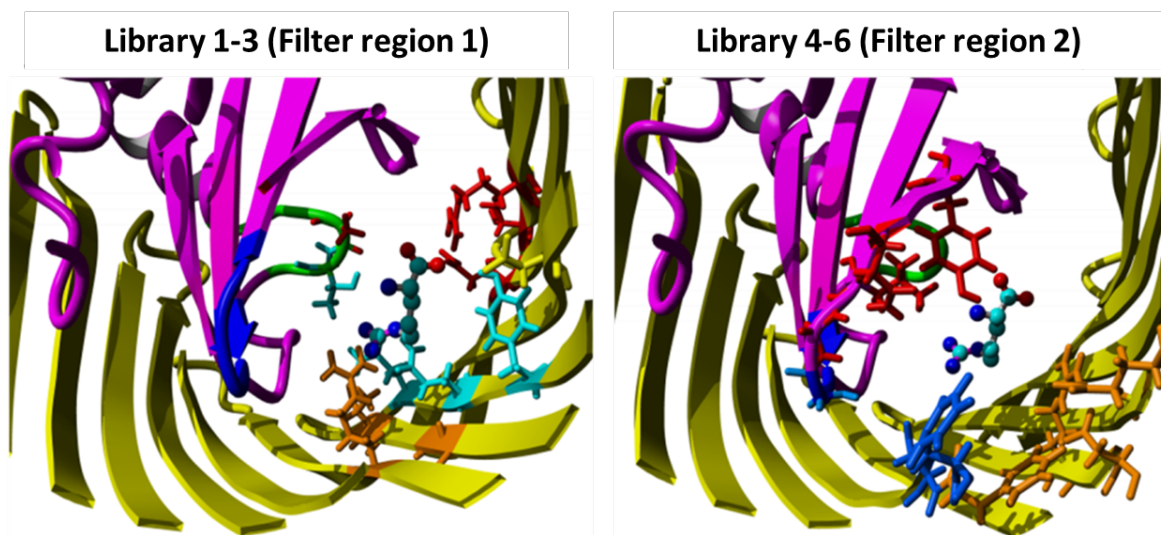


Figure 18. FhuA Δ L (based on FhuA WT) with two found filter regions. The filter regions were generated by deleting two loop regions (Loop 1: green, Loop 2: blue). Highlighted positions were selected for saturation mutagenesis to construct the diversity libraries that are screened for altered enantioselectivity for D / L-arginine. Filter region 1: library 1, red; library 2, cyan; library 3 orange; Filter region 2: library 4, red; library 5, orange; library 6, blue.

3.3 Experimental section

All chemicals were of analytical grade or higher quality and were purchased from Sigma-Aldrich (Steinheim, Germany) and Applichem (Darmstadt, Germany); all enzymes were purchased from New England Biolabs (Frankfurt, Germany), Fermentas (St.Leon-Rot, Germany), or Sigma–Aldrich (Darmstadt, Germany) unless stated otherwise.

Thermal cycler (Mastercycler gradient; Eppendorf, Hamburg, Germany) and thin-wall polymerase chain reaction (PCR) tubes (Multi-ultra tubes; 0.2 mL; Carl Roth, Germany) were used in all PCRs. The amount of DNA in cloning experiments was quantified by using a Nano-Drop photometer (NanoDrop Technologies, Germany).

Target gene

Target gene encoding for FhuA Δ L was used as a template for generation of OmniChange libraries.

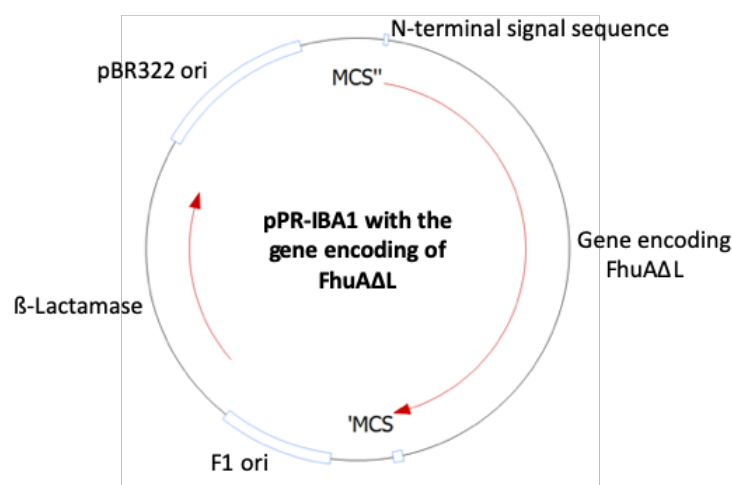


Figure 19. Vector map of FhuA Δ L gene in pPR-IBA1 plasmid.

Bacterial strains

All bacterial strains and plasmids used in this section are respectively given in Table 9. The strain *E. coli* DH5 α was used for generation of high copy numbers of respective plasmids and *E. coli* BE BL21 (DE3) omp8 (*E. coli* omp8) strain was used as an expression strain.

Table 9. Summary of bacterial strains used in this part of thesis

Bacterial strain	Genotype	Function
<i>E. coli</i> DH5 α	F-mcrA Δ (mrr-hsdRMS-mcrBC) endA1 recA1 s ϕ 80dlacZ Δ M15 Δ lacX74 araD139 Δ (ara,leu)7697 galU galK rpsL nupG λ tonA	Plasmid construction and amplification

<i>E. coli</i> BE BL21 (DE3) omp8 (<i>E. coli</i> omp8) strain	F- <i>hsdSB</i> (rB- mB-) <i>gal ompT</i> <i>dcm</i> (DE3) <i>ΔlamB ompF::Tn5</i> <i>ΔompA ΔompC</i>	Expression strain
---	--	-------------------

Media and buffer

Table 10. Summary of media and buffer used in this part of thesis

Media/Buffer	Components
LB media	5 g/L yeast extract, 10 g/L trypton, 10 g/L NaCl
LB plates	5 g/L yeast extract, 10 g/L trypton, 10 g/L NaCl, 15 g/L Agar
TY media	5 g/L yeast extract, 10 g/L trypton, 5 g/L NaCl
SOC media	2 % trypton, 0,5 % yeast extract, 10 mM NaCl, 2.5 mM KCl, 10 mM MgCl ₂ , 10 mM MgSO ₄ , 20 mM glucose
TFBI buffer	pH = 5.8, 30 mM KAc, 50 mM MnCl ₂ , 100 mM RbCl ₂ , 10 mM CaCl ₂ , 15 % (w/v) glycerol
TFBII buffer	pH = 6.8, 10 mM MOPS, 75 mM CaCl ₂ , 10 mM RbCl ₂ , 15 % (w/v) Glycerol,
Tris-KCl buffer	pH 7.4, 10 mM Tris-HCl, 100 mM KCl,
Iodine/ethanol solution for PLICing	100 mM Iodine in ethanol
Cleavage buffer for PLICing	Mix of 5 μL of 0.5 M Tris (pH 9.0), 3 μL of Iodine/ethanol solution and 2 μL ddH ₂ O

Primers

The following table lists the used primers for generation of OmniChange libraries based on FhuAΔL variant. All primers were prepared in-house. Conditions used for PCR is given in the Table 12 and 13.

Table 11. Sequences of the primers used for the generation of OmniChange libraries containing NNK degeneracy codon. Numbering of positions has been done according to FhuA WT sequence (PDB ID: 1BY3¹³¹)

Region	Library name	Oligoname	Sequence ^[a]	GC (%)	T _m (°C)
ΔLoop 1	Library 1	A34 Fwd	gcgcgacagtctNNKACGCCGATTCAAAAAGTG	53.0	65.7

		A34 Rev	aaaggtgtcgttAAATTCGTGATCGAAGCTG	41.9	60.6
		T295 R297 Fwd	aacgacaccttt NNK GTG NNK CAGAACCTGCGC TTTG	50.0	62.0
		T295 R297 Rev	caactgggtatcAACGGAGAAGTTTTGCAG	47.0	61.1
		Q362 Fwd	gataccagttg NNK AGCAAGTTTGCC	50.0	60.7
		Q362 Rev	agactgtcgcgcCGCAATAGTTGC	58.3	63.9
	Library 2	T41 Fwd	cgacagtctgct NNK CCGATTCAAAAAGTG	48.3	61.8
		T41 Rev	gcccgtttgtttCTGTTTATTCAGAATGCGGTAAG G	44.4	63.4
		Y435 Q437 Q439 Fwd	aaacaaacgggcGTT NNK GTT NNK GAT NNK GC GCAGTGGGATAAAAGTG	49.0	69.5
		Y435 Q437 Q439 Rev	agcagactgtcgCGCCGAATAGTTGC	59.3	66.6
	Library 3	T448 G450 Fwd	aaagtgtggtc NNK CTA NNK GGTCGTTATGAC TGG	50.0	65.6
		T448 G450 Rev	ccaggtaaactgTTTGTCATCACGTTTATCGGTC GTCCC	48.7	65.4
		R479 Fwd	cagtttacctgg NNK GGTGGTGTTAACTAC	48.3	61.0
		R479 Rev	gaccagcactttATCCCACTGCGC	58.3	62.3
Δ Loop 2	Library 4	N103 Y105 Fwd	gcagaaggccaaAGCCAG NNK AAC NNK CTGAA TGGCCTGAAG	54.8	69.6
		N103 Y105 Rev	cataatttcagcGCGTTCCAGCATATACGG	46.7	61.1
		G134 G146 Fwd	gctgaaattatgCGTGGC NNK NNK CTGTTGAAT ATGGTC	46.2	65.1
		G134 G146 Rev	ttggccttctgcCGCAAAGCCGCGAATG	60.7	68.7
	Library 5	R452 D454 Fwd	agtgggataaagTGCTGGTCACCCTAGGCGGTN NKT AT NNK TGGGCAGATCAAG	51.9	70.5

		R452 D454 Rev	cgattcgctataGCTGAAGTAAGGTGTTACACC	45.5	61.0
		F500 Fwd	tatagcgaatcg NNK GAACCTTCTTCG	46.3	59.1
		F500 Rev*	ctttatcccactGCGCCTGATCCTGAACATAAAC NNK CGT NNK TTTCTGTTTATTCA	43.1	67.5
	Library 6	G134 Fwd	gaaattatgcgt NNK GGCGGCCTGTTG	53.1	63.2
		G134 Rev	gctatagctgaaGTAAGGTGTTACACC	44.4	56.9
		S499 E501 Fwd	ttcagctatagcGA NNK TTT NNK CCTTCTTCGC AAGTTGGG	45.2	66.1
		S499 E501 Rev	acgcataatttcAGCGCGTTCCAGC	52.0	62.3

[a] small letter-phosphorothioated nucleotides, capital letter-normal nucleotides, bold letters-saturation codon. All primers sequences are in 5' to 3' direction. *Primer F500 Rev has two additional saturation sites (Q431 and G433)

Table 12. Components of PCR mixture for OmniChange libraries generation.

PCR components	Amount
PfuS DNA polymerase buffer (10X)	5 µl
Plasmid template DNA	15-20 ng
dNTP mix	0.2 mM
Forward primer	0.4 µM
Reverse primer	0.4 µM
PfuS DNA polymerase	2 U
ddH ₂ O	Up to 50 µl

Table 13. General PCR conditions used for generation of OmniChange libraries. The exact values for the annealing temperatures (XX: about 5°C below the T_m of primers used) and elongation times (YY: depending upon the length of fragment) varies with the primer pair used. 30 cycles of PCR extension were used for amplification of fragments.

Step	Temperature (°C)	Time
Initial denaturation	98	2 min
Denaturation	98	30 sec
Annealing	XX	30 sec
Extension	72	YY
Final extension	72	5 min

From the PCR sample 5 μ l was run on an agarose gel to determine the estimated quantity of amplified product. To each PCR sample 20 U DpnI (2 μ l) and 7 μ l DpnI buffer was added followed by incubation at 37 °C for 3 hours. The DpnI-treated PCR sample was purified with the PCR cleanup kit (Macherey-Nagel NucleoSpin Extract-II DNA purification kit). After elution into 30 μ l of ddH₂O the DNA concentration was measured using the NanoDrop spectrophotometer.

3.3.1 Iodine cleavage

The vector should be diluted to 0.03-0.04 pmol/ μ l and the inserts to 0.11 pmol/ μ l prior to iodine cleavage. From each DNA fragment (vector and insert) 4 μ l was filled into their own thin-walled PCR tube. For each insert-containing tube another tube filled with water is prepared as vector re-ligation control. The Iodine cleavage mixture is freshly prepared as follows:

- 50 μ l Tris/HCl buffer (500 mM; pH 9.0)
- 30 μ l Iodine-EtOH solution (100 mM)
- 20 μ l ddH₂O

The mixture was thoroughly mixed and stored on ice. To each DNA fragment (and the controls) 2 μ l of Iodine cleavage mix was added. Samples were incubated at 70 °C for 5. The cleaved DNA fragments were kept on ice prior to hybridization.

3.3.2 Hybridization of DNA fragments

All steps were performed at room temperature. The vector sample was split into two PCR tubes and insert 1 was added to one tube and the cleaved ddH₂O to the control tube. They were mixed thoroughly and incubated for 5 minutes. Then the next insert was added to the insert 1-vector mix (and another cleaved ddH₂O to the re-ligation control), mixed again and incubated for 5 minutes. This was repeated with all other remaining inserts and controls. After the last insert was added and incubated the mixture was stored on ice for 5 minutes.

3.3.3 Transformation of assembled OmniChange library

Transformation was done for the vector + insert tube and the vector + cleaved ddH₂O: Verification of the correct assembly was done by colony PCR and saturation at target sites were confirmed by sequencing of plasmid isolated from few clones.

3.4 Result and discussion

Interaction between a selector and a chiral compound can enable chiral recognition. The following section focuses on the generation of OmniChange libraries based on rational model of FhuAΔL in order to impart enantioference to the generated filter regions within FhuAΔL. Structural analysis yielded 23 amino acid positions within 5 Å from the respective filter regions (See section 3.1). These identified positions were grouped into six different OmniChange libraries to perform site saturation mutagenesis using NNK degenerate codons encoding for all 20 proteinogenic amino acids.

3.4.1 Generation of OmniChange libraries

Multiple site saturation mutagenesis libraries were generated with previously described (see section 3.3) OmniChange protocol using FhuAΔL as a template. Primers containing NNK saturation codon are listed in Table 11. All the primers were prepared in-house containing the PTO region for further hybridization using PLICing.¹⁴⁸ Selected position were divided into six libraries with library 1-3 targeting selectivity filter region 1 and library 4-6 targeting selectivity filter region 2. Targeted positions were saturated by using phosphorothiolated primers in PCR to generated fragments of different sizes (Table 14).

Table 14. Number of fragments generated within each library.

Library	Fragments
Library 1	Fragment 1: A34 (744 bp) Fragment 2: T295, R297 (213 bp) Fragment 3: Q362 (4 kb)
Library 2	Fragment 1: T41 (1.1 kb) Fragment 2: Y435, Q437, Q439 (3.8 kb)
Library 3	Fragment 1: T448, G450 (100 bp) Fragment 2: R479 (5 kb)
Library 4	Fragment 1: N103, Y105 (108 bp) Fragment 2: G134, G146 (4.9 kb)
Library 5	Fragment 1: R452, D454 (176 bp) Fragment 2: F500 (4.8 kb)
Library 6	Fragment 1: S499, E501 (3.9 kb) Fragment 2: G134 (1 kb)

Fragments of library 1 (saturation position: Ala34, Thr295, Arg297, Gln362), library 3 (saturation positions: Thr448, Gly450, Arg479) and insert fragment of library 4 (N103/Y105) could also be amplified without any PCR optimization (Figure 20). In order to generate every fragment of each library, correct PCR parameters had to be investigated as they all used a library of primers with random codons for each desired SSM position not fitting the template. Gradient PCR was performed for amplification of all other fragments (“F500”, “G134”, “G134/G146”, “R452/D454”

and “S499/E501”) in order to find out the ideal annealing temperature for each primer pair (Figure 21-24).

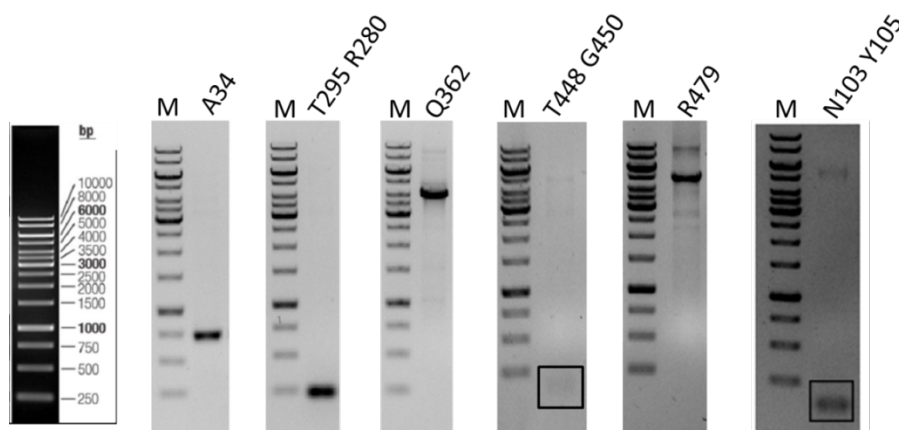


Figure 20. Agarose gel image showing fragment amplification of library 1 (A34, T295, R297, Q362), library 3 (T448, G450, R479) and insert fragment of library 4 (N103/Y105). Annealing temperature of 56°C, 53°C and 59°C were used for generation of fragments for library 1, library 3 and fragment N103/Y105 of library 4 respectively. (Updated figure from thesis of Carsten Ludwig)

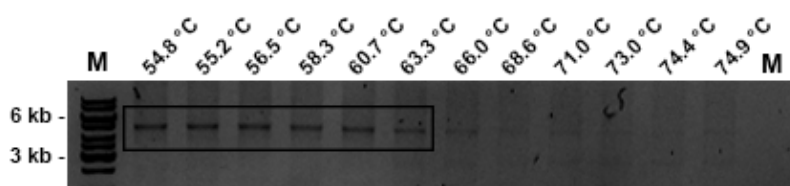


Figure 21. Agarose gel image showing F500 gradient PCR amplification. Gradient PCR was performed with annealing temperatures ranging from 54.8 to 74.9 °C. The best results were achieved with annealing temperatures from 54.8 to 63.3 °C (black box). (Updated figure from thesis of Carsten Ludwig)

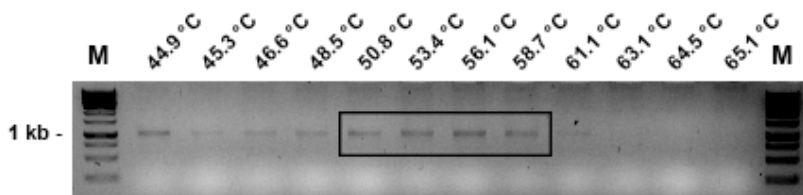


Figure 22. Agarose gel image showing G134 gradient PCR amplification. Gradient PCR was performed with annealing temperatures ranging from 44.9 to 65.1°C. The best results were achieved with annealing temperatures from 50.8 to 58.7°C (black box). (Updated figure from thesis of Carsten Ludwig)

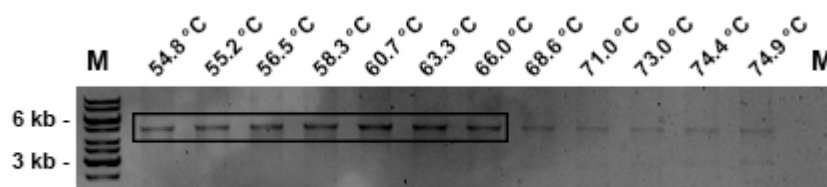


Figure 23. Agarose gel image showing G134 G146 gradient PCR amplification. Gradient PCR was performed with annealing temperatures ranging from 54.8 to 74.9°C. The best results were achieved with annealing temperatures from 54.8 to 66.0°C (black box). (Updated figure from thesis of Carsten Ludwig)

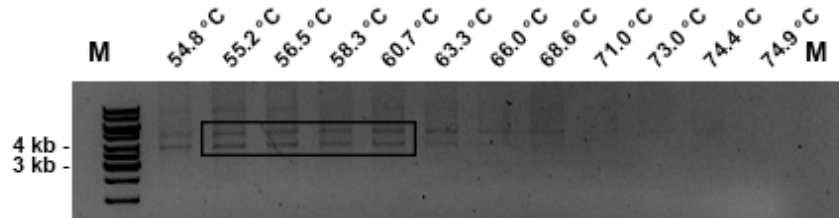


Figure 24. Agarose gel image showing G134 gradient PCR amplification. Gradient PCR was performed with annealing temperatures ranging from 54.8 to 74.9°C. The best results were achieved with annealing temperatures from 55.2 to 60.7°C (black box). (Updated figure from thesis of Carsten Ludwig)

Afterwards sufficient amounts of each fragments were generated. Annealing temperatures and elongation times were chosen based on the gradient PCR experiments. Quality of constructed OmniChange library was checked by sequence analysis of randomly picked clones. Example of sequencing results (Table 15) showed that most of the positions had mutation and only few positions showed wild type genotype. This data showed that diversity quality of generated OmniChange libraries is quite high since none of the investigated clones remained as the original sequence and library could be used for further screening and analysis.

Table 15. Exemplary sequencing results of few clones from library 1 and 4.

Selective Filter region 1				
Library 1	Positionen			
	A34	T278	R280	Q345
Mutant 1	A34G	T278D	R280N	Q345L
Mutant 2	A34V	T278V	R280S	Q345G
Mutant 3	A34Q	T278C	R280C	Q345D
Mutant 4	A34A (silent)	T278	R280-	Q345H
Selective Filter region 2				
Library 4	N97	Y99	G130	G131
Mutant 1	N97C	Y99G	G130R	G131R
Mutant 2	N97N (silent)	Y99L	G130L	G131R
Mutant 3	N97L	Y99W	G130S	G131Y
Mutant 4	N97C	Y99G	G130S	G131T

4 Development and validation of high-throughput screening system for identification of enantioselective FhuA variants

After generation of filter regions and OmniChange libraries, a screening system was developed based on modified citrulline colorimetric screening system adapted to quantify conversion of D- and L- arginine. To achieve high throughput MTP based screening system was developed and validated. Additionally, a characterization system based on chiral HPLC method was also developed in order to characterize the identified variants showing altered enantiopreference after screening.

4.1 Experimental section

All chemicals were of analytical grade or higher quality and were purchased from Sigma-Aldrich (Steinheim, Germany) and Applichem (Darmstadt, Germany); all enzymes were purchased from New England Biolabs (Frankfurt, Germany), Fermentas (St.Leon-Rot, Germany), or Sigma-Aldrich (Darmstadt, Germany) unless stated otherwise.

Thermal cycler (Mastercycler gradient; Eppendorf, Hamburg, Germany) and thin-wall polymerase chain reaction (PCR) tubes (Multi-ultra tubes; 0.2 mL; Carl Roth, Germany) were used in all PCRs. The amount of DNA in cloning experiments was quantified by using a Nano-Drop photometer (NanoDrop Technologies, Germany).

Used gene

Genes used for generation of screening system ADI pkDAO

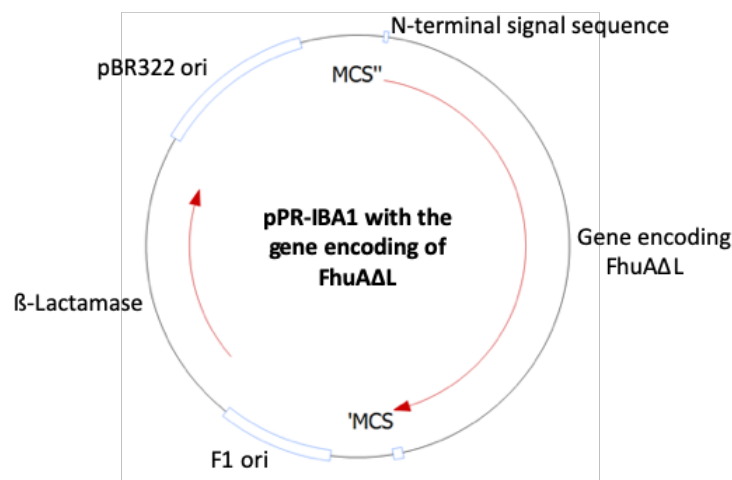


Figure 25. Vector map of FhuAΔL gene in pPR-IBA1 plasmid.

Bacterial strains

All bacterial strains used in this section are given in Table 16. The strain *E. coli* DH5 α was used for generation of high copy numbers of respective plasmids and *E. coli* BE BL21 (DE3) omp8 (*E. coli* omp8) strain was used as an expression strain.

Table 16. Summary of bacterial strains used in this part of thesis

Bacterial strain	Genotype	Function
<i>E. coli</i> DH5 α	F-mcrA Δ (mrr-hsdRMS-mcrBC) endA1 recA1 s ϕ 80dlacZ Δ M15 Δ lacX74 araD139 Δ (ara,leu)7697 galU galK rpsL nupG λ tonA	Plasmid construction and amplification
<i>E. coli</i> BE BL21 (DE3) omp8 (<i>E. coli</i> omp8) strain	F- hsdSB (rB- mB-) gal ompT dcm(DE3) Δ lamB ompF::Tn5 Δ ompA Δ ompC	Expression strain

Media and buffer

Table 17. Summary of media and buffer used in this part of thesis

Media/Buffer	Components
LB media	5 g/L yeast extract, 10 g/L trypton, 10 g/L NaCl
LB plates	5 g/L yeast extract, 10 g/L trypton, 10 g/L NaCl, 15 g/L Agar
TY media	5 g/L yeast extract, 10 g/L trypton, 5 g/L NaCl
SOC media	2 % trypton, 0,5 % yeast extract, 10 mM NaCl, 2.5 mM KCl, 10 mM MgCl ₂ , 10 mM MgSO ₄ , 20 mM glucose
ZYM-5052 auto-induction media ¹⁴⁹	958 ml (1 %Tryptone, 0.5 % yeast extract), 20 ml (25 mM Na ₂ HPO ₄ , 25 mM KH ₂ PO ₄ , 50 mM NH ₄ Cl, 5 mM Na ₂ SO ₄), 20 ml (0.5 %Glycerol, 0.05 % glucose, 0.2 % α -lactose), 2 ml (MgSO ₄ 2 mM), 0.2 ml (0.2X trace elements)
Phosphate buffer saline (PBS)	800 ml of distilled water, 8 g of NaCl., 0.2 g of KCl, 1.44 g of Na ₂ HPO ₄ , 0.24 g of KH ₂ PO ₄ , Adjust the pH to 7.4 with HCl, Add distilled water to a total volume of 1 liter
TFBI buffer	pH = 5.8, 30 mM KAc, 50 mM MnCl ₂ , 100 mM RbCl ₂ , 10 mM CaCl ₂ , 15 % (w/v) glycerol
TFBII buffer	pH = 6.8, 10 mM MOPS, 75 mM CaCl ₂ , 10 mM RbCl ₂ , 15 % (w/v) Glycerol,
Tris-KCl buffer	pH 7.4, 10 mM Tris-HCl, 100 mM KCl,
Iodine/ethanol solution for PLICing	100 mM Iodine in ethanol

Development and validation of high-throughput screening system for identification of
enantioselective FhuA variants

Cleavage buffer for PLICing Mix of 5 μ L of 0.5 M Tris (pH 9.0), 3 μ L of Iodine/ethanol solution and 2 μ L ddH₂O

Primers

Following table lists the primers used for recombination of mutations and to perform colony PCR. All primers were ordered in a salt-free form (Eurofins MWG Operon, Ebersberg, Germany).

Table 18. Summary of primers used in this part of thesis

Function	Primer Name	Sequence	T _m
Change of amino acid Q345H	FhuA Q345H Fwd	GATACCCAGTTGCACAGCAAGTTTGCCAC	68.1 °C
Change of amino acid Q345H	FhuA Q345H Rev	GTGGCAAACCTTGCTGTGCAACTGGGTATC	68.1 °C
Change of amino acid T35Q	YQQT_T35Q_Fwd	CGACAGTCTGCTCTCAGCCGATTCAAAAA GTGC	69.5 °C
Change of amino acid T35Q	YQQT_T35Q_Rev	GCACTTTTTGAATCGGCTGAGCAGACTGT CG	69.5 °C
Change of amino acids Y418G, Q420W and Q422D	YQQT_Y418G_Q420W_Q422D_Fwd	CAGAAACAAACGGGCGTTGGGGTTTAGG ATGATGCGCAGTGGGATAAAGTG	> 75 °C
Change of amino acids Y418G, Q420W and Q422D	YQQT_Y418G_Q420W_Q422D_Rev	CACTTTATCCCACTGCGCATCATCCTAAAC CCCAACGCCCGTTTGTCTG	> 75 °C
TEV internal reverse primer	Internal Primer	CTCGCCACCTTCAACCGAGAAGAAG	66.3 °C
T7 promoter	T7Promoter	TAATACGACTCACTATAGGG	50 °C
Strep tag insertion	FhuA loop Fwd	GGTCTACCCGCAGTTCGAAAAATCTGGT T	> 75 °C
Strep tag insertion	FhuA loop Rev	GCGGGTGAGACCAAGAACCAGAACCCGG AT	> 75 °C
Colony (Strp insertion)	FhuAtev Intern (JT) REV	CTCGCCACCTTCAACCGAGAAGAAG	66.3 °C
Colony (Strp)	Newmiddleprimer (Zhanzhi) FWD	GGCCATTATCTGGCACGT	56.0 °C

insertion)

4.2 Development of whole cell screening system

4.2.1 Cloning and expression of FhuA with amino acid utilizing enzymes (ADI)

For generation of screening system, a D- and L-arginine specific reporter enzyme (arginine deiminase, ADI) was coexpressed with FhuA (ADI-FhuA system). Vector pET-42b(+) containing ADI M21¹⁵⁰ variant was obtained from strain collection. NucleoSpin® Plasmid/Plasmid (NoLid) kit from Machery & Nagel (Düren, Germany) was used for plasmid extraction. The isolated plasmid was quantified (NanoDrop photometer, ND-1000, NanoDrop Technologies, Wilmington, USA), analyzed by sequencing (Eurofins MWG Operon, Ebersberg, Germany) and sequence alignment analysis to confirm the correct DNA sequence of the ADI M21 variant (Clone Manager 9 Professional Edition, Sci-Ed software, Cary, USA). Isolated plasmid was stored at -20°C until transformation. Subsequently the isolated plasmid was transformed into *E. coli* BE BL21 (DE3) Omp8 competent cells. Expression tests were performed before preparing glycerol stocks by mixing 500 µl of 50 % glycerol and 500 µl of overnight grown culture. Following transformation, chemical competent cells were prepared from the cells already transformed with pET-42b(+) vector containing ADI gene (*E. coli* BE BL21 (DE3) Omp8_pET42b_ADI M21 competent cells). OmniChange libraries of FhuA were transformed into these competent cells and were used for screening. Coexpression was confirmed by transforming FhuA gene into *E. coli* BE BL21 (DE3) Omp8_pET42b_ADI M21 competent cells followed by cultivation in ZYM-5052 autoinduction media¹⁴⁹ (37°C, 250 rpm, 200 ml/1 l shaking flask).

4.2.2 Cultivation and expression in 96-well plates

Colonies obtained from OmniChange libraries were cultivated (16 h, 37°C, 900 rpm, 70 % humidity; Multitron Pro, Infors AG, Bottmingen, Switzerland) in 96-well microtiter plates (F-bottomed, polystyrene plates; Greiner bio-one GmbH, Frickenhausen, Germany) containing 150 µl of LB media (0.1 mM ampicillin and 0.05 mM kanamycin). Glycerol stocks were prepared by adding 50 µl of 50 % glycerol solution to each well. Expression (14 h, 30°C, 900 rpm, 70 % humidity; Multitron II, Infors GmbH, Einsbach, Germany) of ADI-FhuA system in 96-deep well microtiter plate (round bottom, polypropylene plates, VWR, Langenfeld, Germany) was performed by inoculating 5 µl of glycerol stock to 500 µl ZYM-5052 autoinduction media (0.1 mM ampicillin and 0.05 mM kanamycin). After cultivation, these clones were used for screening.

4.2.3 Screening of OmniChange libraries

Cell cultures obtained after 14 h of incubation were pelleted by centrifugation (3200 g, 20 min, 4°C; Eppendorf centrifuge 5810 R, Eppendorf AG, Hamburg, Germany). Pelleted cells were

washed once with PBS and again resuspended in 400 µl of PBS. Content of plate were divided into 4 flat bottom microtiter plates and OD₆₀₀ was measured for each plate. Substrate (5 mM L-arginine or 5 mM D-arginine) was added separately to two plates and PBS was added to respective control plates. Plate with L-arginine (and control) was incubated for 20 min and plate with D-arginine (and control) was incubated for 3 h respectively. The arginine deiminase used converts D- and L-arginine, whereby L-arginine is reacted faster by a factor of 10; the overall lower absorption values during the reaction of D-arginine were largely compensated by prolonged incubation times.

Quantification of arginine enantiomer transported through FhuA was done by modified citrulline detection assay.⁷³ After incubation entire content was transferred to a 96-well PCR plate (VWR international bvba, Leuven, Germany) and 60 µl of ferric acid solution and 20 µl of DAM:TSC (1:1) was added. The reaction mixture was further incubated 30 min at 70°C in homemade incubation system for PCR microtiter plate. Colour development was stopped by 5 min incubation on ice followed by centrifugation (3200 g, 20 min, 4°C; Eppendorf centrifuge 5810 R, Eppendorf AG). Supernatant was transferred to F-bottom microtiter plate and absorbance was measured at 530 nm (Tecan Sunrise, Tecan Group AG, Zürich, Switzerland) (Fig. S6). A standard deviation in the 96-well MTP format of 13.6 % and 9.3 % was achieved after optimization for L-arginine and D-arginine, respectively.

4.3 Development of characterization system

4.3.1 Cloning and expression for characterization system

In combination with ADI-FhuA system another coexpression system was generated with D-arginine specific enzyme (pig kidney D-amino acid oxidase, DAO) for characterization of identified FhuA variants from screening. Synthetic gene of DAO mutant 222D224G⁹⁸ (GeneArt Gene Synthesis, ThermoFisher Scientific, Regensburg, Germany) was cloned into pET-42b(+) vector using *Nde*I and *Hind*III restriction enzymes. The vector pET-42b(+)_DAO was transformed into *E. coli* BE BL21 (DE3) Omp8 competent cells. Afterwards, chemical competent cells were prepared from the cells already containing DAO gene (*E. coli* BE BL21 (DE3) Omp8_pET42b_DAO competent cells). Coexpression was confirmed by transforming FhuA gene into *E. coli* BE BL21 (DE3) Omp8_pET42b_DAO competent cells (DAO-FhuA system) followed by cultivation in ZYM-5052 autoinduction media¹⁴⁹ (37°C., 250 rpm, 200 ml/1 l shaking flask).

4.3.2 Chiral HPLC

Resolution of arginine enantiomers was done by using a chiral column (Astec CHIROBIOTIC T, 25 cm x 4.6 mm I.D., 5 µm particles) in analytical HPLC (Nexera X2, Shimadzu Deutschland GmbH, Duisburg, Germany). Both L-arginine and D-arginine were dissolved in PBS (5 mM each). Mobile phase was prepared by mixing PBS, methanol and formic acid (30:70:0.02, pH 3.9). Unless

otherwise indicated, the mobile phase flow rate was 1 ml/min and the UV detection wavelength was 202 nm.

4.3.3 Characterization of identified variants

Parental FhuA variant (FhuA Δ L) and identified variant from screening (FhuAF4) were expressed separately in ADI-FhuA system and DAO-FhuA system as explained above. Coexpressing cells were OD₆₀₀ normalized to 4 and centrifuged (3200 g, 20 min, 4°C; Eppendorf centrifuge 5810 R, Eppendorf AG). Pellets were once washed by resuspending in PBS followed by centrifugation. Obtained pellets were finally resuspended in PBS and mixed together in 1:4.5 ratio (ADI-FhuA:DAO-FhuA cells) according to catalytic properties of ADI and DAO. Mixed cells were incubated (room temperature, rotatory shaking) with racemic mixture of arginine (5 mM of each enantiomer). 200 μ l samples were taken at regular interval and centrifuged. Supernatant obtained were analyzed with chiral HPLC column and calculations of enantiomeric excess and conversion was performed according to reference.¹⁵¹

4.3.4 Quantification of FhuA Δ L and FhuAF4

The amount of outer membrane expressed FhuA was determined by utilizing StrepTactin-Chrome546-conjugate which binds specifically to StrepTactinII sequence (WSHPQFEK).¹⁵² StrepTactinII recognition sequence was introduced in previously identified outer loop 5 (between P405 and V406)¹⁵³ by overlap extension PCR with PTO-overlaps and subsequent PLICing. The primer sequences are summarized in Table 18 and PCR conditions for insertion of strep tag is given in Table 19 and 20. The generated genetic constructs were transformed in *E. coli* BE BL21 (DE3) Omp8 competent cells for expression. Quantification of FhuA WT_Strep, FhuA Δ L_Strep and FhuAF4_Strep was done according to reference.¹⁵³

Table 19. Composition of standard reaction mixture for strep tag insertion PCR.

PCR components	Amount
PfuS DNA polymerase buffer (10X)	5 μ l
Plasmid template DNA	15-20 ng
dNTP mix	0.2 mM
Forward primer	0.4 μ M
Reverse primer	0.4 μ M
PfuS DNA polymerase	2 U
ddH ₂ O	Up to 50 μ l

Table 20. General PCR conditions used for strep tag insertion. 24 cycles of PCR extension were used for amplification.

Step	Temperature (°C)	Time
Initial denaturation	98	1 min

Denaturation	98	30 sec
Annealing	60	1 min
Extension	72	6 min
Final extension	72	8 min

FhuA WT_Strep, FhuA Δ L_Strep and FhuAF4_Strep were expressed for 3 h after induction with IPTG (1mM) as described in previous section. After expression cells expressing FhuA_Strep variants were resuspended in PBS buffer and the OD₆₀₀ was set to 1. In the next step 140 μ l of PBS buffer, 50 μ l of cell suspension and 10 μ l of 1:10 diluted Streptactin-Chromeo546 conjugate (0.5 μ g/ μ l) were pipetted in a 96 well flat bottom MTP (final OD = 0.25). As controls different amounts of Streptactin-Chromeo conjugate were added to PBS buffer (0.05, 0.10, 0.15, 0.20, 0.25, 0.30, 0.4, 0.75) in additional wells to a volume of 200 μ l. The plates were then kept in aluminium foil at room temperature (900 rpm) for 10 min.

Centrifugation was performed for 10 min at 4000 rpm and 4 °C. To wash the pellet the supernatant was discarded and 200 μ l of PBS buffer was added followed by centrifugation for 10 min, 4000 rpm at 4 °C. The supernatant was then discarded and the cells were resuspended in 200 μ l PBS buffer. Fluorescence was directly measured (λ_{ex} = 545 nm, λ_{em} = 561 nm, bandwidth 5 nm, gain 100, 50 flashes, 400 Hz) with Tecan Infinite 1 s shaking.

4.3.5 Steered molecular dynamics simulations

A SMD simulation protocol was developed for diffusion of D- and L- arginine through the channel of FhuA Δ L and FhuAF4 variants. These variants were generated *in silico* within YASARA Structure version 17.8.9¹³² based on the crystal structure of FhuA WT (PDB ID: 1BY3¹³¹). D- and L- arginine were placed above the channel entrance of FhuA Δ L and FhuAF4 variants, respectively. For the pulling of arginine from the top of the FhuA channel, D487 located at the bottom of the FhuA channel was defined as an end point. The size of the simulation box was 100.39 x 76.00 x 61.16 Å with alpha = 90.00, beta = 90.00 and gamma = 90.00. AMBER03 force field¹³⁴ was applied at a temperature of 298 K. During SMD simulations, distances of the arginine and the end point (D487) were analyzed. A pulling force of 5000 pm/ps² on the transported arginine was applied per time step as implemented in YASARA steered MD macro. The arginine was passed through the channel and the selectivity filter regions, which was monitored by time recorded with md_runsteered.mcr script within YASARA.

4.4 Recombination with site directed mutagenesis

Recombination of beneficial mutations from FhuA variant F4 with C11 and F9 was performed separately using FhuA F4 as a template. Primers used for insertion of these mutations are given

in Table 18. Q362H substitution (from FhuA C11) was inserted in one round of SDM. T41Q, Y435G, Q437W and Q439D (from FhuA F9) were inserted in two steps. First T41Q substitution was performed and the product so obtained was used as template for insertion of Y435G, Q437W and Q439D substitutions. PCR conditions used for performing SDM are summarized in Table 21 and 22.

Table 21. Composition of standard reaction mixture for SDM using PCR.

PCR components	Amount
PfuS DNA polymerase buffer (10X)	5 μ l
Plasmid template DNA	15-20 ng
dNTP mix	0.2 mM
Forward primer	0.4 μ M
Reverse primer	0.4 μ M
PfuS DNA polymerase	2 U
ddH ₂ O	Up to 50 μ l

Table 22. General PCR conditions used for SDM. 25 cycles of PCR extension were used for amplification. Any difference in conditions are given in the text (if any).

Step	Temperature (°C)	Time
Initial denaturation	98	2 min
Denaturation	98	30 sec
Annealing	60	45 sec
Extension	72	5 min
Final extension	72	10 min

After PCR, the obtained product was DpnI digested and cleaned as described earlier. Vectors with FhuA genes after recombination were transformed into competent *E. coli* BE BL21 Omp8 strain containing ADI gene to further screen them for their enantiopreference (see section 4.2).

4.5 Result and discussion

The following section describes the development of a MTP based whole cell screening system for identification of chiral FhuA Δ L variants through modified citrulline colorimetric screening system at the computationally proposed filter regions. The generated OmniChange libraries were screened using modified citrulline colorimetric screening system adapted to quantify conversion of D- and L- arginine. The ratio of D-/L-conversion was used as a benchmark to select FhuA variants with altered enantiopreference. Furthermore, the identified variants were characterized using chiral HPLC method developed for separation of arginine enantiomers.

4.5.1 Expression in autoinduction media

Expressing recombinant protein in auto-induction media is based upon the preferences of bacteria to selectively use different carbon sources during diauxic growth and upon the often-observed negative regulation of gene expression by catabolite repression. Auto-induction is more convenient than IPTG induction because the expression strain is simply inoculated into auto-inducing medium and grown to saturation without the need to follow culture growth and add inducer at the proper time. For high-throughput applications, the auto-induction approach has many advantages over traditional induction methods including avoidance of the strong induction and apparent toxicity associated with chemical inducers such as IPTG. ZYM-5052 autoinduction media¹⁴⁹ was chosen for expression of both genes.

The whole cell screening system was developed on the basis of D- and L-arginine specific reporter enzyme (arginine deiminase, ADI) coexpressed with FhuA. After transformation of pET42b_ADI M21¹⁵⁰ into *E. coli* BE BL21 (DE3) Omp8, competent cells were prepared from the cells already transformed with pET-42b(+) vector containing ADI gene (*E. coli* BE BL21 (DE3) Omp8_pET42b_ADI M21 competent cells). Afterwards FhuA WT and FhuA Δ L gene were transformed separately into *E. coli* BE BL21 (DE3) Omp8_pET42b_ADI M21 competent cells. Expression tests were performed before preparing glycerol stocks. Both FhuA and ADI genes were successfully expressed ZYM-5052 autoinduction media. Figure 26 shows the expression band of FhuA and PpADI observed at ~78kDa and ~45 kDa respectively.

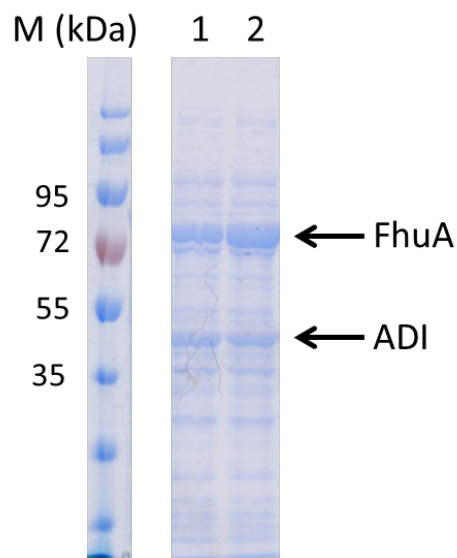


Figure 26. SDS-PAGE gel showing expression of FhuA and ADI. M: Marker (pre-stained PageRuler, Fermentas), Lane 1: *E. coli* BE BL21 (DE3) Omp8_pET42b_ADI M21 and pPR-IBA1_FhuA WT, Lane 2: *E. coli* BE BL21 (DE3) Omp8_pET42b_ADI M21 and pPR-IBA1_FhuA Δ L.

4.5.2 Whole cell citrulline detection assay

A whole cell screening system was successfully developed and validated based on amino acid-utilizing enzymes such as Arginine deiminase (ADI). Arginine deiminase (ADI) was chosen because ADI is able to convert D- and L-arginine. To analyze the enantiopreference of D/L-arginine in the FhuA channels, the channel proteins FhuA were coexpressed with reporter enzymes in *E. coli* BE BL21 (DE3) Omp8. After expression, the cell samples were halved and incubated separately with D- and L-arginine solutions, respectively. The amount of D / L arginine diffused into the *E. coli* cells through the FhuA channels was then converted by ADI enzyme. The reaction was analyzed by colorimetric assay (modified citrulline detection assay) (Figure 27). The color intensity determined photometrically indicates the amount of D- or L-arginine diffused into the cells and converted by ADI. From the individual values of the D- and L-arginine samples, a ratio was calculated (D-arginine / L-arginine), which was compared between FhuA Δ L (parent variant) and the identified FhuA variants after screening. The aim was to find FhuA variants with altered enantioselectivity compared to the starting variant FhuA Δ L.

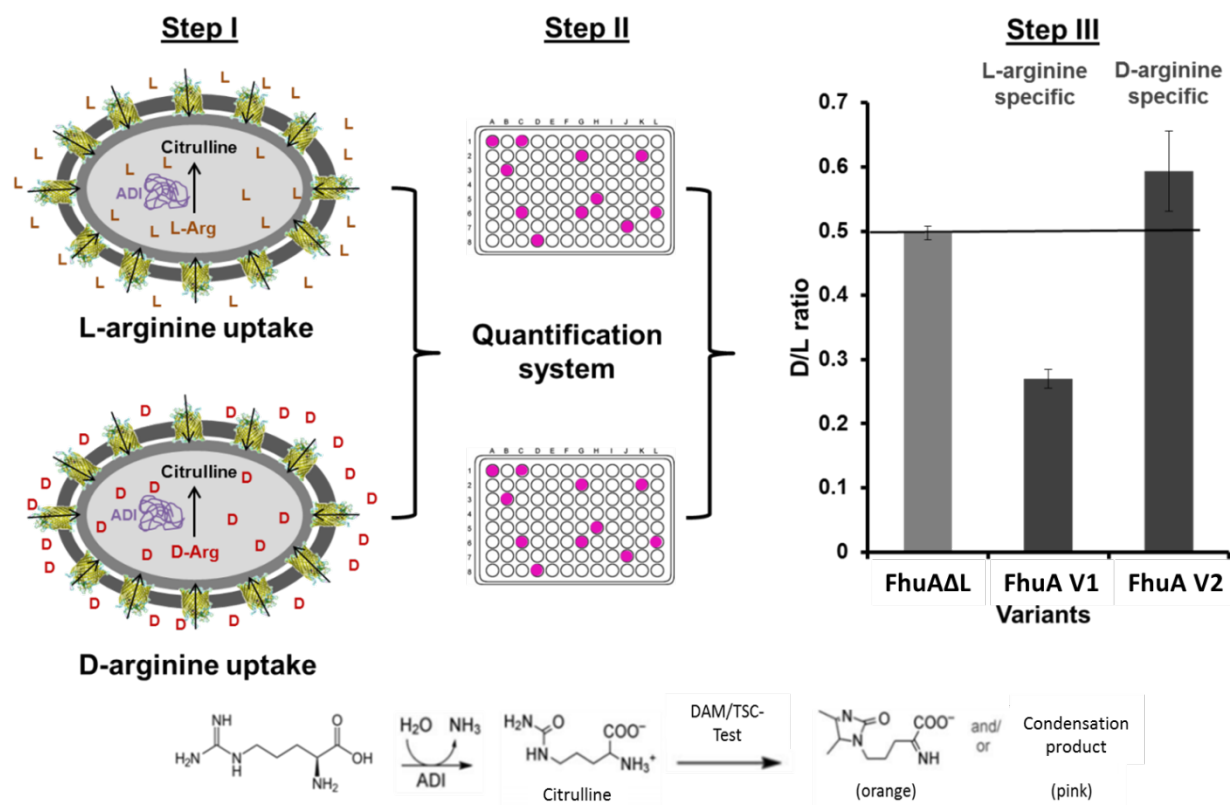


Figure 27 Whole cell screening system. Microtiter plate screening technology based on cytoplasmic expression of ADI and coexpression of FhuA variants in the outer membrane of *E. coli*. Step I: Overnight (~12 hrs) growth of coexpressing *E. coli* cells in ZYM-5052 autoinduction media at 30°C. Cells were pelleted and resuspended in phosphate buffered saline (PBS) pH 7.4 and the content was divided into two separate 96-well microtiter plates (MTPs). Each plate was incubated separately with 5 mM of D- or L-arginine. ADI converts D- and L-arginine which are essentially absorbed through the FhuA variants, to citrulline. By dividing the expression culture into two 96-well microtiter plates, the citrulline product formations of D- and L-arginine are determined and compared in two separate experiments with identical FhuA variants. Step II: Produced citrulline was quantified by modified DAM:TSC (1:1) assay which converts citrulline to a colored compound (absorption at 530 nm). Mechanism of reaction is shown in the bottom of figure. Step III: The ratio of D-/L-conversion was used as benchmark to select FhuA variants with altered enantioselectivity. FhuA V1 and FhuA V2 (variant 1 and variant 2 respectively) are shown as an example where FhuAV1 showed higher transport of L-arginine and FhuAV2 showed higher transport of D-arginine (dark grey bars) when compared to parent FhuAΔL. (Reprinted figure with permission of RSC)¹³⁸

Key performance parameter for a successful screening system to identifying improved variants in microtiter plate based screening systems is the true standard variation of the employed assay. Parameters such as expression in different microtiter plates for a higher yield, incubation time with amino acids and incubation temperature were tested and optimized, as the reaction conditions have crucial importance to be able to identify enantioselective FhuA variants. To

ensure a homogeneous temperature distribution, a new temperature unit was designed and ordered. These optimization steps further improved reaction conditions and resulted in consistent screening and rescreening results with reduced standard deviations.

Standard deviation of the modified citrulline detection assay was reduced by optimizing expression and screening conditions (using auto-induction media and assay conditions such as amount of cell, conversion time and color development procedure). The optimized system resulted in a true standard deviation of 13.6 % for L-arginine conversion and 9.3 % for D-arginine conversion respectively (Figure 28). True coefficient of variation was calculated after subtracting the background. Screening systems with standard deviations up to 15 % have successfully been used in directed evolution experiments.¹⁵⁴ A wide linear detection window is another important factor for identifying beneficial mutants in directed evolution experiments and screening systems for evolved mutants and the screening systems have to be constantly adapted for hitting the linear detection window. A linear detection range up to 6 mM citrulline could be detected using modified citrulline detection assay (Figure 29).

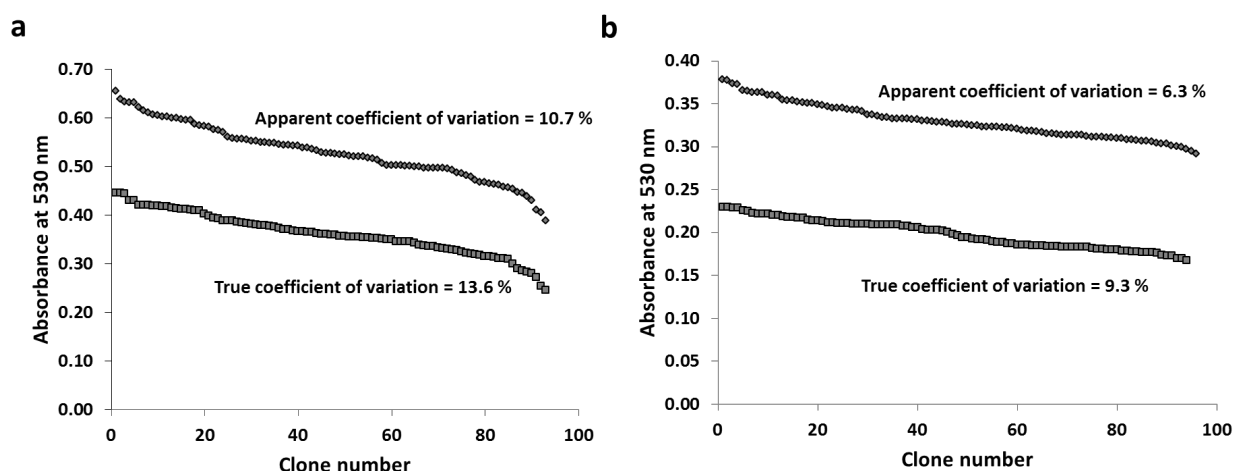


Figure 28. (a) Apparent and true coefficients of variation for L-arginine conversion and (b) apparent and true coefficients of variation for D-arginine conversion. The apparent coefficient of variation was calculated without subtracting the background whereas the true coefficient of variation was calculated after background subtraction.

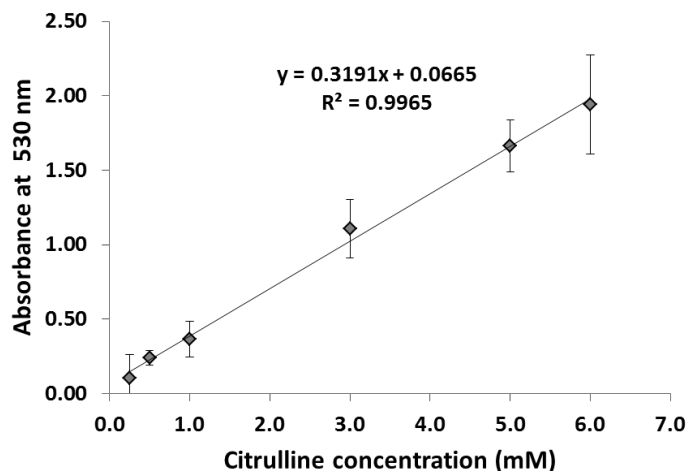


Figure 29. Standard curve for citrulline detection assay in a microtiter format.

4.5.3 Screening of OmniChange libraries

Six OmniChange mutant libraries (1000 variants in each library) based on FhuA Δ L (see chapter 3) were screened with the described whole-cell screening system. From six libraries, 7 promising variants with altered enantiopreference were found compared to the starting variant FhuA Δ L for the diffusion of D / L-arginine (Figure 30). Sequencing revealed that amino acid substitutions are present at the selected positions. These positions represent hotspots that are essential for the development of an enantioselective FhuA channel and allow detailed investigation to improve enantioselectivity. The promising FhuA variants were examined for the required production in terms of their expression to identify the expression variants. Out of the 7 identified variants FhuA C11 (substitution at position Q362H from library 1), FhuA F9 (substitution at position T41Q, Y435G, Q437W and Q439D from library 2) from filter region 1 and variant FhuA F4 (substitution at position G134S and G146T from library 4) from filter region 2 were identified as best variants. All three FhuA variants showed a higher transport of L-arginine compared to the starting variant FhuA Δ L. Although variant FhuA D9 and FhuA C8 showed higher enantiopreference towards L-arginine, these variants showed only silent mutations. This could be attributed to the fact that eventhough silent mutations do not change the amino acid sequence of a protein, but it can strongly influence the amount of protein produced.¹⁵⁵ Two variants (FhuA F12 and FhuA E11) showed slight preference towards higher transport of D-arginine, but the influence of amino acid substitutions were not significant and were very close to standard deviation range. Therefore, these variants were further not tested for characterization.

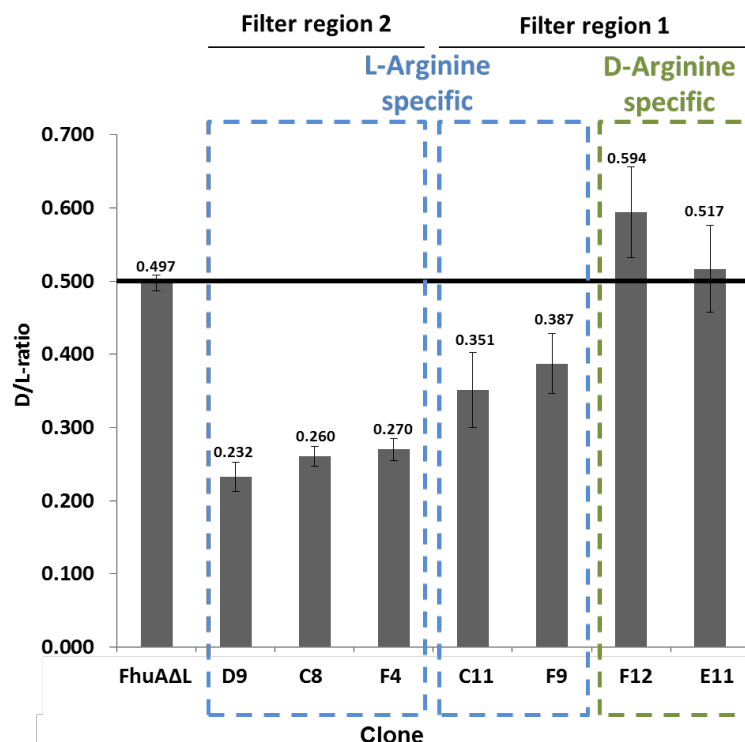


Figure 30. Determination of amino acid selectivity of rationally generated FhuA variants using the whole cell screening system. The D / L ratio shows the enantiopreference of the generated FhuA variants for D- or L-arginine. Average deviations from the mean values are shown as the values reported are the average of three measurements.

4.5.4 Characterization of identified variants

To characterize the chiral FhuA variants, a capillary electrophoretic method was initially developed, which is very well suited for the analysis of UV-absorbing components. Non-UV absorbing components can be screened by dansylation¹⁵⁶ using capillary electrophoresis, although dansylation is not 100% efficient.¹⁵⁶ To avoid the intermediate step of UV labeling, a chiral HPLC method was developed and used for characterization. A chiral column (Astec CHIROBIOTIC T, 25 cm x 4.6 mm I.D., 5 μ m particles) having macrocyclic glycopeptide antibiotic as a chiral stationary phase (CSP) has previously been used for chiral separation of underivatized amino acids.^{18,157} The method was optimized by testing different mobile phases and flow rate to finally get separation of arginine enantiomers (Figure 31).

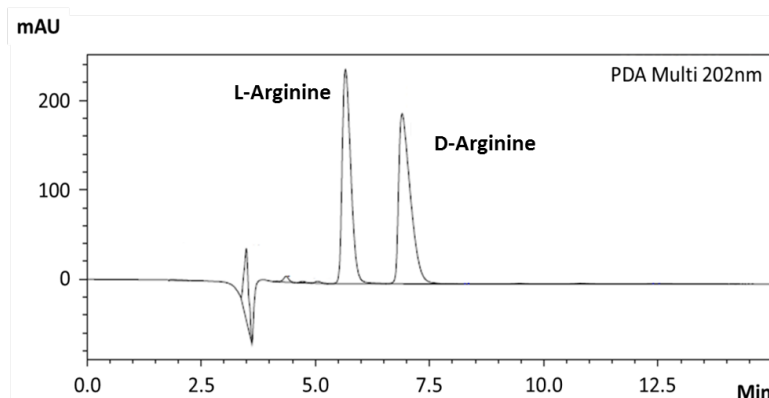


Figure 31. Enantioresolution of arginine enantiomers (5 mM each) using chiral HPLC. Optimized condition used a mixture of PBS, methanol and formic acid (30:70:0.02, pH 3.9) as mobile phase with flow rate of 1 ml/min and the UV detection wavelength at 202 nm. (Reprinted figure with permission of RSC)¹³⁸

The variants found in the screening system showed that L arginine is preferentially taken up by the protein channel of FhuA C11, FhuA F9 and FhuA F4. Of the three previously mentioned variants (FhuA C11, FhuA F9 and FhuA F4), FhuA F4 is the best variant in terms of production as well as the transport of L-arginine. For this purpose FhuA F4 was further characterized using chiral HPLC method. When incubated with a racemic mixture of D / L-arginine, the diffusion of arginine enantiomers through the FhuA channel could be shown through its decrease concentration in the supernatant. Experimentally, the enhanced uptake of L-arginine from the FhuA mutants is determined and compared to the starting variant FhuA Δ L by incubating cells expressing FhuA mutants and amino acid converting enzyme with racemic mixture of arginine. During incubation of FhuA-expressing cells with arginine, 200 μ l samples were taken at regular interval of time. Samples were centrifuged and obtained supernatant were analyzed with chiral HPLC and calculations of enantiomeric excess and conversion was performed according to reference.¹⁵¹ However, no detectable reduction could be demonstrated for D-arginine at comparable measurement conditions with an incubation of up to 8.5 hours in the supernatant (data not shown). This can be attributed to the transport efficiency of the arginine enantiomers through the tailored FhuA channel and ADI enzyme activity. L-arginine is preferentially converted compared to D-arginine when incubating ADI with a racemic mixture of D / L-arginine. Therefore, a second co-expression system with a D-arginine-specific enzyme was developed to eliminate the effect of preference of enzyme for one enantiomer for characterization of the FhuA F4 variant with altered enantiopreference. For this purpose, the porcine kidney D-amino acid oxidase (pkDAO) mutant 222D224G⁹⁸ was expressed together with the FhuA F4 variant (DAO-FhuA system).

Finally, the most beneficial variant FhuAF4 was subjected to a whole cell experiment with a racemic mixture of D-/L-arginine to validate the chiral separation through FhuAF4. In this

experiment the two cell cultures expressing FhuA were grown with Arginine deiminase¹⁵⁰ (ADI; K_{cat} : $18.27 \pm 0.23 \text{ s}^{-1}$, $S_{0.5}$: $0.33 \pm 0.02 \text{ mM}$) for efficient L-arginine conversion and D-amino acid oxidase⁹⁸ (DAO 222D224G; K_{cat} : 240 min^{-1} , K_m : 1.7 mM) for D-arginine conversion. Both cultures were mixed in a ratio of 1:4.5 to compensate for the higher activity of ADI compared to DAO and to enabled comparable conversion of D- and L-arginine. The mixtures of cells were incubated separately with racemic mixture of arginine (5 mM each). Samples were taken at regular intervals and arginine concentrations in the “supernatant” were quantified using a chiral HPLC method (Figure 32a). The translocation efficiency of L-arginine through FhuAF4 was determined by comparing with the parent variant (FhuA Δ L) (Figure 32b).

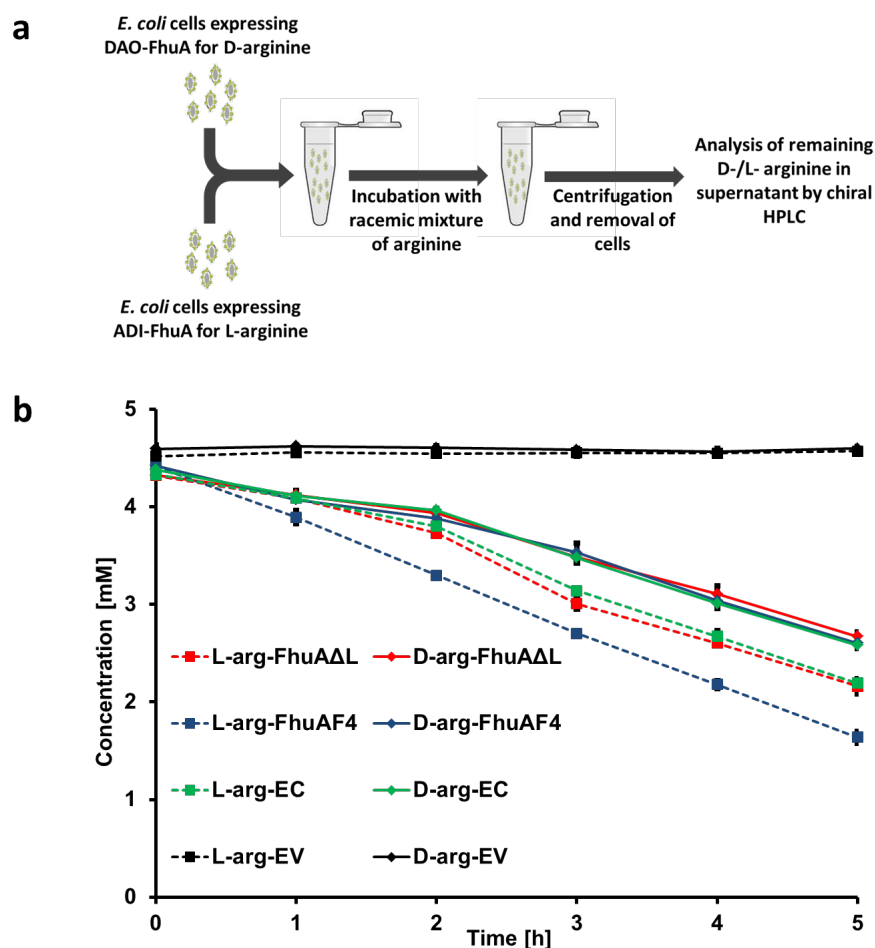


Figure 32. (a) Schematic representation of work flow for characterization of parental and identified FhuA variant using chiral HPLC. *E. coli* cells coexpressing DAO-FhuA and ADI-FhuA were expressed separately. Both cultures were normalized to OD₆₀₀ of 4 and resuspension in PBS buffer pH 7.4 before incubating with racemic mixture of arginine (5 mM each). Samples taken at regular intervals were analyzed with chiral HPLC. **(b)** HPLC quantification of unutilized D-/L-arginine in the supernatant. Unutilized D-arginine (bold line) and L-arginine (dotted line) after incubation with coexpressing *E. coli* cells with the starting variant FhuA Δ L (red lines) and identified variant FhuAF4 (blue lines). ADI/DAO enzyme mix as a control

(EC) expressing only enzymes without FhuA (green lines) and empty vector (EV) control neither expressing ADI/DAO nor FhuA were also run (black lines). FhuAF4 showed higher transport of L-arginine compared to FhuAΔL after incubation with arginine racemate. (Reprinted figure with permission of RSC)¹³⁸

FhuAF4 showed an improved ee % of 23.91 at 52.39 % conversion whereas parent FhuAΔL variant had an ee % of 11.33 at 44.50 % conversion which is close to ee % of 8.35 at 43.14 % conversion of whole *E. coli* cells without recombinantly expressed FhuA (Figure 33 and Table 23). The latter represents the uptake ratio of D-/L-arginine of the selected *E. coli* BE BL21 (DE3) Omp8 strain.

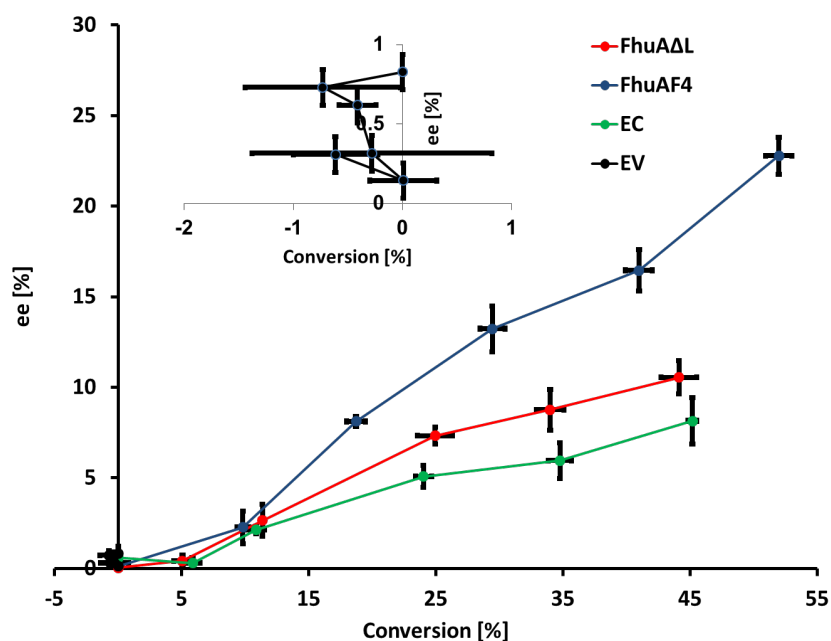


Figure 33. Engineered FhuAF4 variant with improved enantioselectivity for separation of D-/L-arginine based on chiral HPLC. ee vs. conversion for FhuAΔL, FhuAF4 and two controls (EV and EC). FhuAΔL (red line), FhuAF4 (blue line), ADI/DAO enzyme mix as control (EC) expressing only enzymes without FhuA (green lines) and empty vector (EV) control neither expressing ADI/DAO nor FhuA (Black line and inset). FhuAF4 showed an ee of 23.91 % at a conversion of 52.39 % compared to ee of 11.33 % with conversion of 44.50 % with FhuAΔL. (Reprinted figure with permission of RSC)¹³⁸

Table 23. Calculated ee (%) value obtained with parent variant (FhuAΔL) and variant with increased enantiopreference (FhuAF4) after incubation of mixed cells^[a] with arginine racemate.

Variants	ee (%) ^[b]	Conversion (%)
FhuAΔL	11.33	44.50
FhuAF4	23.91	52.39

^a Cells were mixed according to K_{cat} values of ADI (18.27 s^{-1}) and DAO (240 min^{-1}) mutants that ensured equal enzymatic conversion of both enantiomers, ^b ee of D-arginine.

4.5.5 Steered molecular dynamics (SMD) simulations

Steered molecular dynamics (SMD) simulations¹⁵⁸ were carried out for molecular understanding of observed altered enantipreference of FhuAF4 variant towards L-arginine compared to the FhuA Δ L variant. In SMD simulations, arginine was pulled from the top of the FhuA channel towards residue D487 located at the bottom of the FhuA channel. In FhuA Δ L variant, calculated distances between arginine and the end point D487 decreases sharply in the first ≈ 200 ps of the SMD simulations indicating the free diffusion of arginine before entering the selectivity filter region 2 (Figure 34). In FhuA Δ L variant, less interactions of both D- and L-arginine with the filter region 2 were observed and both enantiomers pass freely. Interestingly, in FhuAF4 variant, transport of D-arginine is hindered and steered transport is slowed down, as indicated by a longer residence time close to the selectivity filter region 2. The energetic barrier for transport under constant pulling force in the SMD simulation can be observed as a plateau (Figure 34).

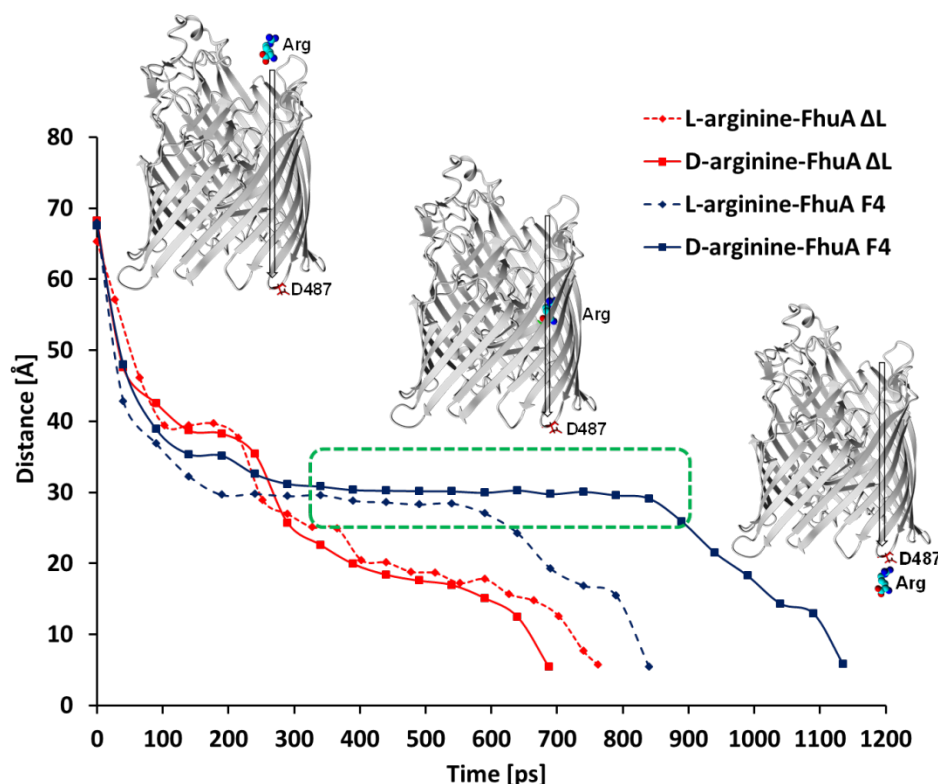


Figure 34. SMD simulations of parent FhuA Δ L and identified variant FhuAF4 showing the change in distance between arginine and the end point D487 during the translocation of D-arginine and L-arginine through FhuA channel (translocation path indicated by an arrow along the selectivity filter regions). A

plateau resulted from the interaction of D- and L-arginine with the selectivity filter region 2 (S134 and T146) is shown with a green dashed box. (Reprinted figure with permission of RSC)¹³⁸

The structural analysis of the geometry in the selectivity filter region 2 showed the persistent formation of hydrogen bonds between D-arginine with S134 and T146 located in filter region 2. On the other hand, L-arginine passes freely compared to D-arginine due to interaction only with S134 within the selectively filter region 2 (Figure 35). More interactions of D-arginine within filter region 2 of FhuAF4 compared to L-arginine resulted in altered enantiopreference.

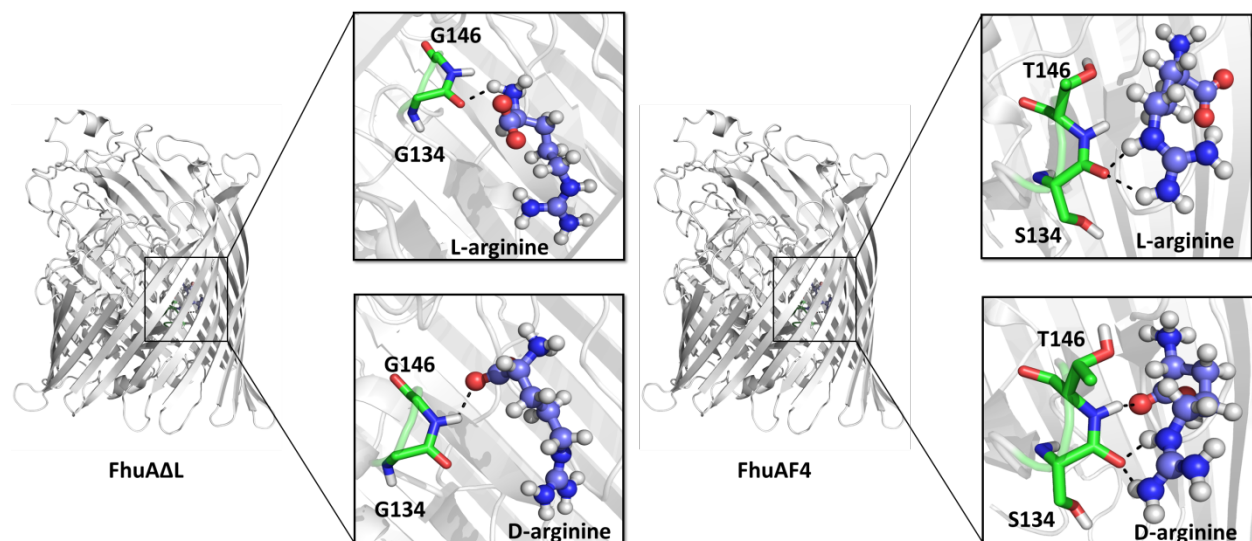


Figure 35. Hydrogen bond interactions in the selectivity filter region 2 during the translocation of arginine enantiomers for parent variant (FhuAΔL) and FhuAF4 variant. Interactions of D- and L-arginine with G134 and G146 of parent variant (FhuAΔL) and with S134 and T146 of FhuAF4 variant is shown. An additional hydrogen bond of D-arginine with T146 was observed compared to L-arginine.

4.6 Recombination of beneficial mutations

After screening all mutant libraries with the whole cell MTP screening system (Figure 27), the selective variant FhuA F4 was identified and amino acid substitutions were confirmed in the filter region 2 (G134S and G146T). Two other selective variants were detected with substitutions in filter region 1: FhuA C11 (Q362) and FhuA F9 (T41Q, Y435G, Q437W, Q439D). All three variants have a higher transport of L-arginine compared to the starting variant FhuA Δ L. The amino acid substitutions from filter region 1 and filter region 2 were recombined by means of site-directed mutagenesis with the aim of investigating further improvements in enantiopreference towards L-arginine transport (Figure 36).

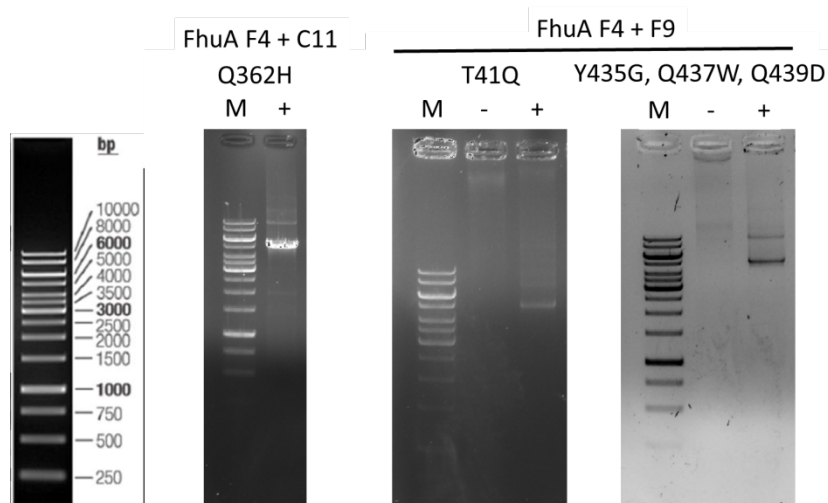


Figure 36. Agarose gel showing recombination of FhuA C11 variant with FhuA F4 and FhuA F9 with FhuA F4 by performing SDM on FhuA F4. FhuA F4 + FhuA F9 recombination was performed in two steps. M= Marker 1 kb; - = Negative control; + = Samples. (Updated figure from thesis of Annkristin Werther)

Further screening of recombined variants was performed using previously described whole cell MTP screening system (Figure 27). FhuA F4 + C11 showed a slightly higher D/L-ratio compared to FhuA F4 variant. On the contrary, the variant FhuA F4 + F9 showed a slightly reduced D/L-ratio. This indicates that FhuA F4 + F9 variant is slightly more selective towards L-arginine compared to F4 variant (Figure 37). But the combination of mutations from the two selectivity filter regions did not result in considerable increase in selectivity towards L-arginine. Slight change in selectivity is still within the standard deviation range and therefore, FhuA F4 still remains the best possible identified variant.

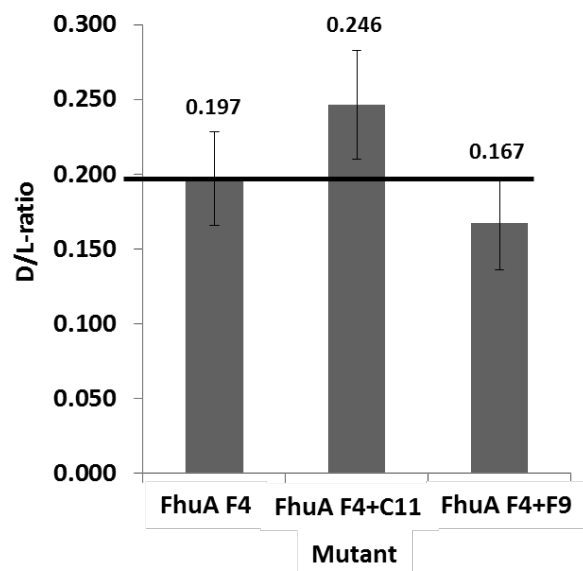


Figure 37. Determination of the amino acid selectivity after recombination of the promising FhuA variants. Shown is the D / L ratio of the single mutant FhuA F4 compared to the combination variants FhuA F4 + C11 and FhuA F4 + F9. The combination of amino acid substitutions in the recombined variants did not result in any notable improvements in enantioselectivity compared to FhuA F4.

4.7 Quantification of FhuA variants on cell surface

Quantification of FhuA variants on *E. coli* cell surface was performed in order to see the influence of imparted mutations in FhuA WT gene on expression of different variants. Additionally, it also showed any influence on transport of amino acids due to expression differences within FhuA variants. Quantification of the expressed FhuA molecules was performed through a StrepTactinII recognition sequence inserted in outer loop of FhuA variants and using Chromeo546 conjugation.^{153,159}

4.7.1 Strep tag insertion by PCR and PLICing

Insertion of Strep tag in outer loop 5 of FhuA¹⁶⁰ was achieved by overlap extension PCR (OE-PCR). The tag was inserted into the genes of three different FhuA variants: FhuA WT, FhuA Δ L and FhuA F4. The entire pPR-IBA1_FhuA plasmids were amplified using forward and reverse primers listed in Table 18. A negative control (without plasmid) was run together with the respective reaction batches for different FhuA variants. The results showed no band for the negative control and a band for all three samples with an approximate size of 5000 bp (Figure 38). Bands for all three FhuA variants showed that amplification was successful and PRC products were generated for each FhuA variant.

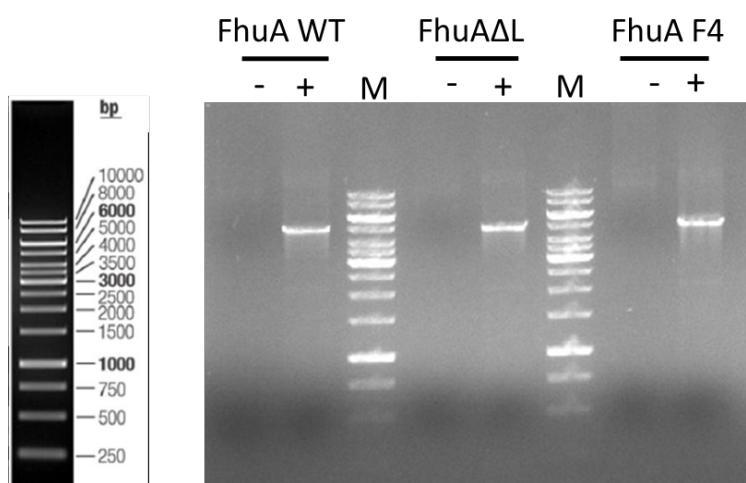


Figure 38. Results of strep tag insertion PCR. Agarose gel (1%) showing PCR amplification of strep tag insertion PCR performed for three different FhuA variants (FhuA WT, FhuA Δ L, FhuA F4). M= Marker (1 kb); - = Negative control; + = Samples. (Updated figure from thesis of Annkristin Werther)

Obtained PCR products were DpnI digested and PCR clean-up was performed to obtain a pure product devoid of any parental vector. Subsequently, PLICing was performed by iodine cleavage and hybridization of previously protected Phosphothioate Oligonucleotide (PTO) region. The ligation mixture was later transformed into *E. coli* BE BL21 Omp8 strains and cultivated overnight on LB agar plates. Some of the colonies were picked and strep tag insertion was checked via colony PCR (Figure 39).

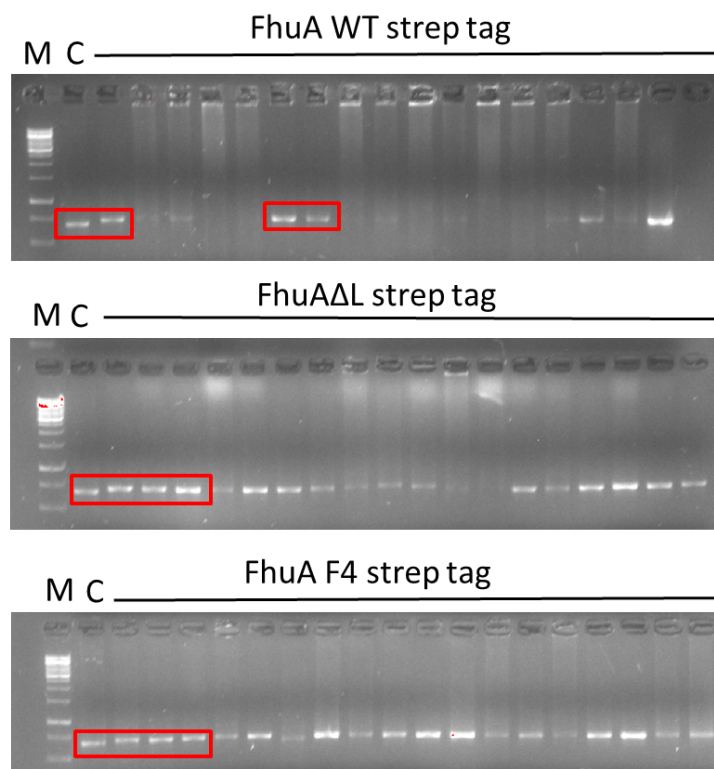


Figure 39. Results of colony PCR for strep tag insertion. Shown is a 1% agarose gel with the results of colony PCR. M = Pre-stained 1 kb protein ladder, C = Control, vector without strep tag insertion, red squares indicate the clones compared to the control, that have been send for sequencing and have been used for cultivation later. (Updated figure from thesis of Annkristin Werther)

For FhuA WT clones 1, 6, 7, 15 and 17 showed insertion of Strep tag (≈ 729 bp) compared to the control (FhuA WT without strep tag, ≈ 681 bp). For FhuA Δ L all clones showed a band that is slightly higher than the control and for FhuA F4 all besides colony 6 show a higher band. Indicating that most clones have been transformed with the vector that inherits the FhuA gene with an additional strep tag sequence. To confirm the insertion of strep tag, the plasmid was isolated from three colonies for each FhuA variant (Figure 39, marked in red boxes) and sent for sequencing. Results from sequencing showed the successful insertion of strep tag in all 9 plasmids.

4.7.2 Expression of strep tagged FhuA variants

All 9 clones that were sent for sequencing were cultivated to see if they would still express properly after insertion of Strep tag in FhuA gene. Cultivation and expression was performed in TY media and samples were taken before induction with IPTG and 3 hours after induction (Figure 40).

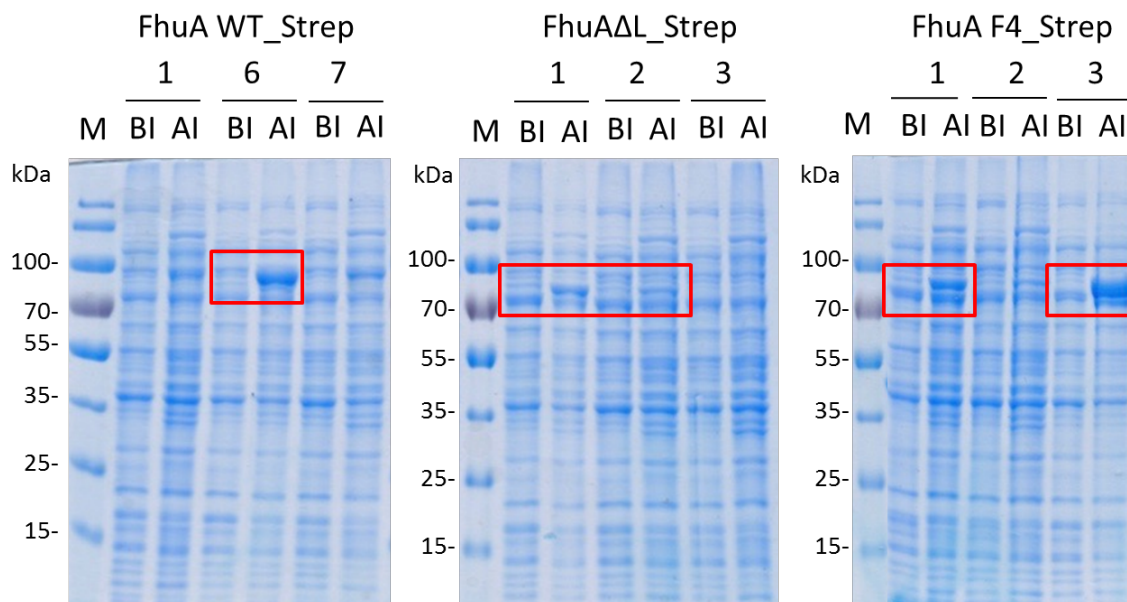


Figure 40. Results of expression of FhuA strep tag variants. Shown are 10% SDS-Gels stained with coomassi blue. Three different clones were cultivated for each FhuA variant and samples were taken before induction (BI) with IPTG and 3 h after induction (AI). Indicated in red squares are the bands of interest with FhuA with a size of 79 kDa. (Updated figure from thesis of Annkristin Werther)

The SDS-Gel showed a thick band for the expression of FhuA WT_strep clone 6, whereas faint bands were observed for clone 1 and 7. Similarly, FhuAΔL_strep clone 1 showed a band for expression, whereas clone 2 showed a very faint expression and clone 3 did not show any FhuA expression after induction. FhuAF4_strep showed thick bands after induction especially for clone 1 and 3 and a very faint expression for clone 2. Wildtype FhuA has a molecular mass of 78.9 kDa²² but FhuAΔL and FhuA F4 are slightly smaller because of the deletion of the two loops of the cork domain. SDS-PAGE showed at least one clone for all three FhuA variants still showed proper expression after insertion of Strep tag.

4.7.3 Quantification of FhuA on cell surface

After expression the samples were centrifuged and the pellet was collected to quantify the amount of FhuA expressed in the outer membrane of *E. coli*. For this purpose FhuA WT_Strep clone 6, FhuAΔL_Strep clone 1 and FhuAF4_Strep clone 3 were used because they showed the highest expression and also sequencing of the whole FhuA gene confirmed no additional mutations. Streptactin-Chromeo546 conjugate (0.5 μg/μl) was used to label the FhuA in the outer membrane of *E. coli*. After various washing steps to wash away the unbound chromeo conjugate, fluorescence was measured (Figure 41). Earlier studies suggested an amount of 4×10^7 cells per 200 μl.¹⁵³ Using this and the measured fluorescence the amount of FhuA per cell was calculated (**Error! Reference source not found.**, Figure 44).

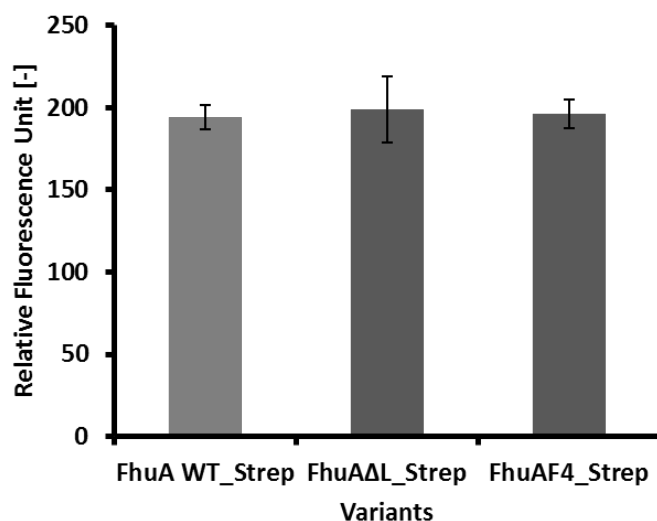


Figure 41. Quantification of FhuA WT_Strep, FhuAΔL_Strep and FhuAF4_Strep on *E. coli* cell surface with Chromeo546-Streptactin-conjugate. Fluorescence measurement (λ_{ex} 545 nm and λ_{em} = 561 nm) in cells expressing FhuA WT_Strep (light grey) and FhuAΔL_Strep and FhuAF4_Strep (dark grey) labelled with Chromeo-Streptactin. An average of ≈ 23000 molecules of FhuA WT_Strep, FhuAΔL_Strep and FhuAF4_Strep were calculated on *E. coli* cell surface after 3 h of expression. (Updated figure from thesis of Annkristin Werther)

A total of ≈ 23136 FhuA WT_Strep molecules per cell were calculated after 3 h of induction with IPTG. Similarly, a total of ≈ 23682 and ≈ 23370 molecules of FhuAΔL_Strep and FhuA F4_strep per cell, respectively, were measured (Table 24). In earlier studies an amount of 54000 molecules of FhuA could be measured for FhuA WT_Strep. A variant with the deletion of the cork domain showed a slightly smaller expression with approximately 44000 molecules¹⁶⁰. These numbers of FhuA molecules were measured after 20 h of expression, whereas here the amount was measured 3 h after induction. This showed that the reengineering of FhuA did not have considerable influence of expression of FhuA variants on *E. coli* cell surface.

Table 24. Calculated number of FhuA_Strep molecules in the outer membrane of *E. coli*. The number of FhuA was calculated after 3 h after induction with IPTG.

	Average RFU	μ l conjugate	n of FhuA per cell
FhuA WT_Strep	194.00	0.16	23136
FhuA Δ L_Strep	198.67	0.17	23682
FhuA F4_Strep	196.00	0.16	23370

5 Summary and conclusion

In the present thesis first proof of principle for chiral resolution of amino acid through an engineered membrane protein was shown. Herein, we reported for the first time chiral resolution through a β -barrel channel based on FhuA, in which two filter regions were identified and redesigned through screening of multi-site saturation mutagenesis (OmniChange) libraries, in order to achieve chiral separation of a D-/L-arginine racemate.

Structurally, FhuA contains a water channel wherein two flexible loops in the cork domain (loop1; residue 35-40 and loop2; residues 135-145) were shortened to generate two selectivity filter regions (filter1 and filter2). Additionally, residues located at the inner interface between barrel and cork domain of FhuA wild type (WT) (PDB ID: 1BY3) were analyzed by *in silico* saturation mutagenesis using FoldX method to identify beneficial substitutions for stabilization of cork domain within the barrel of FhuA. Three substitutions (Q62D, R81W, and N117L) were selected based on largest distance from the generated loop cavity and highest stabilization energy ($\Delta\Delta G < -1$ kcal/mol). Identified positions were substituted by site directed mutagenesis to finally generate a variant FhuA Δ L. FhuA Δ L with the two shortened loops was equally well expressed and circular dichroism (CD) spectra confirmed its β -barrel structure. Calcein release kinetics of polymersomes loaded with a self-quenching concentration of calcein proved that after loop shortening the cork domain keeps its location within the β -barrel of FhuA Δ L.

Furthermore, a directed evolution protocol was developed to identify chiral FhuA Δ L variants through modified citrulline colorimetric screening system at the computationally proposed filter regions. Structural analysis yielded 23 amino acid positions within 5 Å from the respective filter regions. These identified positions were grouped into six different OmniChange libraries to perform site saturation mutagenesis using NNK degenerate codons encoding for all 20 proteinogenic amino acids. The generated libraries were screened using modified citrulline colorimetric screening system adapted to quantify conversion of D- and L- arginine. Each FhuA variant was replicated from a 96-well MTP master plate into two 96-well MTPs and uptake of D- and L- arginine through the FhuA variant in the outer *E. coli* membrane was quantified through the conversion of D- or L-arginine in separated experiments. The ratio of D-/L-conversion was used as a benchmark to select FhuA variants with altered enantioference and independently from the expression level. A total of 6000 clones (library 1-6; 1000 clones per library) were screened and led finally to the identification of the variant FhuAF4 (amino acid substitutions: G134S, G146T; numbering based on PDB ID: 1BY3) showing 1.84 times higher transport of L-arginine compared to FhuA Δ L. Both identified substitutions are located in the selectivity filter region 2 and both variants and the FhuA WT had average of ≈ 23000 FhuA molecules per cell in outer membrane of *E. coli*. Quantification of the expressed FhuA molecules was performed through a StrepTactinII recognition sequence and using Chromeo546 conjugation.

Finally, the most beneficial variant FhuAF4 was subjected to a whole cell experiment with a racemic mixture of D-/L-arginine to validate the chiral separation through FhuAF4. In this experiment the two cell cultures expressing FhuA were grown with Arginine deiminase (ADI; K_{cat} : $18.27 \pm 0.23 \text{ s}^{-1}$, $S_{0.5}$: $0.33 \pm 0.02 \text{ mM}$) for efficient L-arginine conversion and D-amino acid oxidase (DAO 222D224G; K_{cat} : 240 min^{-1} , K_m : 1.7 mM) for D-arginine conversion. Both cultures were mixed in a ratio of 1:4.5 to compensate for the higher activity of ADI compared to DAO and to enable comparable conversion of D- and L-arginine. The mixtures of cells were incubated separately with racemic mixture of arginine (5 mM each). Samples were taken at regular intervals and arginine concentrations in the “supernatant” were quantified using a chiral HPLC method. The translocation efficiency of L-arginine through FhuAF4 was determined by comparing with the parent variant (FhuA Δ L). FhuAF4 showed an improved ee % of 23.91 at 52.39 % conversion whereas parent FhuA Δ L variant had an ee % of 11.33 at 44.50 % conversion which is close to ee % of 8.35 at 43.14 % conversion of whole *E. coli* cells without recombinantly expressed FhuA. The latter represents the uptake ratio of D-/L-arginine of the selected *E. coli* BE BL21 (DE3) Omp8 strain.

Steered molecular dynamics (SMD) simulations were carried out for molecular understanding of observed altered enantioselectivity of FhuAF4 variant towards L-arginine compared to the FhuA Δ L variant. In SMD simulations, arginine was pulled from the top of the FhuA channel towards residue D487 located at the bottom of the FhuA channel. In FhuA Δ L variant, calculated distances between arginine and the end point D487 decrease sharply in the first ≈ 200 ps of the SMD simulations indicating the free diffusion of arginine before entering the selectivity filter region 2. In FhuAF4 variant, less interactions of both D- and L-arginine with the filter region 2 were observed and both enantiomers pass freely. Interestingly, in FhuAF4 variant, transport of D-arginine is hindered and steered transport is slowed down, as indicated by a longer residence time close to the selectivity filter region 2. The energetic barrier for transport under constant pulling force in the SMD simulation can be observed as a plateau.

The structural analysis of the geometry in the selectivity filter region 2 showed the persistent formation of hydrogen bonds between D-arginine with S134 and T146 located in filter region 2. On the other hand, L-arginine passes freely compared to D-arginine due to interaction only with S134 within the selectivity filter region 2. More interactions of D-arginine within filter region 2 of FhuAF4 compared to L-arginine resulted in altered enantioselectivity.

In conclusion, we have designed a novel whole cell screening system and the filter region 2 to engineer chiral FhuA channel proteins on the example of D-/L-arginine separation. Interestingly, even a subtle change of just two amino acids considerably influenced the selectivity of FhuA channel. It is likely that with the identified filter region and OmniChange libraries further improvements are achievable for other amino acids and a broader range of enantiomers. The chiral FhuA channel proteins would be an excellent scaffold for generation of chiral membrane

based on protein polymer conjugates with a high potential for novel and scalable downstream processes.

Work done in the present thesis is an important step towards utilization of porins for generation of chiral porin-polymer membranes. This work shows first proof of principle that porins can be engineered for chiral separation of compounds. Additionally, simulation studies provide valuable insights in investigation of a chiral recognition of amino acids based on the engineered channel protein FhuA. Generation of an engineered chiral selective porin and its utilization in porin based membranes is the first step towards a novel, scalable and cost-effective downstream processing strategy when compared to industrially used methods such as crystallization.

References

- 1 Lehninger, A. L., Nelson, D. & Cox, M. M. (Springer Verlag, Berlin, Heidelberg, New York, 2001).
- 2 Smith, S. W. Chiral toxicology: it's the same thing...only different. *Toxicol Sci* **110**, 4-30, doi:10.1093/toxsci/kfp097 (2009).
- 3 Caner, H., Groner, E., Levy, L. & Agranat, I. Trends in the development of chiral drugs. *Drug Discov Today* **9**, 105-110 (2004).
- 4 Maier, N. M., Franco, P. & Lindner, W. Separation of enantiomers: needs, challenges, perspectives. *J Chromatogr A* **906**, 3-33 (2001).
- 5 Jirage, K. B. & Martin, C. R. New developments in membrane-based separations. *Trends Biotechnol* **17**, 197-200, doi:10.1016/S0167-7799(98)01296-7 (1999).
- 6 Rouhi, A. M. Chirality at work. *Chemical & engineering news* **81**, 56-56 (2003).
- 7 Sheldon, R. A. *Chirotechnology: industrial synthesis of optically active compounds*. (CRC press, 1993).
- 8 Lin, G., You, Q. & Cheng, J. Chiral Drugs. *Chemistry and Biological Action*. Wiley, ed **1** (2011).
- 9 Flack, H. Louis Pasteur's discovery of molecular chirality and spontaneous resolution in 1848, together with a complete review of his crystallographic and chemical work. *Acta. Crystallogr. A* **65**, 371-389 (2009).
- 10 Lorenz, H. & Seidel-Morgenstern, A. Processes to separate enantiomers. *Angew. Chem. Int. Ed.* **53**, 1218-1250 (2014).
- 11 Crosby, J. Synthesis of optically active compounds: a large scale perspective. *Tetrahedron* **47**, 4789-4846 (1991).
- 12 Kotha, S. Opportunities in asymmetric synthesis: an industrial prospect. *Tetrahedron* **50**, 3639-3662 (1994).
- 13 Kinbara, K. Design of resolving agents based on crystal engineering. *Synlett* **2005**, 0732-0743 (2005).
- 14 Alexakis, A., Frutos, J. C., Mutti, S. & Mangeney, P. Chiral Diamines for a New Protocol To Determine the Enantiomeric Composition of Alcohols, Thiols, and Amines by ³¹P, ¹H, ¹³C, and ¹⁹F NMR. *J. Org. Chem.* **59**, 3326-3334 (1994).
- 15 Collet, A., Brienne, M. J. & Jacques, J. Optical resolution by direct crystallization of enantiomer mixtures. *Chem. Rev.* **80**, 215-230 (1980).

-
- 16 Alvarez Rodrigo, A., Lorenz, H. & Seidel-Morgenstern, A. Online monitoring of preferential crystallization of enantiomers. *Chirality* **16**, 499-508 (2004).
- 17 Okamoto, Y. & Yashima, E. Polysaccharide derivatives for chromatographic separation of enantiomers. *Angew. Chem. Int. Ed.* **37**, 1020-1043 (1998).
- 18 Armstrong, D. W. Chiral stationary phases for high performance liquid chromatographic separation of enantiomers: a mini-review. *Journal of liquid chromatography* **7**, 353-376 (1984).
- 19 Ghanem, A. & Aboul-Enein, H. Y. Application of lipases in kinetic resolution of racemates. *Chirality* **17**, 1-15 (2005).
- 20 Vedejs, E. & Jure, M. Efficiency in nonenzymatic kinetic resolution. *Angew. Chem. Int. Ed.* **44**, 3974-4001 (2005).
- 21 Ferguson, A. D., Breed, J., Diederichs, K., Welte, W. & Coulton, J. W. An internal affinity-tag for purification and crystallization of the siderophore receptor FhuA, integral outer membrane protein from Escherichia coli K-12. *Protein Sci* **7**, 1636-1638, doi:10.1002/pro.5560070719 (1998).
- 22 Ferguson, A. D., Hofmann, E., Coulton, J. W., Diderichs, K. & Welte, W. in *Science* Vol. 282 2215-2220 (1998).
- 23 Gutschmann, T., Heimbürg, T., Keyser, U., Mahendran, K. R. & Winterhalter, M. Protein reconstitution into freestanding planar lipid membranes for electrophysiological characterization. *nature protocols* **10**, 188 (2015).
- 24 Wimley, W. C. The versatile beta-barrel membrane protein. *Curr Opin Struct Biol* **13**, 404-411 (2003).
- 25 Sansom, M. S. & Kerr, I. D. Transbilayer pores formed by beta-barrels: molecular modeling of pore structures and properties. *Biophys J* **69**, 1334-1343, doi:10.1016/S0006-3495(95)80000-7 (1995).
- 26 Killmann, H., Benz, R. & Braun, V. Conversion of the FhuA transport protein into a diffusion channel through the outer membrane of Escherichia coli. *The EMBO Journal* **12**, 3007-3016 (1993).
- 27 Nallani, M., Benito, S., Onaca, O., Graff, A., Lindemann, M., Winterhalter, M., Meier, W. & Schwaneberg, U. A nanocompartment system (Synthosome) designed for biotechnological applications. *J Biotechnol* **123**, 50-59, doi:10.1016/j.jbiotec.2005.10.025 (2006).
- 28 Polgár, L. (Springer-Verlag, Berlin, 1999).
- 29 Wolfe, A. J., Mohammad, M. M., Thakur, A. K. & Movileanu, L. Global redesign of a native beta-barrel scaffold. *Biochim Biophys Acta* **1858**, 19-29, doi:10.1016/j.bbamem.2015.10.006 (2016).

-
- 30 Krewinkel, M., Dworeck, T. & Fioroni, M. Engineering of an E. coli outer membrane protein FhuA with increased channel diameter. *J Nanobiotechnology* **9**, 33, doi:10.1186/1477-3155-9-33 (2011).
- 31 Koebnik, R., Locher, K. P. & Van Gelder, P. Structure and function of bacterial outer membrane proteins: barrels in a nutshell. *Mol Microbiol* **37**, 239-253 (2000).
- 32 Onaca, O., Sarkar, P., Roccatano, D., Friedrich, T., Hauer, B., Grzelakowski, M., Guven, A., Fioroni, M. & Schwaneberg, U. Functionalized nanocompartments (synthosomes) with a reduction-triggered release system. *Angew Chem Int Ed Engl* **47**, 7029-7031, doi:10.1002/anie.200801076 (2008).
- 33 Güven, A., Fioroni, M., Hauer, B. & Schwaneberg, U. Molecular understanding of sterically controlled compound release through an engineered channel protein (FhuA). *Journal of nanobiotechnology* **8**, 14 (2010).
- 34 Güven, A., Dworeck, T., Fioroni, M. & Schwaneberg, U. Residue K556-A Light Triggerable Gatekeeper to Sterically Control Translocation in FhuA. *Advanced Engineering Materials* **13**, B324-B329 (2011).
- 35 Liu, Z., Ghai, I., Winterhalter, M. & Schwaneberg, U. Engineering enhanced pore sizes using FhuA Δ 1-160 from E. coli outer membrane as template. *ACS sensors* **2**, 1619-1626 (2017).
- 36 Muhammad, N., Dworeck, T., Fioroni, M. & Schwaneberg, U. Engineering of the E. coli outer membrane protein FhuA to overcome the hydrophobic mismatch in thick polymeric membranes. *Journal of nanobiotechnology* **9**, 8 (2011).
- 37 Philippart, F., Arlt, M., Gotzen, S., Tenne, S. J., Bocola, M., Chen, H. H., Zhu, L., Schwaneberg, U. & Okuda, J. A hybrid ring-opening metathesis polymerization catalyst based on an engineered variant of the beta-barrel protein FhuA. *Chemistry* **19**, 13865-13871, doi:10.1002/chem.201301515 (2013).
- 38 Kasianowicz, J. J., Brandin, E., Branton, D. & Deamer, D. W. Characterization of individual polynucleotide molecules using a membrane channel. *Proceedings of the National Academy of Sciences* **93**, 13770-13773 (1996).
- 39 Mathé, J., Aksimentiev, A., Nelson, D. R., Schulten, K. & Meller, A. Orientation discrimination of single-stranded DNA inside the α -hemolysin membrane channel. *Proceedings of the National Academy of Sciences* **102**, 12377-12382 (2005).
- 40 Meller, A., Nivon, L., Brandin, E., Golovchenko, J. & Branton, D. Rapid nanopore discrimination between single polynucleotide molecules. *Proceedings of the National Academy of Sciences* **97**, 1079-1084 (2000).
- 41 Laszlo, A. H., Derrington, I. M., Brinkerhoff, H., Langford, K. W., Nova, I. C., Samson, J. M., Bartlett, J. J., Pavlenok, M. & Gundlach, J. H. Detection and mapping of 5-methylcytosine and 5-hydroxymethylcytosine with nanopore MspA. *Proceedings of the National Academy of Sciences* **110**, 18904-18909 (2013).

-
- 42 Chang, J., Li, H., Hou, T. & Li, F. based fluorescent sensor for rapid naked-eye detection of acetylcholinesterase activity and organophosphorus pesticides with high sensitivity and selectivity. *Biosensors and Bioelectronics* **86**, 971-977 (2016).
- 43 Murata, K., Mitsuoka, K., Hirai, T., Walz, T., Agre, P., Heymann, J. B., Engel, A. & Fujiyoshi, Y. Structural determinants of water permeation through aquaporin-1. *Nature* **407**, 599 (2000).
- 44 Kumar, M., Grzelakowski, M., Zilles, J., Clark, M. & Meier, W. Highly permeable polymeric membranes based on the incorporation of the functional water channel protein Aquaporin Z. *Proceedings of the National Academy of Sciences* **104**, 20719-20724 (2007).
- 45 Adler-Nissen, J. Limited enzymic degradation of proteins: A new approach in the industrial application of hydrolases. *Journal of Chemical Technology and Biotechnology* **32**, 138-156 (1982).
- 46 Arnold, F. H. & Moore, J. C. in *New Enzymes for Organic Synthesis* 1-14 (Springer, 1997).
- 47 Lutz, S. & Bornscheuer, U. T. *Protein engineering handbook*. Vol. 1 (Wiley Online Library, 2009).
- 48 Spickermann, D., Kara, S., Barackov, I., Hollmann, F., Schwaneberg, U., Duenkelmann, P. & Leggewie, C. Alcohol dehydrogenase stabilization by additives under industrially relevant reaction conditions. *Journal of molecular catalysis B: enzymatic* **103**, 24-28 (2014).
- 49 Hilterhaus, L., Liese, A., Kettling, U. & Antranikian, G. *Applied biocatalysis: from fundamental science to industrial applications*. (John Wiley & Sons, 2016).
- 50 Chen, R. Enzyme engineering: rational redesign versus directed evolution. *Trends in biotechnology* **19**, 13-14 (2001).
- 51 Lim, B. N., Choong, Y. S., Ismail, A., Glökler, J., Konthur, Z. & Lim, T. S. Directed evolution of nucleotide-based libraries using lambda exonuclease. *Biotechniques* **53**, 357-364 (2012).
- 52 Stemmer, W. P. DNA shuffling by random fragmentation and reassembly: in vitro recombination for molecular evolution. *Proceedings of the National Academy of Sciences* **91**, 10747-10751 (1994).
- 53 Kuchner, O. & Arnold, F. H. Directed evolution of enzyme catalysts. *Trends in biotechnology* **15**, 523-530 (1997).
- 54 Mills, D. R., Peterson, R. & Spiegelman, S. An extracellular Darwinian experiment with a self-duplicating nucleic acid molecule. *Proceedings of the National Academy of Sciences of the United States of America* **58**, 217 (1967).

-
- 55 Chen, K. & Arnold, F. H. Tuning the activity of an enzyme for unusual environments: sequential random mutagenesis of subtilisin E for catalysis in dimethylformamide. *Proceedings of the National Academy of Sciences* **90**, 5618-5622 (1993).
- 56 Wong, T. S., Roccatano, D. & Schwaneberg, U. Steering directed protein evolution: strategies to manage combinatorial complexity of mutant libraries. *Environmental microbiology* **9**, 2645-2659 (2007).
- 57 Wong, T. S., Zhurina, D. & Schwaneberg, U. The diversity challenge in directed protein evolution. *Combinatorial chemistry & high throughput screening* **9**, 271-288 (2006).
- 58 Cadwell, R. C. & Joyce, G. F. Randomization of genes by PCR mutagenesis. *Genome research* **2**, 28-33 (1992).
- 59 Cirino, P. C., Mayer, K. M. & Umeno, D. in *Directed evolution library creation* 3-9 (Springer, 2003).
- 60 Patrick, W. M., Firth, A. E. & Blackburn, J. M. User-friendly algorithms for estimating completeness and diversity in randomized protein-encoding libraries. *Protein engineering* **16**, 451-457 (2003).
- 61 Wong, T. S., Tee, K. L., Hauer, B. & Schwaneberg, U. Sequence saturation mutagenesis (SeSaM): a novel method for directed evolution. *Nucleic Acids Research* **32**, e26-e26 (2004).
- 62 Chen, R. A general strategy for enzyme engineering. *Trends Biotechnol* **17**, 344-345 (1999).
- 63 Santiago, G., Martínez-Martínez, M., Alonso, S., Bargiela, R., Coscolín, C., Golyshin, P. N., Guallar, V. & Ferrer, M. Rational engineering of multiple active sites in an ester hydrolase. *Biochemistry* **57**, 2245-2255 (2018).
- 64 Ozaki, S.-i., Matsui, T., Roach, M. P. & Watanabe, Y. Rational molecular design of a catalytic site: engineering of catalytic functions to the myoglobin active site framework. *Coordination Chemistry Reviews* **198**, 39-59 (2000).
- 65 Xu, L.-H. & Du, Y.-L. Rational and semi-rational engineering of cytochrome P450s for biotechnological applications. *Synthetic and systems biotechnology* (2018).
- 66 Ruff, A. J., Dennig, A. & Schwaneberg, U. To get what we aim for—progress in diversity generation methods. *The FEBS journal* **280**, 2961-2978 (2013).
- 67 Dennig, A., Shivange, A. V., Marienhagen, J. & Schwaneberg, U. OmniChange: the sequence independent method for simultaneous site-saturation of five codons. *PloS one* **6**, e26222 (2011).
- 68 Shivange, A. V., Dennig, A. & Schwaneberg, U. Multi-site saturation by OmniChange yields a pH-and thermally improved phytase. *Journal of biotechnology* **170**, 68-72 (2014).

-
- 69 Dennig, A., Marienhagen, J., Ruff, A. J. & Schwaneberg, U. in *Directed Evolution Library Creation* 139-149 (Springer, 2014).
- 70 Horn, F. The breakdown of arginine to citrulline by *Bacillus pyocyaneus*. *Hoppe Seylers Z Physiol Chem* **216**, 244-247 (1933).
- 71 Lu, X., Li, L., Wu, R., Feng, X., Li, Z., Yang, H., Wang, C., Guo, H., Galkin, A. & Herzberg, O. Kinetic analysis of *Pseudomonas aeruginosa* arginine deiminase mutants and alternate substrates provides insight into structural determinants of function. *Biochemistry* **45**, 1162-1172 (2006).
- 72 Das, K., Butler, G. H., Kwiatkowski, V., Clark Jr, A. D., Yadav, P. & Arnold, E. Crystal structures of arginine deiminase with covalent reaction intermediates: implications for catalytic mechanism. *Structure* **12**, 657-667 (2004).
- 73 Zhu, L., Tee, K. L., Roccatano, D., Sonmez, B., Ni, Y., Sun, Z. H. & Schwaneberg, U. Directed evolution of an antitumor drug (arginine deiminase PpADI) for increased activity at physiological pH. *ChemBioChem* **11**, 691-697 (2010).
- 74 Schofield, P. J., Edwards, M. R., Matthews, J. & Wilson, J. R. The pathway of arginine catabolism in *Giardia intestinalis*. *Molecular and biochemical parasitology* **51**, 29-36 (1992).
- 75 Biagini, G. A., Yarlett, N., Ball, G. E., Billetz, A. C., Lindmark, D. G., Martinez, M. P., Lloyd, D. & Edwards, M. R. Bacterial-like energy metabolism in the amitochondriate protozoan *Hexamita inflata*. *Molecular and biochemical parasitology* **128**, 11-19 (2003).
- 76 YARLETT, N., LINDMARK, D. G., GOLDBERG, B., Ali Moharrami, M. & BACCHI, C. J. Subcellular localization of the enzymes of the arginine dihydrolase pathway in *Trichomonas vaginalis* and *Tritrichomonas foetus*. *Journal of Eukaryotic Microbiology* **41**, 554-559 (1994).
- 77 Linstead, D. & Cranshaw, M. A. The pathway of arginine catabolism in the parasitic flagellate *Trichomonas vaginalis*. *Molecular and biochemical parasitology* **8**, 241-252 (1983).
- 78 Takaku, H., Takase, M., Abe, S. I., Hayashi, H. & Miyazaki, K. In vivo anti-tumor activity of arginine deiminase purified from *Mycoplasma arginini*. *International journal of cancer* **51**, 244-249 (1992).
- 79 Wheatley, D. N. Controlling cancer by restricting arginine availability—arginine-catabolizing enzymes as anticancer agents. *Anti-cancer drugs* **15**, 825-833 (2004).
- 80 Scott, L., Lamb, J., Smith, S. & Wheatley, D. Single amino acid (arginine) deprivation: rapid and selective death of cultured transformed and malignant cells. *British journal of cancer* **83**, 800 (2000).
- 81 Wheatley, D. N. in *Seminars in cancer biology*. 247-253 (Elsevier).

-
- 82 Takaku, H., Matsumoto, M., Misawa, S. & Miyazaki, K. Anti-tumor activity of arginine deiminase from *Mycoplasma arginini* and its growth-inhibitory mechanism. *Japanese journal of cancer research* **86**, 840-846 (1995).
- 83 Sugimura, K., Ohno, T., Fukuda, S., Wada, Y., Kimura, T. & Azuma, I. Tumor growth inhibitory activity of a lymphocyte blastogenesis inhibitory factor. *Cancer research* **50**, 345-349 (1990).
- 84 Storr, J. & Burton, A. The effects of arginine deficiency on lymphoma cells. *British journal of cancer* **30**, 50 (1974).
- 85 Szlosarek, P. W., Klabatsa, A., Pallaska, A., Sheaff, M., Balkwill, F. R. & Fennell, D. (AACR, 2006).
- 86 Smith, S. M., Uslaner, J. M. & Hutson, P. H. The therapeutic potential of D-amino acid oxidase (DAAO) inhibitors. *The open medicinal chemistry journal* **4**, 3 (2010).
- 87 Pollegioni, L., Fukui, K. & Massey, V. Studies on the kinetic mechanism of pig kidney D-amino acid oxidase by site-directed mutagenesis of tyrosine 224 and tyrosine 228. *Journal of Biological Chemistry* **269**, 31666-31673 (1994).
- 88 Dixon, M. & Kleppe, K. D-Amino acid oxidase II. Specificity, competitive inhibition and reaction sequence. *Biochimica et Biophysica Acta (BBA)-Nucleic Acids and Protein Synthesis* **96**, 368-382 (1965).
- 89 Pollegioni, L., Piubelli, L., Sacchi, S., Pilone, M. & Molla, G. Physiological functions of D-amino acid oxidases: from yeast to humans. *Cellular and molecular life sciences* **64**, 1373-1394 (2007).
- 90 Krebs, H. A. Metabolism of amino-acids: Deamination of amino-acids. *Biochemical Journal* **29**, 1620 (1935).
- 91 Massey, L. K., Sokatch, J. R. & Conrad, R. S. Branched-chain amino acid catabolism in bacteria. *Bacteriological reviews* **40**, 42 (1976).
- 92 Fuchs, S. A., Berger, R., Klomp, L. W. & de Koning, T. J. D-amino acids in the central nervous system in health and disease. *Molecular genetics and metabolism* **85**, 168-180 (2005).
- 93 Hashimoto, A., Nishikawa, T., Konno, R., Niwa, A., Yasumura, Y., Oka, T. & Takahashi, K. Free D-serine, D-aspartate and D-alanine in central nervous system and serum in mutant mice lacking D-amino acid oxidase. *Neuroscience letters* **152**, 33-36 (1993).
- 94 Pilone, M. D-Amino acid oxidase: new findings. *Cellular and Molecular Life Sciences CMLS* **57**, 1732-1747 (2000).
- 95 Wilson, P. D. Enzyme changes in ageing mammals. *Gerontology* **19**, 79-125 (1973).

-
- 96 D'Aniello, A., D'Onofrio, G., Pischetola, M., D'Aniello, G., Vetere, A., Petrucelli, L. & Fisher, G. H. Biological role of D-amino acid oxidase and D-aspartate oxidase. Effects of D-amino acids. *Journal of Biological Chemistry* **268**, 26941-26949 (1993).
- 97 Helfman, P. M., Bada, J. L. & Shou, M.-Y. Considerations on the role of aspartic acid racemization in the aging process. *Gerontology* **23**, 419-425 (1977).
- 98 Setoyama, C., Nishina, Y., Mizutani, H., Miyahara, I., Hirotsu, K., Kamiya, N., Shiga, K. & Miura, R. Engineering the substrate specificity of porcine kidney d-amino acid oxidase by mutagenesis of the "active-site lid". *Journal of biochemistry* **139**, 873-879 (2006).
- 99 Schwechheimer, C. & Kuehn, M. J. Outer-membrane vesicles from Gram-negative bacteria: biogenesis and functions. *Nature reviews microbiology* **13**, 605 (2015).
- 100 Palivan, C. G., Goers, R., Najer, A., Zhang, X., Car, A. & Meier, W. Bioinspired polymer vesicles and membranes for biological and medical applications. *Chemical society reviews* **45**, 377-411 (2016).
- 101 Sutisna, B., Polymeropoulos, G., Mygiakis, E., Musteata, V., Peinemann, K.-V., Smilgies, D.-M., Hadjichristidis, N. & Nunes, S. P. Artificial membranes with selective nanochannels for protein transport. *Polymer Chemistry* **7**, 6189-6201 (2016).
- 102 Taubert, A. Controlling water transport through artificial polymer/protein hybrid membranes. *Proceedings of the National Academy of Sciences* **104**, 20643-20644 (2007).
- 103 Meller, A. & Branton, D. Single molecule measurements of DNA transport through a nanopore. *Electrophoresis* **23**, 2583-2591 (2002).
- 104 Chaize, B., Colletier, J.-P., Winterhalter, M. & Fournier, D. Encapsulation of enzymes in liposomes: high encapsulation efficiency and control of substrate permeability. *Artificial cells, blood substitutes, and biotechnology* **32**, 67-75 (2004).
- 105 Jahadi, M. & Khosravi-Darani, K. Liposomal encapsulation enzymes: from medical applications to kinetic characteristics. *Mini reviews in medicinal chemistry* **17**, 366-370 (2017).
- 106 Municoy, S. & Bellino, M. A liposome-actuated enzyme system and its capability as a self-biomineralized silica nanoreactor. *RSC Advances* **7**, 67-70 (2017).
- 107 Bangham, A. D. & Horne, R. Negative staining of phospholipids and their structural modification by surface-active agents as observed in the electron microscope. *Journal of molecular biology* **8**, 660-IN610 (1964).
- 108 Torchilin, V. P. Recent advances with liposomes as pharmaceutical carriers. *Nature reviews Drug discovery* **4**, 145 (2005).

-
- 109 Lasic, D. & Papahadjopoulos, D. Liposomes revisited. *Science* **267**, 1275-1277 (1995).
- 110 Sharma, A. & Sharma, U. S. Liposomes in drug delivery: progress and limitations. *International journal of pharmaceutics* **154**, 123-140 (1997).
- 111 Gregoriadis, G. Engineering liposomes for drug delivery: progress and problems. *Trends in biotechnology* **13**, 527-537 (1995).
- 112 Langer, R. Drug delivery and targeting. *NATURE-LONDON*-, 5-10 (1998).
- 113 Allen, T. M. & Cullis, P. R. Liposomal drug delivery systems: from concept to clinical applications. *Advanced drug delivery reviews* **65**, 36-48 (2013).
- 114 Samad, A., Sultana, Y. & Aqil, M. Liposomal drug delivery systems: an update review. *Current drug delivery* **4**, 297-305 (2007).
- 115 Mozafari, M. R. Liposomes: an overview of manufacturing techniques. *Cellular and Molecular Biology Letters* **10**, 711 (2005).
- 116 Discher, D. E. & Ahmed, F. Polymersomes. *Annu. Rev. Biomed. Eng.* **8**, 323-341 (2006).
- 117 LoPresti, C., Lomas, H., Massignani, M., Smart, T. & Battaglia, G. Polymersomes: nature inspired nanometer sized compartments. *Journal of Materials Chemistry* **19**, 3576-3590 (2009).
- 118 Bermudez, H., Brannan, A. K., Hammer, D. A., Bates, F. S. & Discher, D. E. Molecular weight dependence of polymersome membrane structure, elasticity, and stability. *Macromolecules* **35**, 8203-8208 (2002).
- 119 Messenger, L., Gaitzsch, J., Chierico, L. & Battaglia, G. Novel aspects of encapsulation and delivery using polymersomes. *Current opinion in pharmacology* **18**, 104-111 (2014).
- 120 Onaca, O., Nallani, M., Ihle, S., Schenk, A. & Schwaneberg, U. Functionalized nanocompartments (Synthosomes): Limitations and prospective applications in industrial biotechnology. *Biotechnology Journal: Healthcare Nutrition Technology* **1**, 795-805 (2006).
- 121 Helenius, A. & Simons, K. Solubilization of membranes by detergents. *Biochimica et Biophysica Acta (BBA)-Reviews on Biomembranes* **415**, 29-79 (1975).
- 122 le Maire, M., Champeil, P. & Møller, J. V. Interaction of membrane proteins and lipids with solubilizing detergents. *Biochimica et Biophysica Acta (BBA)-Biomembranes* **1508**, 86-111 (2000).

-
- 123 Seddon, A. M., Curnow, P. & Booth, P. J. Membrane proteins, lipids and detergents: not just a soap opera. *Biochimica et Biophysica Acta (BBA)-Biomembranes* **1666**, 105-117 (2004).
- 124 Shikata, T., Hirata, H. & Kotaka, T. Micelle formation of detergent molecules in aqueous media: viscoelastic properties of aqueous cetyltrimethylammonium bromide solutions. *Langmuir* **3**, 1081-1086 (1987).
- 125 Lund, S., Orłowski, S., De Foresta, B., Champeil, P., Le Maire, M. & Møller, J. Detergent structure and associated lipid as determinants in the stabilization of solubilized Ca²⁺-ATPase from sarcoplasmic reticulum. *Journal of Biological Chemistry* **264**, 4907-4915 (1989).
- 126 Dworeck, T., Petri, A.-K., Muhammad, N., Fioroni, M. & Schwaneberg, U. FhuA deletion variant Δ 1-159 overexpression in inclusion bodies and refolding with Polyethylene-Poly (ethylene glycol) diblock copolymer. *Protein expression and purification* **77**, 75-79 (2011).
- 127 Tenne, S.-J., Kinzel, J., Arlt, M., Sibilla, F., Bocola, M. & Schwaneberg, U. 2-Methyltetrahydrofuran and cyclopentylmethylether: Two green solvents for efficient purification of membrane proteins like FhuA. *Journal of Chromatography B* **937**, 13-17 (2013).
- 128 Michaux, C., Pomroy, N. C. & Privé, G. G. Refolding SDS-denatured proteins by the addition of amphipathic cosolvents. *Journal of molecular biology* **375**, 1477-1488 (2008).
- 129 Michaux, C., Roussel, G., Lopes-Rodrigues, M., Matagne, A. & Perpète, E. Unravelling the mechanisms of a protein refolding process based on the association of detergents and co-solvents. *Journal of Peptide Science* **22**, 485-491 (2016).
- 130 Kinzel, J., Sauer, D. F., Bocola, M., Arlt, M., Garakani, T. M., Thiel, A., Beckerle, K., Polen, T., Okuda, J. & Schwaneberg, U. 2-Methyl-2, 4-pentanediol (MPD) boosts as detergent-substitute the performance of β -barrel hybrid catalyst for phenylacetylene polymerization. *Beilstein journal of organic chemistry* **13**, 1498-1506 (2017).
- 131 Locher, K. P., Rees, B., Koebnik, R., Mitschler, A., Moulinier, L., Rosenbusch, J. P. & Moras, D. Transmembrane signaling across the ligand-gated FhuA receptor: crystal structures of free and ferrichrome-bound states reveal allosteric changes. *Cell* **95**, 771-778 (1998).
- 132 Krieger, E. & Vriend, G. YASARA View—molecular graphics for all devices—from smartphones to workstations. *Bioinformatics* **30**, 2981-2982 (2014).
- 133 Van Durme, J., Delgado, J., Stricher, F., Serrano, L., Schymkowitz, J. & Rousseau, F. A graphical interface for the FoldX forcefield. *Bioinformatics* **27**, 1711-1712 (2011).
- 134 Duan, Y., Wu, C., Chowdhury, S., Lee, M. C., Xiong, G., Zhang, W., Yang, R., Cieplak, P., Luo, R. & Lee, T. A point-charge force field for molecular mechanics simulations of proteins based on condensed-phase quantum mechanical calculations. *J. Comput. Chem.* **24**, 1999-2012 (2003).

-
- 135 Tenne, S.-J. & Schwaneberg, U. First insights on organic cosolvent effects on FhuA wildtype and FhuA Δ 1-159. *International journal of molecular sciences* **13**, 2459-2471 (2012).
- 136 Bonhivers, M., Plancon, L., Ghazi, A., Boulanger, A., Le Maire, M., Lambert, O., Rigaud, J. & Letellier, L. FhuA, an Escherichia coli outer membrane protein with a dual function of transporter and channel which mediates the transport of phage DNA. *Biochimie* **80**, 363-369 (1998).
- 137 Sauer, D. F., Bocola, M., Broglia, C., Arlt, M., Zhu, L. L., Brocker, M., Schwaneberg, U. & Okuda, J. Hybrid ruthenium ROMP catalysts based on an engineered variant of β -barrel protein FhuA Δ CVFtev: effect of spacer length. *Chemistry—An Asian Journal* **10**, 177-182 (2015).
- 138 Anand, D., Dhoke, G. V., Gehrman, J., Garakani, T. M., Davari, M. D., Bocola, M., Zhu, L. & Schwaneberg, U. Chiral separation of d/l-arginine with whole cells through an engineered FhuA nanochannel. *Chemical Communications* **55**, 5431-5434 (2019).
- 139 Savitzky, A. & Golay, M. J. Smoothing and differentiation of data by simplified least squares procedures. *Analytical chemistry* **36**, 1627-1639 (1964).
- 140 Surrey, T. & Jähnig, F. Kinetics of folding and membrane insertion of a β -barrel membrane protein. *Journal of Biological Chemistry* **270**, 28199-28203 (1995).
- 141 Kragh-Hansen, U., le Maire, M. & Møller, J. V. The mechanism of detergent solubilization of liposomes and protein-containing membranes. *Biophysical Journal* **75**, 2932-2946 (1998).
- 142 Daskal, I., Ramirez, S. A., Ballal, R. N., Spohn, W. H., Wu, B. & Busch, H. Detergent lysis for isolation of intact polysomes of Novikoff hepatoma ascites cells. *Cancer research* **36**, 1026-1034 (1976).
- 143 Caligur, V. Detergents and solubilization reagents. *BioFiles for File Science Research* **3**, 1-36 (2008).
- 144 Arlt, M. *Design of biohybrid catalysts for metathesis reactions*, Universitätsbibliothek der RWTH Aachen, (2015).
- 145 Tenne, S.-J. & Schwaneberg, U. *Engineering of FhuA into an ideal scaffold for metallozymes*, Hochschulbibliothek der Rheinisch-Westfälischen Technischen Hochschule Aachen, (2012).
- 146 Allen, T. Calcein as a tool in liposome methodology. *Liposome technology* **3**, 177-182 (1984).
- 147 Hamann, S., Kiilgaard, J. F., Litman, T., Alvarez-Leefmans, F. J., Winther, B. R. & Zeuthen, T. Measurement of cell volume changes by fluorescence self-quenching. *Journal of fluorescence* **12**, 139-145 (2002).
- 148 Blanus, M., Schenk, A., Sadeghi, H., Marienhagen, J. & Schwaneberg, U. Phosphorothioate-based ligase-independent gene cloning (PLICing): An enzyme-free and sequence-independent cloning method. *Analytical biochemistry* **406**, 141-146 (2010).

-
- 149 Studier, F. W. Protein production by auto-induction in high-density shaking cultures. *Protein expression and purification* **41**, 207-234 (2005).
- 150 Cheng, F., Kardashliev, T., Pitzler, C., Shehzad, A., Lue, H., Bernhagen, J. r., Zhu, L. & Schwaneberg, U. A competitive flow cytometry screening system for directed evolution of therapeutic enzyme. *ACS Synth. Biol.* **4**, 768-775 (2015).
- 151 Chen, C. S., Fujimoto, Y., Girdaukas, G. & Sih, C. J. Quantitative analyses of biochemical kinetic resolutions of enantiomers. *J. Am. Chem. Soc.* **104**, 7294-7299 (1982).
- 152 Skerra, A. & Schmidt, T. G. in *Methods in enzymology* Vol. 326 271-304 (Elsevier, 2000).
- 153 Ruff, A. J., Arlt, M., van Ohlen, M., Kardashliev, T., Konarzycka-Bessler, M., Bocola, M., Dennig, A., Urlacher, V. B. & Schwaneberg, U. An engineered outer membrane pore enables an efficient oxygenation of aromatics and terpenes. *Journal of Molecular Catalysis B: Enzymatic* **134**, 285-294 (2016).
- 154 Despotovic, D., Vojcic, L., Prodanovic, R., Martinez, R., Maurer, K.-H. & Schwaneberg, U. Fluorescent assay for directed evolution of perhydrolases. *Journal of biomolecular screening* **17**, 796-805 (2012).
- 155 Kudla, G., Murray, A. W., Tollervey, D. & Plotkin, J. B. Coding-sequence determinants of gene expression in *Escherichia coli*. *science* **324**, 255-258 (2009).
- 156 Gros, C. & Labouesse, B. Study of the dansylation reaction of amino acids, peptides and proteins. *European journal of biochemistry* **7**, 463-470 (1969).
- 157 Armstrong, D. W., Liu, Y. & Ekborgott, K. H. A covalently bonded teicoplanin chiral stationary phase for HPLC enantioseparations. *Chirality* **7**, 474-497 (1995).
- 158 Isralewitz, B., Gao, M. & Schulten, K. Steered molecular dynamics and mechanical functions of proteins. *Curr. Opin. Struct. Biol.* **11**, 224-230 (2001).
- 159 Schmidt, T. G. & Skerra, A. The Strep-tag system for one-step purification and high-affinity detection or capturing of proteins. *Nature protocols* **2**, 1528 (2007).
- 160 Ruff, A. J., Arlt, M., van Ohlen, M., Kardashliev, T., Konarzycka-Bessler, M., Bocola, M., Denning, A., Urlacher, V. B. & Schwaneberg, U. in *J. Mol. Cat B* Vol. 134 285-294 (2016).

Appendix

Vector maps of pPR-IBA1 expression vector

Features of pPR-IBA1

	from bp	to bp
forward primer binding site	20	39
multiple cloning site	100	183
Strep-tag	184	213
reverse primer binding site	264	283
f1 origin	425	863
AmpR resistance gene	1011	1870

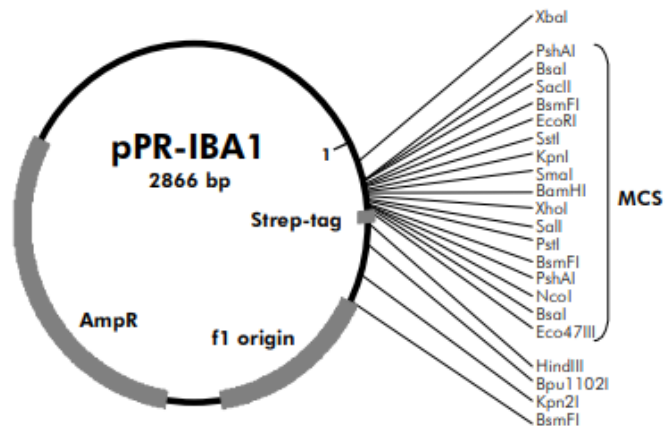


Figure 42. Vector map of expression vector used for FhuA expression in this thesis (IBA GmbH).

Vector maps of the expression vector pET 42b (+)

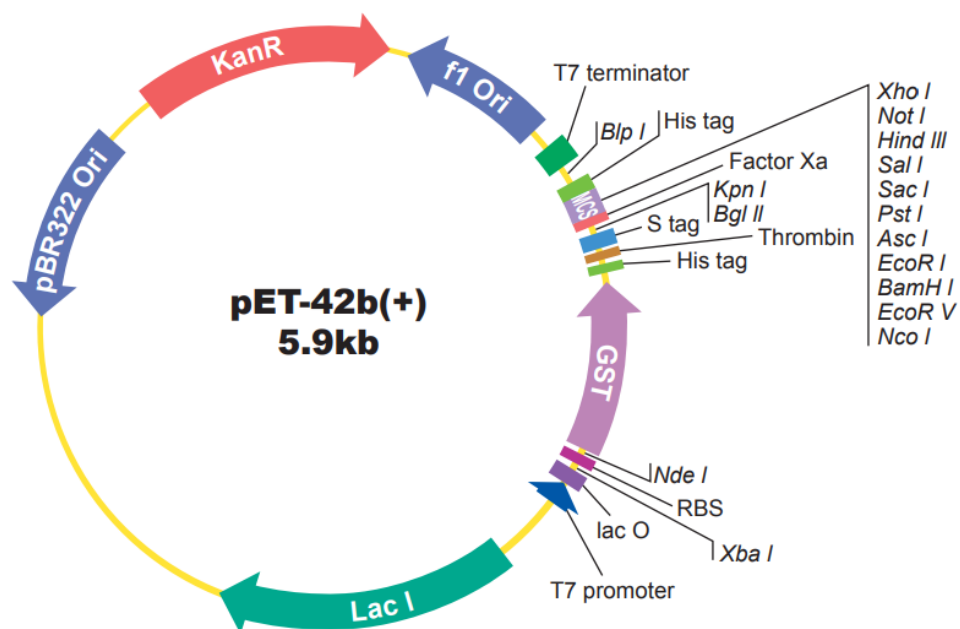


Figure 43. Vector map of expression vector used for ADI and pkDAO expression in this thesis (GenScript).

DNA sequence of gene encoding for FhuA WT

ATGGCGCGTTCCAAAACCTGCTCAGCCAAAACACTCACTGCGTAAAATCGCAGTTGTAGTAGCCACAGCGGTTAGCG
 GCATGTCTGTTTATGCACAGGCAGCGGTTGAACCGAAAGAAGACACTATCACCGTTACCGCTGCACCTGCGCCGCA
 AGAAAGCGCATGGGGGCTGCTGCAACTATTGCGGCGCGACAGTCTGCTACCGGCACTAAACCGATACGCCGAT
 TCAAAAAGTGCCACAGTCTATTTCTGTTGTGACCGCCGAAGAGATGGCGCTGCATCAGCCGAAGTCGGTAAAAGA
 AGCGCTTAGCTACACGCCGGGTGTCTCTGTTGGTACGCGTGGCGCATCCAACACCTATGACCACCTGATCATTGCG
 GGCTTTGCGGCAGAAGGCCAAAGCCAGAATAACTATCTGAATGGCCTGAAGTTGCAGGGCAACTTCTATAACGAT
 GCGGTCAATTGACCCGTATATGCTGGAACGCGCTGAAATTATGCGTGGCCCGGTTTCCGTGCTTTACGGTAAAAGCA
 GTCCTGGCGGCTGTTGAATATGGTCAGCAAGCGTCCGACCACCGAACCCTGAAAGAAGTTCAGTTTAAAGCCG
 GTACTGACAGCCTGTTCCAGACTGGTTTTGACTTTAGCGATTGTTGGATGATGACGGTGTACTCTTATCGCCTG
 ACCGGTCTTGCGCGTTCTGCCAATGCCAGCAGAAAAGGGTCAGAAGAGCAGCGTTATGCTATTGCACCGGCGTTCA
 CCTGGCGTCCGGATGATAAAACCAATTTTACCTTCCTTTCTTACTTCCAGAACGAGCCGGAACCGGTTATTACGGC
 TGGTTGCCGAAAGAGGGAACCGTTGAGCCGCTGCCGAACGGTAAGCGTCTGCCGACAGACTTTAATGAAGGGGC
 GAAGAACAACACCTATTCTCGTAATGAGAAGATGGTCGGCTACAGCTTCGATCACGAATTTAACGACACCTTTACT
 GTGCGTCAGAACCTGCGCTTTGCTGAAAACAAAACCTCGAAAACAGCGTTTATGTTACGGCGTCTGCTCCGATC
 CGGCGAATGCTTACAGCAAACAGTGTGCGGCATTAGCGCCAGCGGATAAAGGCCATTATCTGGCACGTAAATACG
 TCGTTGATGATGAGAAGCTGCAAACTTCTCCGTTGATACCCAGTTGCAGAGCAAGTTTGCCACTGGCGATATCGA
 CCACACCCTGCTGACCGGTGTGCACTTTATGCGTATGCGTAATGACATCAACGCCTGGTTTGGTTACGACGACTCTG
 TGCCACTGCTCAATCTGTACAATCCGGTGAATACCGATTTGCACTTCAATGCCAAAGATCCGGCAAACCTCCGGCCCT
 TACCGCATTCTGAATAAACAGAAACAAACGGGCGTTTATGTTTACAGGATCAGGCGCAGTGGGATAAAGTGTGGTC
 ACCCTAGGCGGTGCTTATGACTGGGCAGATCAAGAATCTCTTAACCGCGTTGCCGGGACGACCGATAAACGTGAT
 GACAAACAGTTTACCTGGCGTGGTGGTGTAACTACCTGTTTGATAATGGTGTAAACACCTTACTTCAGCTATAGCGA
 ATCGTTTGAACCTTCTTCGCAAGTTGGGAAGGATGGTAATATTTTCGCACCGTCTAAAGGTAAGCAGTATGAAGTC
 GCGGTGAAATATGTACCGGAAGATCGTCCGATTGTAGTTACTGGTGCCGTGTATAATCTCACTAAACCAACAACC
 TGATGGCGGACCTGAGGGTCTCTTCTCGGTTGAAGGTGGCGAGATCCGCGCACGTGGCGTAGAAATCGAAG
 CGAAAGCGGCGCTGTCGGCGAGTGTTAACGTAGTCGGTCTTATACTTACACCGATGCGGAATACACCACCGATAC
 TACCTATAAAGGCAATACGCCTGCACAGGTGCCAAAACACATGGCTTCGTTGTGGGCTGACTACACCTTCTTTGACG
 GTCCGCTTTCAGGTCTGACGCTGGGCACCGGTGGTCGTTATACTGGCTCCAGTTATGGTGATCCGGCTAACTCCTTT
 AAAGTGGGAAGTTATACGGTCGTGGATGCGTTAGTACGTTATGATCTGGCGCGAGTCGGCATGGCTGGCTCCAAC
 GTGGCGCTGCATGTTAACAACCTGTTTCGATCGTGAATACGTCGCCAGCTGCTTTAACACTTATGGCTGCTTCTGGGG
 CGCAGAACGTCAGGTCGTTGCAACCGCAACCTTCCGTTTCTAA

Amino acid sequence of gene encoding for FhuA WT

MARSKTAQPKHSLRKIAVVVATAVSGMSVYAQAAVEPKEDTITVTAAPAPQESAWGPAATIAARQSATGKTDTPIQK
 VPQISVVTAEEMALHQPKSVKEALSYTPGVSVGTRGASNTYDHLIRGFAAEGQSQNNYLNGLKLQGNFYNDVIDPY
 MLERAIEIMRGPVSVLYGKSSPGLLNMVSKRPTTEPLKEVQFKAGTDSLFTGTFDFSDSLDDGVYSYRLTGLARSANA
 QQKGSEEQRYAIAAFTWRPDDKTNFTLSFYQNEPETGYYGWLPKEGTVEPLPNGKRLPTDFNEGAKNNTYSRNEKM
 VGYSFDHEFNDFTVRQNLRFENKTSQNSVYGYGVCSDPANAYSKQCAALAPADKGHYLARKYVVDDEKLQNFVSDT
 QLQSKFATGDIDHTLLTGVD FMRMRNDINAWFGYDDSVPLLNLYNPVNTDFDFNAKDPANSGPYRILNKQKQTVGVV
 QDQAQWDKVLVTLGGRYDWADQESLNRVAGTTDKRDDKQFTWRGGVNYLFDNGVTPYFSYSEFEPSSQVGKDGNI

FAPSKGKQYEVGVKYPEDRPIVVTGAVYNLTKTNNLMADPEGSSFFSVEGGEIRARGVEIEAKRPLSASVNVVGSYTYTD
AEYTTDTTYKGNTPAQVPKHMASLWADYTFFDGPLSGLTLGTGGRYTGSSYGDPA NSFKVGSYTVVDALVRYDLARVG
MAGSNVALHVNNLFDREYVASCNTYGCFWGAERQVVATATFRF

DNA sequence of gene encoding for FhuA Δ L

ATGGCGGTTCCAAAACACTGCTCAGCCAAAACACTCACTGCGTAAAATCGCAGTTGTAGTAGCCACAGCGGTTAGCG
 GCATGTCTGTTTATGCACAGGCAAGCGCATGGGGGCTGCTGCAACTATTGCGGCGGACAGTCTGCTACGCCGAT
 TCAAAAAGTGCCACAGTCTATTTCTGTTGTGACCGCCGAAGAGATGGCGCTGCATGACCCGAAGTCGGTAAAAGA
 AGCGCTTAGCTACACGCCGGGTGTCTCTGTTGGTACGTGGGGCGCATCCAACACCTATGACCACCTGATCATTGCG
 GGCTTTGCGGCAGAAGGCCAAAGCCAGAATAACTATCTGAATGGCCTGAAGTTGCAGGGCAACTTCTATCTCGATG
 CGGTCATTGACCCGTATATGCTGGAACGCGCTGAAATTATGCGTGGCGGCGGCCTGTTGAATATGGTCAGCAAGC
 GTCCGACCACCGAACCGCTGAAAGAAGTTCAGTTTAAAGCCGGTACTGACAGCCTGTTCCAGACTGGTTTTGACTT
 TAGCGATTCTGTTGGATGATGACGGTGTCTTACTCTTATCGCCTGACCGGTCTTGCGCGTTCTGCCAATGCCACAGCAGA
 AAGGGTCAGAAGAGCAGCGTTATGCTATTGCACCGGCGTTACCTGGCGTCCGGATGATAAAACCAATTTTACCTT
 CCTTCTTACTTCCAGAACGAGCCGGAACCGGTTATTACGGCTGGTTGCCGAAAGAGGGGAACCGTTGAGCCGCTG
 CCGAACGGTAAGCGTCTGCCGACAGACTTTAATGAAGGGGCGAAGAACAACACCTATTCTCGTAATGAGAAGATG
 GTCGGCTACAGCTTCGATCACGAATTTAACGACACCTTTACTGTGCGTCAGAACCTGCGCTTTGCTGAAAACAAAAC
 CTCGAAAACAGCGTTTATGGTTACGGCGTCTGCTCCGATCCGGCGAATGCTTACAGCAAACAGTGTGCGGCATTA
 GCGCCAGCGGATAAAGGCCATTATCTGGCACGTAAATACGTCGTTGATGATGAGAAGCTGCAAACTTCTCCGTTG
 ATACCCAGTTGCAGAGCAAGTTTGCCACTGGCGATATCGACCACACCCTGCTGACCGGTGTCGACTTTATGCGTAT
 GCGTAATGACATCAACGCCTGGTTTGGTTACGACGACTCTGTGCCACTGCTCAATCTGTACAATCCGGTGAATACCG
 ATTCGACTTCAATGCCAAAGATCCGGCAAACCTCCGGCCCTTACCGCATTCTGAATAAACAGAAACAAACGGGCGT
 TTATGTTTCAAGGATCAGGCGCAGTGGGATAAAGTGCTGGTCACCCTAGGCGGTCGTTATGACTGGGCAGATCAAGA
 ATCTCTTAACCGCGTTGCCGGGACGACCGATAAACGTGATGACAAACAGTTTACCTGGCGTGGTGGTGTAACTAC
 CTGTTTGATAATGGTGTAACACCTTACTTCAGCTATAGCGAATCGTTTGAACCTTCTTCGCAAGTTGGGAAGGATGG
 TAATATTTTCGCACCGTCTAAAGGTAAGCAGTATGAAGTCGGCGTGAAATATGTACCGGAAGATCGTCCGATTGTA
 GTTACTGGTGCCGTGTATAATCTCACTAAAACCAACAACCTGATGGCGGACCCTGAGGGTTCCTTCTCTCGGTTGA
 AGGTGGCGAGATCCGCGCACGTGGCGTAGAAATCGAAGCGAAAGCGGCGCTGTCGGCGAGTGTTAACGTAGTCG
 GTTCTTATACTTACACCGATGCGGAATACACCACCGATACTACCTATAAAGGCAATACGCCTGCACAGGTGCCAAA
 ACACATGGCTTCGTTGTGGGCTGACTACACCTTCTTTGACGGTCCGCTTTCAGGTCTGACGCTGGGCACCGGTGGTC
 GTTATACTGGCTCCAGTTATGGTGATCCGGCTAACTCCTTTAAAGTGGAAGTTATACGGTCGTGGATGCGTTAGT
 ACGTTATGATCTGGCGCGAGTCGGCATGGCTGGCTCCAACGTGGCGCTGCATGTTAAACACCTGTTTCGATCGTGAA
 TACGTCGCCAGCTGCTTTAACACTTATGGCTGCTTCTGGGGCGCAGAACGTCAGGTCGTTGCAACCGCAACCTTCC
 GTTCTAA

Amino acid sequence of gene encoding for FhuA Δ L

MARSKTAQPKHSLRKIAVVVATAVSGMSVYAQAAVEPKEDTITVTAAPAPQESAWGPAATIAARQSATGKTDTPIQK
 VPQISVVTAEEMLHDPKSVKEALSYTPGVSVGTWGASNTYDHLIRGFAAEGQSQNNYLNGLKLQGNFYLDAVIDPY
 MLERAIEIMRGPVSVLYGKSSPGLLNMVSKRPTEPLKEVQFKAGTDSLFTGDFSDSLDDGVSYSRLTGLARSANA
 QQKGSEEQRYAIAPAFTWRPDDKNFTFLSYFQNEPETGYYGWLPKEGTVEPLPNGKRLPTDFNEGAKNNYTSRNEKM
 VGYSFDHEFNDTFTVRQNLRFENKTSQNSVYGVVCSDPANAYSKQCAALAPADKGHYLARKYVVDDEKLQNFVSDT
 QLQSKFATGDIDHTLLTGVD FMRMRNDINAWFGYDDSVPLNLYNPVNTDFDFNAKDPANSGPYRILNKQKQTVGVV
 QDQAQWQDKVLVTLGGRYDWADQESLNRVAGTTDKRDDKQFTWRGGVNYLFDNGVTPYFSYSEFEPSSQVQKDGNI
 FAPSKGKQYEVGVKYPEDRPIVVTGAVYNLTNTNLMADPEGSFFSVEGGEIRARGVEIEAKRPLSASVNVVGSYTYTD

AEYTTDTTYKGNTPAQVPKHMASLWADYTFFDGPLSGLTLGTGGRYTGSSYGD
PANSFKVGSYTVVDALVRYDLARVG
MAGSNVALHVNNLFDREYVASCNTYGC
FWGAERQVVATATFRF

DNA sequence of gene encoding for FhuAF4

ATGGCGGTTCCAAAACCTGCTCAGCCAAAACACTCACTGCGTAAAATCGCAGTTGTAGTAGCCACAGCGGTTAGCG
 GCATGTCTGTTTATGCACAGGCAAGCGCATGGGGGCTGCTGCAACTATTGCGGCGGACAGTCTGCTACGCCGAT
 TCAAAAAGTGCCACAGTCTATTTCTGTTGTGACCGCCGAAGAGATGGCGCTGCATGACCCGAAGTCGGTAAAAGA
 AGCGCTTAGCTACACGCCGGGTGTCTCTGTTGGTACGTGGGGCGCATCCAACACCTATGACCACCTGATCATTGCG
 GGCTTTGCGGCAGAAGGCCAAAGCCAGAATAACTATCTGAATGGCCTGAAGTTGCAGGGCAACTTCTATCTCGATG
 CGGTCATTGACCCGTATATGCTGGAACGCGCTGAAATTATGCGTGGCTCGACGCTGTTGAATATGGTCAGCAAGCG
 TCCGACCACCGAACCGCTGAAAGAAGTTCAGTTTAAAGCCGGTACTGACAGCCTGTTCCAGACTGGTTTTGACTTTA
 GCGATTCTGTTGGATGATGACGGTGTCTTACTCTTATCGCCTGACCGGTCTTGCGCGTTCTGCCAATGCCAGCAGAAA
 GGGTCAGAAGAGCAGCGTTATGCTATTGCACCGGCGTTACCTGGCGTCCGGATGATAAAACCAATTTTACCTTCC
 TTTCTTACTTCCAGAACGAGCCGGAACCGGTTATTACGGCTGGTTGCCGAAAGAGGGGAACCGTTGAGCCGCTGCC
 GAACGGTAAGCGTCTGCCGACAGACTTTAATGAAGGGGCGAAGAACAACACCTATTCTCGTAATGAGAAGATGGT
 CGGCTACAGCTTCGATCACGAATTTAACGACACCTTTACTGTGCGTCAGAACCTGCGCTTTGCTGAAAACAAAACCT
 CGAAAACAGCGTTTATGGTTACGGCGTCTGCTCCGATCCGGCGAATGCTTACAGCAAACAGTGTGCGGCATTAGC
 GCCAGCGGATAAAGGCCATTATCTGGCACGTAAATACGTCGTTGATGATGAGAAGCTGCAAACCTTCTCCGTTGAT
 ACCCAGTTGCAGAGCAAGTTTGCCACTGGCGATATCGACCACACCTGCTGACCGGTGTCGACTTTATGCGTATGC
 GTAATGACATCAACGCCTGGTTTGGTTACGACGACTCTGTGCCACTGCTCAATCTGTACAATCCGGTGAATACCGAT
 TTCGACTTCAATGCCAAAGATCCGGCAAACCTCCGGCCCTTACCGCATTCTGAATAAACAGAAACAAACGGGCGTTT
 ATGTTTCAGGATCAGGCGCAGTGGGATAAAGTGTGGTCAACCTAGGCGGTCGTTATGACTGGGCAGATCAAGAAT
 CTCTTAACCGCGTTGCCGGGACGACCGATAAACGTGATGACAAACAGTTTACCTGGCGTGGTGGTGTAACTACCT
 GTTTGATAATGGTGTAACACCTTACTTACGCTATAGCGAATCGTTTGAACCTTCTTCGCAAGTTGGGAAGGATGGTA
 ATATTTTCGCACCGTCTAAAGGTAAGCAGTATGAAGTCGGCGTGAAATATGTACCGGAAGATCGTCCGATTGTAGT
 TACTGGTGCCGTGTATAATCTCACTAAAACCAACAACCTGATGGCGGACCCTGAGGGTTCCTTCTTCTCGGTTGAAG
 GTGGCGAGATCCGCGCACGTGGCGTAGAAATCGAAGCGAAAGCGGCGCTGTCGGCGAGTGTTAACGTAGTCGGT
 TCTTATACTTACACCGATGCGGAATACACCACCGATACTACCTATAAAGGCAATACGCCTGCACAGGTGCCAAAAC
 ACATGGCTTCTGTTGTTGGGCTGACTACACCTTCTTTGACGGTCCGCTTTCAGGTCTGACGCTGGGCACCGGTGGTCTG
 TATACTGGCTCCAGTTATGGTGATCCGGCTAACTCCTTTAAAGTGGGAAGTTATACGGTCGTGGATGCGTTAGTAC
 GTTATGATCTGGCGCGAGTCGGCATGGCTGGCTCCAACGTGGCGCTGCATGTTAACAACCTGTTTCGATCGTGAATA
 CGTCGCCAGCTGCTTTAACACTTATGGCTGCTTCTGGGGCGCAGAACGTCAGGTCGTTGCAACCGCAACCTTCCGTT
 TCTAA

Amino acid sequence of gene encoding for FhuAF4

MARSKTAQPKHSLRKIAVVVATAVSGMSVYAQAAVEPKEDTITVTAAPAPQESAWGPAATIAARQSATGKTDTPIQK
 VPQISISVVTAEEMALHDPKSVKEALSYTPGVSVGTWASNTYDHLIRGFAAEGQSQNNYLNGLKLQGNFYLDAVIDPY
 MLERAIEIMRSPVSVLYGKSPTGLNLMVSKRPTTEPLKEVQFKAGTDSLFTQGFDFSDSLDDGVVSYRLTGLARSANAQ
 QKGSEEQRYAIAPAFTWRPDDKTNFTLSYFQNEPETGGYGWLPKEGTVEPLPNGKRLPTDFNEGAKNNTYSRNEKMOV
 GYSFDHEFNDFTVRQNLRAFNKTSQNSVYGYGVCDPANAYSKQCAALAPADKGHYLARKYVVDDEKLQNFSDVTQ
 LQSKFATGDIHTLLTGVDfMRMRNDINAWFGYDDSVPLNLYNPVNTDFDFNAKDPANSGPYRILNKQKQTVVYVQ
 DQAQWDKVLVTLGGRYDWADQESLNRVAGTTDKRDDKQFTWRGGVNYLFDNGVTPYFSYSESEFESSQVGKDNIF
 APSKGKQYEVGVKYPEDRPIVVTGAVYNLTKTNNLMADPEGSFFSVEGGEIRARGVEIEAKRPLSASVNVVGSYTYTDA

EYTTDTTYKGNTPAQVPKHMASLWADYTFFDGPLSGLTLGTGGRYTGSSYGDPA NSFKVGSYTVVDALVRYDLARVGM
AGSNVALHVNNLFDREYVASCNTYGCFWGAERQVVATATFRF

DNA sequence of gene encoding for FhuA Δ Strep tag

ATGGCGGTTCCAAAACCTGCTCAGCCAAAACACTCACTGCGTAAAATCGCAGTTGTAGTAGCCACAGCGGTTAGCG
 GCATGTCTGTTTATGCACAGGCAAGCGCATGGGGGCTGCTGCAACTATTGCGGCGGACAGTCTGCTACGCCGAT
 TCAAAAAGTGCCACAGTCTATTTCTGTTGTGACCGCCGAAGAGATGGCGCTGCATGACCCGAAGTCGGTAAAAGA
 AGCGCTTAGCTACACGCCGGGTGTCTCTGTTGGTACGTGGGGCGCATCCAACACCTATGACCACCTGATCATTGCG
 GGCTTTGCGGCAGAAGGCCAAAGCCAGAATAACTATCTGAATGGCCTGAAGTTGCAGGGCAACTTCTATCTCGATG
 CGGTCATTGACCCGTATATGCTGGAACGCGCTGAAATTATGCGTGGCGGCGGCCTGTTGAATATGGTCAGCAAGC
 GTCCGACCACCGAACCGCTGAAAGAAGTTCAGTTTAAAGCCGGTACTGACAGCCTGTTCCAGACTGGTTTTGACTT
 TAGCGATTCTGTTGGATGATGACGGTGTCTTACTCTTATCGCCTGACCGGTCTTGCGCGTTCTGCCAATGCCAGCAGA
 AAGGGTCAGAAGAGCAGCGTTATGCTATTGCACCGGCGTTACCTGGCGTCCGGATGATAAAACCAATTTTACCTT
 CCTTCTTACTTCCAGAACGAGCCGGAACCGGTTATTACGGCTGGTTGCCGAAAGAGGGAAACCGTTGAGCCGCTG
 CCGAACGGTAAGCGTCTGCCGACAGACTTTAATGAAGGGGCGAAGAACAACACCTATTCTCGTAATGAGAAGATG
 GTCGGCTACAGCTTCGATCACGAATTTAACGACACCTTTACTGTGCGTCAGAACCTGCGCTTTGCTGAAAACAAAAC
 CTCGAAAACAGCGTTTATGGTTACGGCGTCTGCTCCGATCCGGCGAATGCTTACAGCAAACAGTGTGCGGCATTA
 GCGCCAGCGGATAAAGGCCATTATCTGGCACGTAAATACGTCGTTGATGATGAGAAGCTGCAAACTTCTCCGTTG
 ATACCCAGTTGCAGAGCAAGTTTGCCACTGGCGATATCGACCACACCCTGCTGACCGGTGTCGACTTTATGCGTAT
 GCGTAATGACATCAACGCCTGGTTTGGTTACGACGACTCTGTGCCACTGCTCAATCTGTACAATCCGGGTTCTGGTT
 CTTGGTCTCACCCGAGTTTCAAAAATCTGGTTCTGGTGTGAATACCGATTTGACTTCAATGCCAAAGATCCGGCA
 AACTCCGGCCCTTACCGCATTCTGAATAAACAGAAACAAACGGGCGTTTATGTTTCAAGGATCAGGCGCAGTGGGATA
 AAGTGCTGGTCACCCTAGGCGGTCGTTATGACTGGGCAGATCAAGAATCTCTTAACCGCGTTGCCGGGACGACCG
 ATAAACGTGATGACAAACAGTTTACCTGGCGTGGTGGTGTAACTACCTGTTTGATAATGGTGTAACACCTTACTTC
 AGCTATAGCGAATCGTTTGAACCTTCTCGCAAGTTGGGAAGGATGGTAATATTTTCGCACCGTCTAAAGGTAAGC
 AGTATGAAGTCGGCGTGAAATATGTACCGGAAGATCGTCCGATTGTAGTTACTGGTGCCGTGTATAATCTCACTAA
 AACCAACAACCTGATGGCGGACCCTGAGGGTTCCTTCTCTCGTTGAAGGTGGCGAGATCCGCGCACGTGGCGT
 AGAAATCGAAGCGAAAGCGGCGCTGTCGGCGAGTGTTAACGTAGTCGGTCTTATACTTACACCGATGCGGAATA
 CACCACCGATACTACCTATAAAGGCAATACGCTGCACAGGTGCCAAACACATGGCTTCGTTGTGGGCTGACTAC
 ACCTTCTTTGACGGTCCGCTTTCAGGTCTGACGCTGGGCACCGGTGGTCGTTATACTGGCTCCAGTTATGGTGATCC
 GGCTAACTCCTTTAAAGTGGGAAGTTATACGGTCGTGGATGCGTTAGTACGTTATGATCTGGCGCGAGTCGGCATG
 GCTGGCTCCAACGTGGCGCTGCATGTTAAACACCTGTCGATCGTGAATACGTCGCCAGCTGCTTTAACACTTATGG
 CTGCTTCTGGGGCGCAGAACGTCAGGTCGTTGCAACCGCAACCTTCCGTTTCTAA

Amino acid sequence of gene encoding for FhuA Δ Strep tag

MARSKTAQPKHSLRKIAVVVATAVSGMSVYAQA AVEPKEDTITVTAAPAPQESAWGPAATIAARQSATGKTDTPIQK
 VPQISISVVTAEEMALHDPKSVKEALSYTPGVSVGTWASNTYDHLIRGFAAEGQSQNNYLNLKLQGNFYLDAVIDPY
 MLERAIEIMRGPVSVLYGKSSPGLLNMVSKRPTEPLKEVQFKAGTDSLFTGDFDSDSLDDGVYSYRLTGLARSANA
 QQKGSEEQRYAIAFAFTWRPDDKNFTFLSYFQNEPETGYYGWLPKEGTVEPLPNGKRLPTDFNEGAKNNTYSRNEKM
 VGYSFDHEFNDFTVRQNLRFANKTQSNSVYGYGVCSDPANAYSKQCAALAPADKGHYLARKYVVDDEKLQNFVSDT
 QLQSKFATGDIDHTLLTGVD FMRMNDINAWFGYDDSVLLNLYNPWSPQFEKVNTDFDFNAKDPANSGPYRILNK
 QKQTVGVYVDQAQWDKVLVTLGGRYDWADQESLNRVAGTTDKRDDKQFTWRGGVNYLFDNGVTPYFSYSESEFESS
 QVGKDGNI FAPSKGKQYEVGVKYPEDRPIVVTGAVYNLTKTNLMADPEGSFFSVEGGEIRARGVEIEAKRPLSASVN

VVGSYTYTDAEYTTDTTYKGNTPAQVPKHMASLWADYTFFDGPLSGLTLGTGGRYTGSSYGDPANSFKVGSYTVVDAL
VRYDLARVGMAGSNVALHVNNLFDREYVASCNTYGCFWGAERQVVATATFRF

DAN sequence of gene encoding for FhuA F4 Strep tag

ATGGCGGTTCCAAAACCTGCTCAGCCAAAACACTCACTGCGTAAAATCGCAGTTGTAGTAGCCACAGCGGTTAGCG
 GCATGTCTGTTTATGCACAGGCAAGCGCATGGGGGCTGCTGCAACTATTGCGGCGGACAGTCTGCTACGCCGAT
 TCAAAAAGTGCCACAGTCTATTTCTGTTGTGACCGCCGAAGAGATGGCGCTGCATGACCCGAAGTCGGTAAAAGA
 AGCGCTTAGCTACACGCCGGGTGTCTCTGTTGGTACGTGGGGCGCATCCAACACCTATGACCACCTGATCATTGCG
 GGCTTTGCGGCAGAAGGCCAAAGCCAGAATAACTATCTGAATGGCCTGAAGTTGCAGGGCAACTTCTATCTCGATG
 CGGTCATTGACCCGTATATGCTGGAACGCGCTGAAATTATGCGTGGCTCGACGCTGTTGAATATGGTCAGCAAGCG
 TCCGACCACCGAACCGCTGAAAGAAGTTCAGTTTAAAGCCGGTACTGACAGCCTGTTCCAGACTGGTTTTGACTTTA
 GCGATTCTGTTGGATGATGACGGTGTCTTACTCTTATCGCCTGACCGGTCTTGCGCGTTCTGCCAATGCCAGCAGAAA
 GGGTCAGAAGAGCAGCGTTATGCTATTGCACCGGCGTTCACCTGGCGTCCGGATGATAAAACCAATTTTACCTTCC
 TTTCTTACTTCCAGAACGAGCCGGAACCGGTTATTACGGCTGGTTGCCGAAAGAGGGGAACCGTTGAGCCGCTGCC
 GAACGGTAAGCGTCTGCCGACAGACTTTAATGAAGGGGCGAAGAACAACACCTATTCTCGTAATGAGAAGATGGT
 CGGCTACAGCTTCGATCACGAATTTAACGACACCTTTACTGTGCGTCAGAACCTGCGCTTTGCTGAAAACAAAACCT
 CGAAAACAGCGTTTATGGTTACGGCGTCTGCTCCGATCCGGCGAATGCTTACAGCAAACAGTGTGCGGCATTAGC
 GCCAGCGGATAAAGGCCATTATCTGGCACGTAAATACGTCGTTGATGATGAGAAGCTGCAAACCTTCTCCGTTGAT
 ACCCAGTTGCAGAGCAAGTTTGCCACTGGCGATATCGACCACACCCTGCTGACCGGTGTCGACTTTATGCGTATGC
 GTAATGACATCAACGCCTGGTTTGGTTACGACGACTCTGTGCCACTGCTCAATCTGTACAATCCGGGTTCTGGTTCT
 TGGTCTCACCCGAGTTTCAAAAATCTGGTTCTGGTGTGAATACCGATTCGACTTCAATGCCAAAGATCCGGCAAA
 CTCCGGCCCTTACCGCATTCTGAATAAACAGAAACAAACGGGCGTTTATGTTTACAGGATCAGGCGCAGTGGGATAAA
 GTGCTGGTCACCCTAGGCGGTCGTTATGACTGGGCAGATCAAGAATCTCTTAACCGCGTTGCCGGGACGACCGATA
 AACGTGATGACAAACAGTTTACCTGGCGTGGTGGTGTAACTACCTGTTTGATAATGGTGTAAACCTTACTTCAGC
 TATAGCGAATCGTTTGAACCTTCTTCGCAAGTTGGGAAGGATGGTAATATTTTCGCACCGTCTAAAGGTAAGCAGT
 ATGAAGTCGGCGTGAAATATGTACCGGAAGATCGTCCGATTGTAGTTACTGGTGCCGTGTATAATCTCACTAAAAC
 CAACAACCTGATGGCGGACCCTGAGGGTTCCTTCTTCTCGGTTGAAGGTGGCGAGATCCGCGCACGTGGCGTAGA
 AATCGAAGCGAAAGCGGCGCTGTGCGCGAGTGTTAACGTAGTCGGTTCTTATACTTACACCGATGCGGAATACACC
 ACCGATACTACCTATAAAGGCAATACGCCTGCACAGGTGCCAAAACACATGGCTTCGTTGTGGGCTGACTACACCT
 TCTTTGACGGTCCGCTTTCAGGTCTGACGCTGGGCACCGGTGGTCTTATACTGGCTCCAGTTATGGTGATCCGGCT
 AACTCCTTTAAAGTGGGAAGTTATACGGTCGTGGATGCGTTAGTACGTTATGATCTGGCGCGAGTCGGCATGGCTG
 GCTCCAACGTGGCGCTGCATGTTAACAACCTGTTGATCGTGAATACGTCGCCAGCTGCTTTAACACTTATGGCTGC
 TTCTGGGGCGCAGAACGTCAGGTCGTTGCAACCGCAACCTTCCGTTTCTAA

Amino acid sequence of gene encoding for FhuA F4 Strep tag

MARSKTAQPKHSLRKIAVVVATAVSGMSVYAQAAVEPKEDTITVTAAPAPQESAWGPAATIAARQSATGKTDTPIQK
 VPQISVVTAEEMLHDPKSVKEALSYTPGVSVGTWGASNTYDHLIRGFAAEGQSQNNYLNGLKLQGNFYLDAVIDPY
 MLERAIEIMRSPVSVLYGKSSPTGLLNMVSKRPTTEPLKEVQFKAGTDSLFTQGFDFSDSLDDGVYSYRLTGLARSANAQ
 QKGSEEQRYAIAPAFTWRPDDKTNFTLSYFQNEPETGGYGWLPKEGTVEPLPNGKRLPTDFNEGAKNNYSRNEKMMV
 GYSFDHEFNDTFTVRQNLRAFNKTSQNSVYGYGVCDPANAYSKQCAALAPADKGHYLARKYVVDDEKLQNFVSDTQ
 LQSKFATGDIDHTLLTGVD FMRMRNDINAWFGYDDSVPLNLYNPWSHPQFEKVNTDFDFNAKDPANSGPYRILNKQ
 KQTGVVYVDQAQWDKVLVTLGGRYDWADQESLNRVAGTTDKRDDKQFTWRGGVNYLFDNGVTPYFSYSESEFESSQ
 VGKDGNI FAPSKGKQYEVGVKYPEDRPIVVTGAVYNLTKTNNLMADPEGSFFSVEGGEIRARGVEIEAKRPLSASVNVV

GSYTYTDAEYTTDTTYKGNTPAQVPKHMASLWADYTFDGPLSGLTLGTGGRYTGSSYGD PANSEFKVGSYTVVDALVR
YDLARVGMAGSNVALHVNNLFDREYVASCNTYGCFWGAERQVVATATFRF

DNA sequence of gene encoding for pig kidney D-amino acid oxidase (pkDAO)

ATGCGTGTTGTTGTTATTGGTGCCGGTGTGATTGGTCTGAGCACCGCACTGTGTATTCATGAACGTTATCATTCACT
TCTGCAGCCGCTGGATGTTAAAGTTTATGCAGATCGTTTTACCCGTTTACCACCACCGATGTTGCAGCAGGTCTGT
GGCAGCCGTATACCAGCGAACCGAGCAATCCGCAAGAAGCAAATTGGAATCAGCAGACCTTTAACTATCTGCTGA
GCCATATTGGTAGCCCGAATGCAGCAAATATGGGTCTGACACCGGTTAGCGGCTATAACCTGTTTCGTGAAGCAGT
TCCGGATCCGTATTGGAAGATATGGTTCTGGGTTTTCTGAAACTGACACCGCGTGAAGTGGACATGTTTCCGGAT
TATCGTTATGGTTGGTTTAACACCAGCCTGATTCTGGAAGGTCGTAAATATCTGCAGTGGCTGACCGAACGTCTGA
CAGAACGTGGTGTGAAATTTTCTGCGTAAAGTTGAGAGCTTTGAAGAGGTTGCACGTGGTGGTGCAGATGTTAT
TATCAATTGTACCGGTGTTTGGGCAGGCGTGTGCAGCCGGATCCGCTGTTACAGCCTGGTCTGGTGCAGATTATC
AAAGTTGATGCACCGTGGCTGAAAACTTTATCATTACCCATGATCTGGAACGCGACATTGGCAATAGCCCGTATA
TCATTCCGGGTCTGCAGGCAGTTACCTTAGGTGGCACCTTTCAGGTTGGTAATTGGAACGAAATTAACAACATCCA
GGATCACAACACCATTTGGGAAGGTTGTTGTCGTCTGGAACCGACGCTGAAAGATGCAAAAATTGTTGGTGAATAT
ACCGGTTTTCTCCGGTTCGTCCGCAGGTTGCCTGGAACGTGAACAGCTGCGTTTTGGTAGCAGCAATACCGAAG
TGATTCATAACTATGGTCATGGTGGTTATGGTCTGACCATTATTGGGGTTGTGCACTGGAAGTTGCAAACTGTTT
GGTAAAGTTCTGGAAGAACGTAATCTGCTGACAATGCCTCCGAGCCATCTGTAA

Amino acid sequence of gene encoding for pig kidney D-amino acid oxidase (pkDAO)

MRVVVIGAGVIGLSTALCIHERYHSLVQLDVKVYADRFTPFTTTDVAAGLWQPYTSEPSNPQEANWNQQTFNILLSHI
GSPNAANMGLTPVSGYNLFREAVPDYPWKDMVLGFRKLTPRELDMPDYRYGWFNTSLILEGRKYLQWLTERLTERG
VKFFLRKVESFEEVARGGADVINCTGVWAGVLQPDLLQPRGQIIKVDAPWLKNFIITHDLERDIGNSPYIIPGLQAVT
LGGTFQVGNWNEINNIQDHNTIWEGCCRLEPTLKDAKIVGEYTGFRPVRPQVRLEREQLRFGSSNTEVIHNYGHGGYGL
TIHWGCALEVAKLFGKVLERNLLTMPPSHL

DNA sequence of gene encoding for arginine diminas (ADI)

ATGTCCGCTGAAACACAGAAGTACGGTGTCCACTCCGAAGCAGGCAAGCTGCGCAAGGTAATGGTCTGCGCTCCGGGACTGG
CGCACAGGCGCCTGACCCCGAGCAACCGCCATGAGCTGCTGTTGACGAAGTGATCTGGGTGCGACCAGGCCAAGCGCGACCA
CTTCGACTTCGTACCAAGATGCGCGAGCGCGGCGTGGATGTGCTGGAAATGCATAACCTGCTACCGGATATCGTGCAGAACC
CCGAGGCCCTGAAGTGGATCCTCGACCGCAAGATCACCCCTGACACCGTCGGGGTGGGCCTGACCAACGAAGTGCAGCTG
GCTGGAGGGCCAGGAGCCACGCCACCTCGCCGAGTTCCTGATCGGCGGCGTGACGTCCCAGGACCTGCCGGAGAGCGAAGGT
GCCAGCGTGGTCAAGATGTACAACGACTACCCGGGCCACTCCAGCTTCATCCTGCCGCCGCTGCCAACACCCAGTTCACCCGC
GACACCACCTGCTGGATCTACGGCGGCGTGACCCTCAACCCGATGTACTGGCCGGCGCGACGCCAGGAAACCCTGCTGACCAC
CGCCATCTACAAGTTCACCCCGAGTTCACCAAGGCCGACTTCCAGGTCTGGTACGGCGACCCGGACCAAGAGCACGGCCAGG
CCACCCTCGAAGGCGGCGACGTCATGCCGATTGGCAAGGGCATCGTGCTGATCGGCATGGGTGAGCGCACCTCGCGCCAGGC
CATCGGCCAACTGGCACAGAACCTCTTCGCCAAGGGCGCAGTGAGCAAGTGATCGTCGCCGGGGCTGCCGAAGTCCCGTGCG
GCCATGCACCTGGACACCGTGTTCACTTCTGCGACCGCGACCTGCTCACGGTTTTCCCGAAAGTGGTGCGCGAGATCGTGCCG
TTCATCATCCGCGGACGAAAGCAAGCCCTACGGCATGGACGTACGCCGCGAGAACAAGTCGTTTCATCGAGGTGGTCGGCGA
GCAGCTGGGCGTCAAGCTGCGTGTGGTCGAGACCGGCGGCAACAGCTTCGCCCGCGAGCGCGAGCAGTGGGATGACGGCAA
CAACGTGGTGGCGCTGGAGCCAGGTGTGGTCATCGGCTACGACCGCAACACCTACACCAATACCTTGCTGCGCAAGGCCGGGA
TAGAGGTCATCACCATCAGTGCCGGCGAACTGGGCCGGGGCCGTGGCGGCGGCCGTTGCATGACCTGCCCGATCGTGCGCGA
CCCGATCAACTACTAA

Formula used for calculation of the amount of FhuA on E.coli cell surface

$$V_{\text{Chromo}} = \frac{y - a}{b} = \frac{y - 1.3726}{1008.6}$$

$$n_{\text{cells (in 200 } \mu\text{l)}} = \frac{n_{\text{cells per ml at OD0.25)}}{5} = \frac{2 * 10^8}{5} = 4 * 10^7$$

$$n_{\text{FhuA}} = \frac{\frac{V_{\text{Chromo}} * C_{\text{Chromo-stock}}}{M_{\text{Chromo-conjugate}}} * N_A}{n_{\text{cells (in 200}\mu\text{l)}}$$

$$= \frac{\frac{V_{\text{Chromo}} \mu\text{l} * 0.5 \mu\text{g}/\mu\text{l}}{53000 \text{ g/mol}} * 6.022 * 10^{23} * \text{mol}^{-1}}{4 * 10^7}$$

Figure 44. Calculation of the amount of FhuA in the outer membrane of E. coli. Y is the value that was measured during fluorescence assay with Streptactin-Chromo546 conjugate. V_{Chromo} was then calculated using the standard curve

Publications and patent

Journals

Anand D., Dhoke G., Gehrmann J., Mirzaei Garakani T., Davari M., Bocola M., Zhu L., Schwaneberg U. [#] Chiral separation of D/L arginine with whole cells through an engineered FhuA channel, *Chemical Communications*, 2019,**55**, 5431-5434

Charan H., Glebe U., **Anand D.**, Kinzel J., Zhu L., Bocola M., Mirzaei Garakani T., Schwaneberg U. and Böker A.[#]; Nano-thin walled micro-compartments from transmembrane protein-polymer conjugates, *Soft Matter*, **2017**, 13, 2866-2875..

Charan H.*, Kinzel J.*, Glebe U., **Anand D.**, Mirzaei Garakani T., Zhu L., Bocola M., Schwaneberg U.[#] and Böker A.[#]; Grafting PNIPAAm from β -barrel shaped transmembrane nanopores, *Biomaterials*, **2016**, 107, 115-123.

Patent

Porous thin film membrane, method for producing same and possible uses.

Pub. No.: US2019/0091636 A1, Pub. Date: March 28, 2019.

BMBF status seminar

Publication: Kinzel J., Glebe U., **Anand D.**, Charan H., Mirzaei Garakani T., Bocola M., Zhu L., Dai X., Böker A. and Schwaneberg U.[#]; Auf dem Weg zu chiralen Protein-Membranen, *Tagungsband 18. Heiligenstädter Kolloquium*, **2016**, 42, 217-224.

* Authors contributed equally

[#] Corresponding authors

Declaration

I hereby declare that all information in this document has been obtained and presented in accordance with academic rules and ethical conduct. I also declare that, as required by these rules and conduct, I have fully cited and referenced all material and results that are not original to this work.

Aachen, June 22, 2020

(Deepak Anand)

Acknowledgement

First of all, I am deeply grateful to my supervisor Prof. Dr. Ulrich Schwaneberg for giving me the opportunity to work on the project 'Chiral membranes' for my PhD thesis in his research group. Thank you for the challenging project, your trust in me, and for continual and unwavering encouragement and scientific guidance over the years.

The presented work in this thesis is part of a tandem project 'Chiral Membranes', which is in the framework of the innovation Biotechnologie 2020+ of the German Federal Ministry of Education and Research (BMBF, Förderkennzeichen: 031A164). The BMBF is kindly acknowledged for financial support.

I would like to thank Prof. Dr. Alexander Böker for acceptance of being my second referee in my PhD defense committee and taking the time to evaluate my thesis. I would also like to thank Prof. Dr. _____ for agreeing to be part of my PhD defense committee as third referee. Furthermore, I would like to thank Prof. Dr. _____ for being in committee as chairman.

I would also like to take this opportunity to thank Dr. Leilei Zhu and Dr. Tayebbeh Mirzaei Garakani who guided me through different parts of my PhD. I acknowledge them for taking over the supervision of my lab work, for discussions, promoting to get some 'HiWi hours' for our project as well as supporting me in preparation of presentations and reports.

I am thankful to Prof. Alexander Böker and his research group for being great tandem partners, in particular Dr. Ulrich Glebe, Dr. Himanshu Charan, Maria Mathiru and Magnus Schwieters. It was a pleasure working with you. We faced and solved important challenges and finally published the results together. Thank you all for playing a very important part in improving my interdisciplinary communication skills.

I would like to give my special thanks to Dr. Julia Gehrmann for being such a great project partner. Time that we spent together in lab always gave me strength facing this really challenging project.

Many thanks to Dr. Marco Bocola, Dr. Mehdi Davari and Dr. Gaurao V. Dhoke for the invaluable support in FhuA modeling and teaching me the usage of YASARA. Thanks a lot for your support for writing the manuscript which actually was a hard task.

I would like to thank Dr. Ketaki Belsare, Dr. Gaurao V. Dhoke, Subratat Pramanik, Volkan Besirlioglu, Khalil Essani and Dr. Martin Thiele for their great moral support during hard times and for making working in lab a fun experience.

My master and research students Carolin Göbel, Marc Sevenic, Oliver Klaas, Martin Woloszyn, Carsten Ludwig, Annkristin Werther and HiWi Daniel Sexauer are acknowledged for their help in the progress of my projects and valuable experiences about supervision.

I acknowledge the whole Schwaneberg group (past and present) and members of the MolMed and Interdisciplinary subgroup for the scientific discussions and the friendly working atmosphere in a multicultural environment, which I appreciated a lot.

My heart pours with gratitude for my family who stood by me in all ups and downs. As a child I have always looked upto my “Mummy and Papa” who were always there for me and I still look upto both of you. It would have not been possible for me to achieve what I did till now in my life without your support and trust. What can I say about my brother Ankush! I don’t say enough to you, but you are my first friend and my life would have been incomplete without you. I still remember the pen you gave me when I was coming to Germany. For me it signified to study hard and achieve great. Trust me, my brother and friend, I did my best even when going got hard. Thanks for being in my life and completing it.

Last but not least, a very special thanks to a special person who has always been there for me no matter the situation. Her special support when I was down with lots of things that were going around me, gave me strength to move forward even when path was not clear. I will forever be indebted and grateful for all your support.

Curriculum Vitae

Personal Information

Name: Deepak Anand
Date of Birth: 15.10.1987
Place of Birth: Manali, India
Nationality: Indian

Education

07.2013 – 10.2019 PhD Fellow, Institute of Biotechnology, RWTH Aachen.

07.2011 - 06.2013 Master of technology. Indian Institute of Technology, Guwahati, India.
Major field of study: Biotechnology.
Master thesis title: “Advancement of SeSaM method with nucleotide analogs”.

07.2011 - 06.2013 Master of Science. Himachal Pradesh University, H.P., India.
Major field of study: Biotechnology.
Master thesis title: “Partial genomic characterization of *Sasurea lappa* plant using random amplified polymorphic DNA (RAPD) technique.”

10.2009 - 09.2012 Bachelor studies. Himachal Pradesh University, H.P., India.
Major field of study: Biotechnology.
Bachelor training: “Fermentation technology in triple antigen (DPT) section in Central Research Institute (CRI), Kasauli, H.P. India”.

Deepak Anand, Aachen